MATHEMATICAL AND STATISTICAL MODELS OF CULEX MOSQUITO ABUNDANCE AND TRANSMISSION DYNAMICS OF WEST NILE VIRUS WITH WEATHER IMPACT

LONGBIN CHEN

A DISSERTATION SUBMITTED TO
THE FACULTY OF GRADUATE STUDIES
IN PARTIAL FULFILMENT OF THE REQUIREMENTS
FOR THE DEGREE OF
DOCTOR OF PHILOSOPHY

GRADUATE PROGRAM IN MATHEMATICS AND STATISTICS
YORK UNIVERSITY
TORONTO, ONTARIO

October 2017

Abstract

West Nile virus (WNV) is a serious public health concern worldwide. Mosquitoes are the key factor in the transmission of the disease. Forecasting mosquito abundance and modeling WNV transmission dynamics with weather conditions are challenging scientific tasks due to the significant weather impact and the magnitude of uncertainty associated with incomplete information. In this dissertation, we employ mathematical and statistical methods to model and forecast the mosquito abundance, the WNV transmission and WNV risk with the weather impact.

Compartmental models for WNV transmission usually assume that mosquito population grows with a constant recruiting rate. However in reality, the mosquito abundance is closely related to weather conditions. In the first part, we improve a generalized linear model (GLM) for *Culex* mosquito abundance with the weather effect. Then we integrate the GLM with a compartmental model for WNV transmission to build a hybrid model. The hybrid model can better capture the reported WNV human infection case pattern in Peel Region, Ontario. As far as we know,

this hybrid model is novel and has never been proposed in the literature of modeling WNV transmission.

In order to better describe the *Culex* mosquito behaviors of the whole year, in the second part, we first separate the year into two periods. Then we build a matrix population model for each period respectively. Our simulation results show that our model captures the trends of available mosquito data very well.

It is important to model the spatial variation of mosquito population for each region. The classical statistical models are not suitable when some important explanatory factors for each trap are either missing or unobservable. Therefore, in the third part, we study the spatio-temporal distribution of *Culex* mosquito population by estimating the collective impact of all the unobservable information for each trap. The results demonstrate that the model has a high level of accuracy in comparison with the classical GLM.

In the last part, we show our work in forecasting weekly *Culex* mosquito abundance since 2011 in Peel Region, Ontario. Then we forecast WNV risk using the hybrid model.

Acknowledgements

First and foremost, I would like to express my special appreciation and thanks to my advisor Professor Huaiping Zhu for his solid support of my Ph.D. study and research, for his patience, enthusiasm, motivation, and immense knowledge. His guidance helped me throughout my Ph.D. study and writing of this thesis. His advice on both research as well as on my career have been priceless. My co-supervisor, Professor Steven Wang has always been there to listen and give invaluable advice. I am profoundly grateful to him for the long discussions. I would like to thank him for carefully reading and commenting on revisions of this manuscript. I would also like to thank Professor Xin Gao and Professor Beate Sander for their insightful comments on my research and continuous support during my Ph.D. studies.

I am grateful to York University and Department of Mathematics and Statistics for the financial support and help they provided during my graduate studies. I also would like to thank the members of LAMPS who have contributed immensely to my personal and professional time at York University. This group has been a source

of friendships, good advice, and collaboration. I cannot finish without thanking my family. For my parents, they raised me with love and supported me in all my pursuits. Last but not the least, I would like to thank all my friends for all the assistance and encouragement.

Table of Contents

List of Tables

List of Figures

1 Introduction

West Nile virus (WNV) is a menace to public health and causes a huge economic burden. As a mosquito-borne disease, WNV first arrived in North American at New York City in 1999. It rapidly spread across the North America continent. The largest outbreak to date in the USA was in 2003, and there were 9862 reported cases of WNV including 264 deaths. The virus arrived in Ontario of Canada in 2000. It caused the largest national outbreak in Canada in 2007 with 2215 reported cases of human infection (CDC 2012a, PHAC 2012). In 2012, a large outbreak and a milder one occurred in the USA and Canada respectively, with a total of 5674 WNV human infection cases (286 deaths) in the USA and 428 cases in Canada. The number of reported human infection cases of WNV varies over the years. Figure 1.1 shows the number of reported WNV human infection cases in Canada and Ontario from 2002 to 2016.

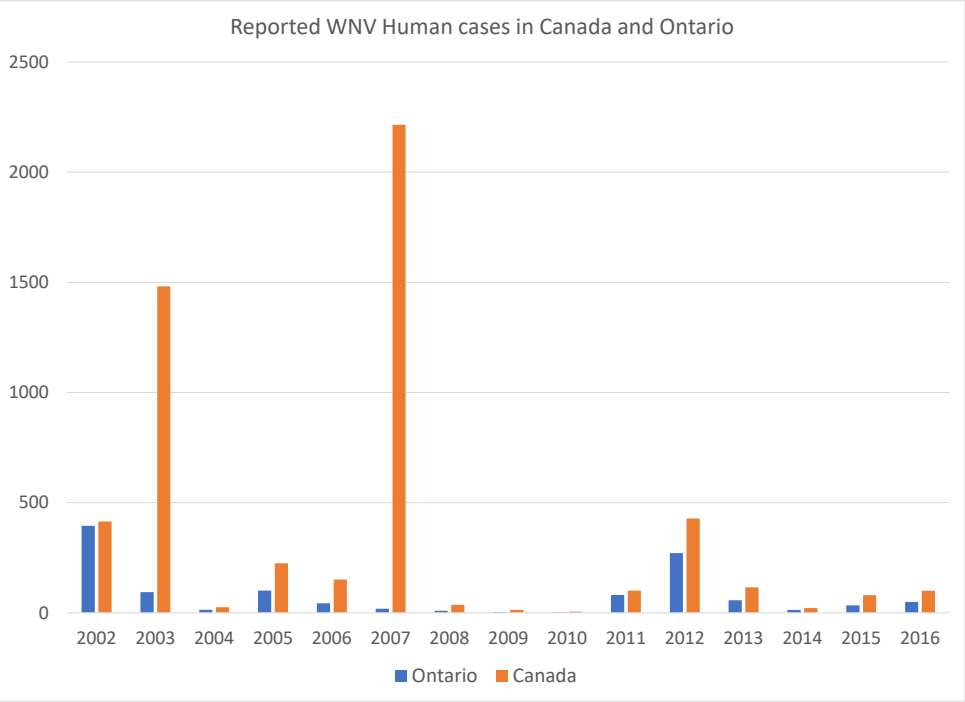

Figure 1.1: WNV reported cases in Canada and Ontario from 2002 to 2016. Data source: Public Health Agency of Canada and Public Health Ontario.

About 20% infected humans would develop mild symptoms including fever. About 1 in 150 infected people would develop a severe illness, which affects the central nervous system and can cause death (CDC 2012b). Prevention of the disease becomes extremely important since no specific treatment or vaccine is available for WNV infection now. Avoiding mosquito bites is the most effective measure to prevent

the disease as mosquitoes are the medium to transmit the disease (CDC 2012b). For each mosquito bite, the risk of infection depends on whether the mosquito is infected. Thus, predicting WNV risk and mosquito abundance is important task in the control and prevention of WNV. Weather conditions not only affect the abundance and the behavior of vector mosquitoes but also determines the outbreak and spreading of WNV. Therefore in this dissertation, we use mathematical and statistical methods to study the effect of weather conditions on mosquito abundance and WNV transmission. And we forecast weekly mosquito abundance and WNV risk with the effect of weather conditions.

1.1 West Nile virus transmission cycle

The transmission cycle of WNV is shown in Figure 1.2. Female mosquitoes become infected by feeding on infectious hosts, and infected mosquitoes pass the virus to other hosts including birds, horses, humans and other mammals through biting for blood meals (PEE 2002, Thomas and Urena 2001). Large non-human mammals (such as horses) and humans are dead-end hosts for the virus due to the low viral level of virus in their blood (Hayes et al. 2005). They cannot transmit the virus back to mosquitoes.

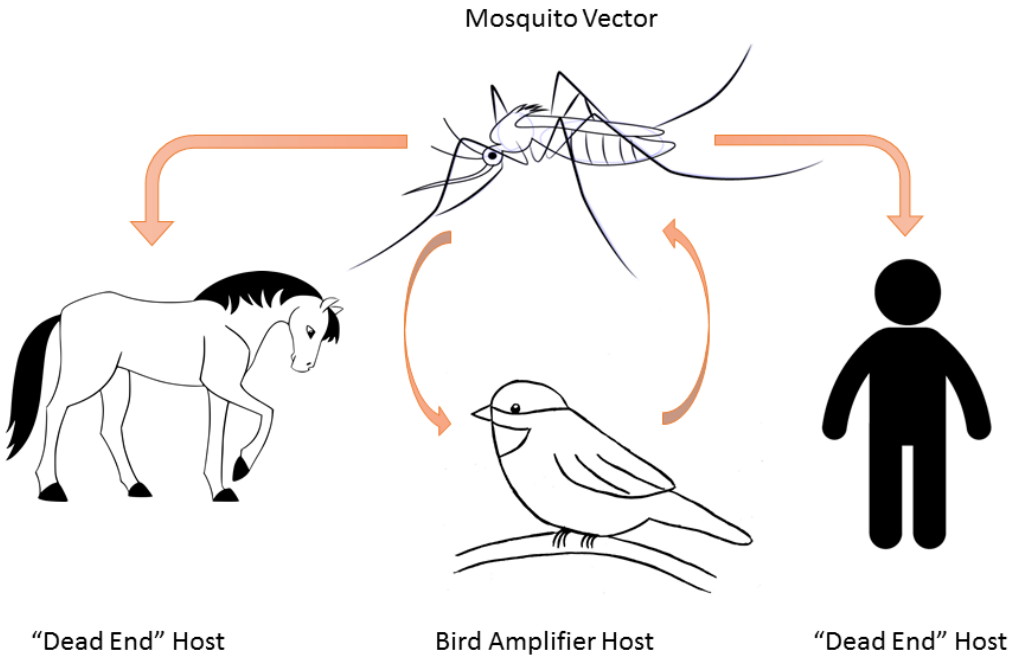

Figure 1.2: WNV transmission cycle.

Although the WNV infected mosquitoes can pass the virus to their offsprings, the filial infection rate is small (0.28%) (Anderson and Main 2006). Therefore we will not consider the vertical transmission as in other studies (Bowman et al. 2005, Wonham et al. 2004).

1.2 Mosquito life cycle with the effect of weather

Mosquito life cycle is significantly affected by environmental conditions such as temperature and precipitation. There are four separate stages in the whole life cycle of

mosquitoes which is shown in Figure 1.3. Mosquito eggs will hatch to larva usually in one or two days depending on temperature (Impoinvil et al. 2007, Koenraadt et al. 2003). Larva will develop into pupa when they accumulate enough heat and food. We do not consider the effect of food on mosquito develop and assume there always is enough food. The adult mosquitoes will then emerge from pupa with enough heat accumulation. Usually adult female mosquitoes can live up to about one month and adult male mosquitoes can live up to about one week (Becker et al. 2010). Three stages of the mosquito life cycle (eggs, larva, pupa) are closely related to water. Therefore, the reproduction and development of mosquitoes are highly dependent on environmental conditions especially temperature and precipitation (Cailly et al. 2012, Gardner et al. 2012, Jones et al. 2012a, Wang et al. 2011).

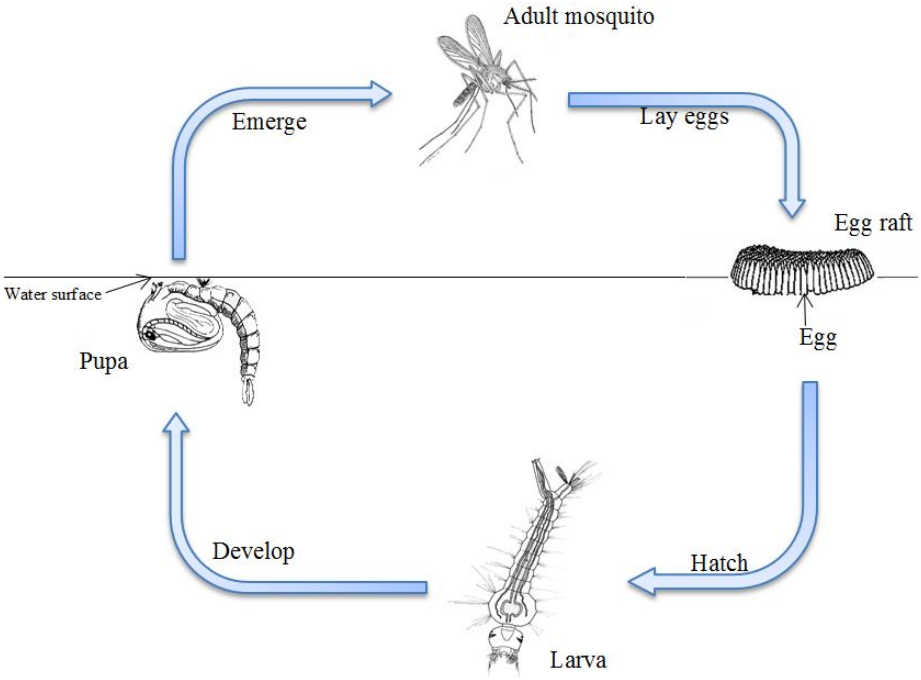

Figure 1.3: Mosquito life cycle.

Mosquito behaviors are also affected by weather conditions. The adult mosquito daily mortality rate is affected by both temperature and precipitation (Brady et al. 2013, Jones et al. 2012a, Reisen 1995, Rubel et al. 2008, Yang et al. 2009). Temperature and precipitation also have impact on mosquito biting behaviors (Dickerson et al. 2012, Jones et al. 2012a, Reisen et al. 1992b, Rubel et al. 2008). Furthermore, in areas where the weather conditions do not support year round mosquito development, mosquitoes have to go through the overwintering diapause to survive in unfavorable weather condition.

As the primary vector for WNV, *Culex pipiens/restuans* mosquitoes play the key role in transmission and spreading of WNV. Thus we focus on modeling the abundance and behaviors of the *Culex pipiens/restuans* mosquitoes in this dissertation.

1.3 Mosquito population models

For non-structured single species models, the most basic and famous model is the logistic growth population model, which is developed by Pierre-Francois Verhulst (Bacar 2011), and is rediscovered and popularized by Raymond Pearl and Lowell Reed (Pearl and Reed 1920). The delay is introduced to the logistic model by Hutchinson (1948). Much research has been done to extend the models and study their properties (Arino et al. 2006, Blythe et al. 1982, Cooke et al. 1999). For mosquito population model, Wan and Zhu (2014) formulate a new model with maturation delay for mosquito population incorporating the impact of blood meal resource for mosquito reproduction. They show the impact of blood meal resource in a given region determines the mosquito abundance and may induce Hopf bifurcation. The new model for mosquito also suggests that the resources for mosquito reproduction should not be ignored. These models are all great contributions to the modeling studies, but they lack the structure of mosquito population.

For the structured population models, Bernardelli (1941), Leslie (1945, 1948),

Lewis (1942) develop the age-structured matrix models independently. These models classify the population into discrete age classes and incorporate age-specific vital rates such as survival probability. Lefkovitch (1965) develops a stage-structured model for species whose life cycle can be divided into different stages. Moon (1976) develops a matrix model for the dynamics of *Culex tarsalis* mosquitoes. The model includes the life states through which the mosquito proceeds. The transition probabilities from one state (egg, larva, pupa, and adult) to another is derived in the study. These transition probabilities depend on the duration of stay and mortality in each state. A formula is derived for the expected number of mosquitoes alive at any time during the spring or summer. Focks et al. (1993) build a dynamic life table model for *Ades aegypti* which considered the effect of weather and. Ahumada et al. (2004) develop a matrix population model to study the *Culex quinquefasciatus* mosquito population along an elevational gradient on the Island of Hawaii. They study how the elevational gradients, rainfall, and temperature affect mosquito population. Their model predicts that mosquitoes at lower elevations can grow under a broader range of rainfall parameters than middle and high elevation populations. Schaeffer et al. (2008) develop a matrix mosquito population model for *Aedes (Stegomyia) africanus* and *Aedes (Diceromyia) furcifer (Diptera: Culicidae)* mosquitoes. The authors consider water availability in breeding sites as the primary environmen-

tal factor affecting the mosquito life cycle. The results show a good match between the simulated populations and the field data over the period considered. The works of Ahumada et al. (2004) and Schaeffer et al. (2008) are great contributions to mosquito abundance models. However, the above mosquito population models can not be used to model *Culex* mosquitoes in Southern Ontario since they do not consider the effect of mosquito overwintering diapause. Lončarić and Hackenberger (2013) present a stage and age structured mosquito population model including the effect of temperature, rainfall, photoperiod, and the flooding dynamics. Although hey also consider the overwintering diapause, they only assume that the mosquito population remains constant in overwintering diapause.

Additionally, there are some statistical studies about the relationship between mosquito abundance and environmental factors. DeGaetano (2004) uses a multiple linear regression model to explore the relationship between the monthly average adult mosquito (*Culex*) abundance and some meteorological factors. The factors including monthly average maximum, minimum and mean air temperature, total precipitation, maximum daily rainfall, etc. Pecoraro et al. (2007) discuss the climatic and landscape correlations for potential WNV mosquito vectors (including *Aedes vexanx*, *Anopheles punctipennis*, *Coquillettidia perturbans*, *Culex pipiens*, *Culex tarsalis* and *Culiseta inornata*) in the Seattle region by a multiple linear regression. They find

that the temperature and mosquito abundance are positively correlated, while precipitation is not strongly correlated. Trawinski and MacKay (2008) propose a time series analysis model to forecast WNV mosquito vector (*Aedes vexans* and *Culex pipiens/restuans*) populations in Erie County, New York. Their results indicate that the most significant meteorological variables for forecasting *Aedes vexans* abundance and *Cluex pipiens/restuans* abundance are different. Walsh et al. (2007) use a poisson regression to examine the effect of off-season factors (such as average maximum temperature, total heating degree-days). Their results suggest that some of the off-season factors can be used as predictive variables for mosquito abundance. Wang et al. (2011) apply a generalized linear model (GLM) to predict the abundance of *Culex* mosquitoes in Peel Region, they use daily weather data (temperature and precipitation) and weekly *Culex* mosquito surveillance data to fit the model.

1.4 WNV transmission models

Since the emergence of WNV in North America in 1999, much work has been done to model, analyze the transmission dynamics, and control the virus. The first epidemic model analyzing WNV transmission is presented by Thomas and Urena (2001) to investigate the interaction between the virus life cycle and the consequent effect on humans. Wonham et al. (2004) examine the WNV transmission between the

mosquito and bird population by using a system of differential equations. A similar model of WNV transmission between vector (mosquito) and the avian population is demonstrated by Cruz-Pacheco et al. (2005). They also estimate Basic Reproductive Number R_0 for several species of birds using experimental and field data. A theoretical frame work is presented by Kenkre et al. (2005) to analyze the epidemic of WNV. It also provides the mosquito diffusion and birds migration. C. Bowman and Zhu (2005) propose a single-season ordinary differential equation model which includes human population to assess control strategies against WNV. Lewis et al. (2006) utilize the reaction-diffusion equations and cooperative nature of cross-infection of WNV to study the existence of traveling wave solutions and estimated the spatial spread rate of the infection. Wan and Zhu (2010) study the backward bifurcation in some of the available compartment models for WNV, they conclude that the higher mortality rate of host birds due to infection determines the existence of backward bifurcation. The existence of backward bifurcation suggests that an endemic of the virus will depend on the initial population sizes of the vector and host. Different species of birds have different responses to the virus. For example, American crows suffer a higher mortality rate from the infection of the virus. Later on, Abdelrazec et al. (2013) establish and analyze a system of ordinary differential equations model by considering the avian species as corvids and non-corvids. They also discuss the

roles of corvids and non-corvids birds in the virus transmission.

1.5 Overview of the dissertation

We use both mathematical models and statistical models to study the impact of weather conditions on mosquito population and the transmission dynamics of WNV. We take an innovative approach to forecast mosquito abundance and WNV risk with real weather conditions. Moreover, we propose a matrix population model considering the mosquito overwintering diapause through dividing a year into two periods. We also develop a model for the mosquito population spatio-temporal distribution, and these novel models are the essential part to study WNV overwintering survival and spatial distribution. In addition, our models can be adopted to model other similar mosquito-borne disease such as Dengue fever and Zika.

In Chapter 1, we introduce the background of mosquito-borne diseases. We also describe the mosquito biology and impact of weather on mosquitoes abundance, mosquito biting preference,and virus transmission. We provide a survey on current mosquito abundance models and WNV transmission models.

Although compartmental models for WNV transmission can explain the WNV transmission mechanism very well, they usually assume mosquito population remains constant or grows with a constant recruiting rate. However, this assumption is not

suitable since the mosquito population is heavily affected by weather conditions. In Chapter 2, we first improve the statistical model in Wang et al. (2011), then we integrate the statistical model for mosquito abundance with an compartmental WNV transmission model. We also consider the effect of temperature and precipitation on the mosquito behaviors in the hybrid model. We estimate some parameters of the model and compare the effect of different weather patterns. Simulation results show that the hybrid model can capture the trend of the WNV human infection cases very well in Peel Region. The results also indicate that the impact of temperature is more significant than that of precipitation. This hybrid model is novel for modeling WNV transmission since it supply a better way of incorporating the daily weather conditions, therefore allow us to develop a forecasting capacity for mosquito abundance and risk of WNV.

In Peel Region of Ontario, Canada, the winter weather conditions cannot support the mosquito development. The mosquitoes have to go through the overwintering diapause to survive. Thus the overwintering diapause plays the key role in the survival of mosquitoes and WNV. In Chapter 3, we first divide the whole year into two periods, then we build a matrix mosquito population for each period considering the effect of temperature. We also analyze the theoretical properties of our model when the temperature is assumed to be a constant. Our simulation results show

that our model can capture the trend of mosquito surveillance data very well in Peel Region of Ontario.

It is important to model the spatial variation of mosquito population for each region. Some of the important factors for each trap may be missing or just unobservable. Missing factors may include land use conditions, elevation, humidity, and photoperiod at each trap. In Chapter 4, we study the spatio-temporal distribution of mosquito population by using a hidden dimension method to estimate the collective impact of all the unobservable information for each trap. The method is applied to mosquito surveillance data in Peel Region, Ontario, Canada. The simulation results demonstrate that the method significantly improves the modeling accuracy, and show a good match with the observed mosquito abundance data. We also derive the conditions when the mean square error (MSE) of GLM with missing information is smaller than that without missing information.

In Chapter 5, we will discuss the forecasting capacity of our models and present our practice of forecasting weekly average trapped mosquito abundance in Peel Region during summer weeks. By comparing with the observed mosquito abundance data, our model can provide a reasonable fit to the available data. We also forecast the WNV risk in Peel Region by using vector infection rate as the risk index. In Chapter 6, we conclude this dissertation and provide a discussion.

2 Weather driven hybrid model for the transmission of West Nile virus

2.1 Introduction

There have been extensive modeling studies of the virus since the emergence of WNV in North America (Abdelrazec et al. 2013, C. Bowman and Zhu 2005, Cruz-Pacheco et al. 2005, Kenkre et al. 2005, Lewis et al. 2006, Thomas and Urena 2001, Wan and Zhu 2010, Wonham et al. 2004). All of these modeling studies reveal some basic features of the WNV transmission, but these models ignore the effect of some important weather factors on the mosquito population and transmission of WNV.

Mosquito abundance and biting behaviors are considerably affected by weather conditions, including temperature, precipitation, day length, and etc. These weather factors also have an impact on the transmission of WNV (Dohm et al. 2002). For adult mosquitoes, environmental conditions also have an impact on mortality rate

and biting behaviors (Reisen et al. 1992b, Rubel et al. 2008).

Many statistical models have been used to study the relationship between mosquito abundance and environmental factors, such as temperature, rainfall, humidity, etc. Some of them focus on finding the most significant weather factors (Pecoraro et al. 2007, Trawinski and MacKay 2008), and some of the models using larger time scales (one month) for the impact of weather (DeGaetano 2004, Walsh et al. 2007). These statistical models show the importance of understanding how weather conditions affect the count of mosquitoes. However, we cannot use these models in our study since we need a model that can fit and predict the *Culex* mosquito surveillance data. Wang et al. (2011) apply a generalized linear model to predict the abundance of *Culex* mosquitoes (the primary WNV vector in Ontario) in Peel Region. Their model reaches a reasonable accuracy, thus we introduce and modify their model.

In this chapter, we build a hybrid model to study the WNV transmission dynamics considering the effect of temperature and precipitation. The hybrid model consists of a statistical model for the abundance of *Culex* mosquitoes and a compartmental model for WNV transmission between mosquito, bird, and human. We also incorporate the weather effect on mosquito mortality rate, mosquito biting preference, and mosquito biting rate in our model.

This chapter is organized as the following. We introduce the mosquito surveillance

data and the statistical model for *Culex* mosquito abundance model in Section 2.2. In Section 2.3, we introduce a compartmental model for WNV transmission without weather effect. Then we show the hybrid model integrating the statistical model for *Culex* mosquito abundance and the compartmental model in Section 2.4. In Section 2.5, we estimate the unknown parameters and show simulation results under different weather patterns. We provide a brief conclusion and a short discussion in Section 2.6.

2.2 Mosquito surveillance data and the model of the *Culex* mosquito abundance with weather conditions

Our mosquito data come from the mosquito surveillance program which is initiated in Ontario in 2001 by the Ontario Ministry of Health and Long-Term Care. There are 31 permanent, fixed monitoring traps in Peel Region, Ontario. Mosquitoes are collected weekly on Tuesdays or Wednesdays from mid-June to early October. Then the trapped mosquitoes are brought to the laboratory where they are identified to species level and tested for WNV. The average *Culex* mosquito trap count in Peel Region from 2003 to 2010 are shown in Figure 2.1.

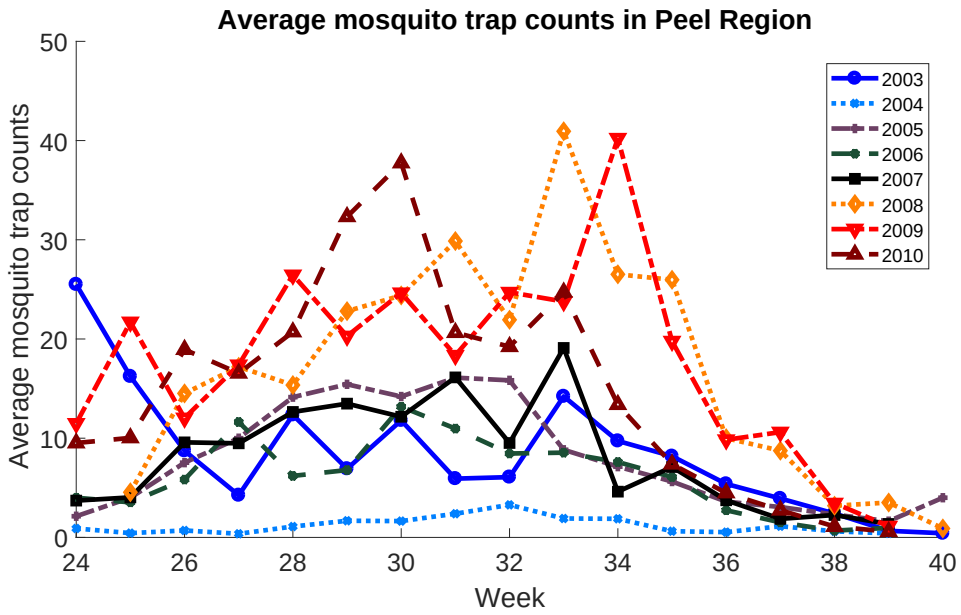

Figure 2.1: Average mosquito trap counts in Peel Region from 2003 to 2010.

Wang et al. (2011) use a generalized linear model with temperature and precipitation for the weekly forecasting of the *Culex* mosquito abundance. In their model, they use the growing degree-days to trace the effect of the daily average temperature on *Culex* mosquito abundance. Following the notations in Wang et al. (2011), the growing degree-days dd is defined as following:

$$dd = \begin{cases} 0°C, & \text{if } T_m \leq 9°C, \\ T_m - 9°C, & \text{if } T_m > 9°C, \end{cases} \tag{2.1}$$

where T_m is daily mean temperature, $9°C$ is the baseline temperature. Below $9°C$, immature *Culex* mosquitoes development will stop or become much slower (Wang

et al. 2011). The generalized linear model in Wang et al. (2011) has the following form,

$$\begin{aligned} E(y) &= \mu, \\ g(\mu) &= log(\mu) = \eta, \\ \eta &= \beta_0 + \beta_1(ddm)^2 + \beta_2 ddm + \beta_3(ppm)^2 + \beta_4 ppm, \end{aligned} \tag{2.2}$$

where y is arithmetic mean of mosquito count per trap night in Peel Region. The y is assumed to follow gamma distribution in Wang et al. (2011), so we have $y \sim Gamma(\alpha, \beta)$. The expectation of y is $E(y) = \mu$. The linear predictor is η which is related to the expected value μ through the link function $g(\mu) = log(\mu)$. Here ddm is the arithmetic mean of daily dd and ppm is the arithmetic mean of daily precipitation.

With the surveillance data for *Culex* mosquito trap counts in Peel Region from 2002 to 2008, they find that the arithmetic means of daily dd from 11 days before each collection ($ddm^{[11]}$) and arithmetic means of daily precipitation from 35 days before each collection ($ppm^{[35]}$) have the most significant impact on the mosquito count.

Temperature and precipitation also have the interactive effect on mosquito population (Alto and Juliano 2001), so we add the term $ddm * ppm$ and get the modified

model as following,

$$\begin{aligned} &E(y) = \mu, \\ &g(\mu) = log(\mu) = \eta, \\ &\eta = \beta_0 + \beta_1 (ddm)^2 + \beta_2 ddm + \beta_3 (ppm)^2 + \beta_4 ppm + \beta_5 ddm * ppm. \end{aligned} \tag{2.3}$$

We apply model (2.3) for *Culex* mosquito trap count in Peel Region from 2002 to 2012 and find that $ddm^{[10]}$ and $ppm^{[42]}$ have the most significant impact on mosquito count. Therefore we use $ddm^{[10]}$ and $ppm^{[42]}$.

Although the mosquito larviciding treatment was conducted in urban and suburban areas of Peel Region during summer time, the effect of larviciding can be ignored since it does not affect the effective trapping zone of the traps in the mosquito surveillance program in Peel Region. Therefore we will not consider the effect of larviciding and other incidental adult mosquito control from the local population.

Let $\overline{N}_M(t)$ be the average *Culex* mosquito trap count in Peel Region on day t, we have

$$\begin{aligned} ln(\overline{N}_M(t)) =& \beta_0 + \beta_1 (ddm_t^{[10]})^2 + \beta_2 ddm^{[10]} + \beta_3 (ppm_t^{[42]})^2 + \beta_4 ppm_t^{[42]} \\ &+ \beta_5 ddm_t^{[10]} * ppm_t^{[42]}, \end{aligned} \tag{2.4}$$

where

$$ddm_t^{[10]} = \frac{1}{10} \sum_{i=1}^{10} dd_{t-i}, \tag{2.5}$$

$$ppm_t^{[42]} = \frac{1}{42}\sum_{i=1}^{42} pp_{t-i}, \tag{2.6}$$

dd_t is growing degree-day on day t and pp_t is precipitation on day t. The value of estimated coefficients (β_0, β_1, β_2, β_3, β_4, and β_5) used in the model (2.4) are shown in Table 2.1. The coefficients were estimated by iterative weighted least squares method through *glmfit* function in MATLAB.

Coefficients	Value
β_0	-2.8048
β_1	-0.0124
β_2	0.5105
β_3	-0.0614
β_4	1.0005
β_5	-0.0353

Table 2.1: Estimated coefficients of model (2.4).

As one example, observed *Culex* mosquito average trap count and predicted *Culex* mosquito average trap count by model (2.4) in Peel Region in year 2011 are shown in Figure 2.2.

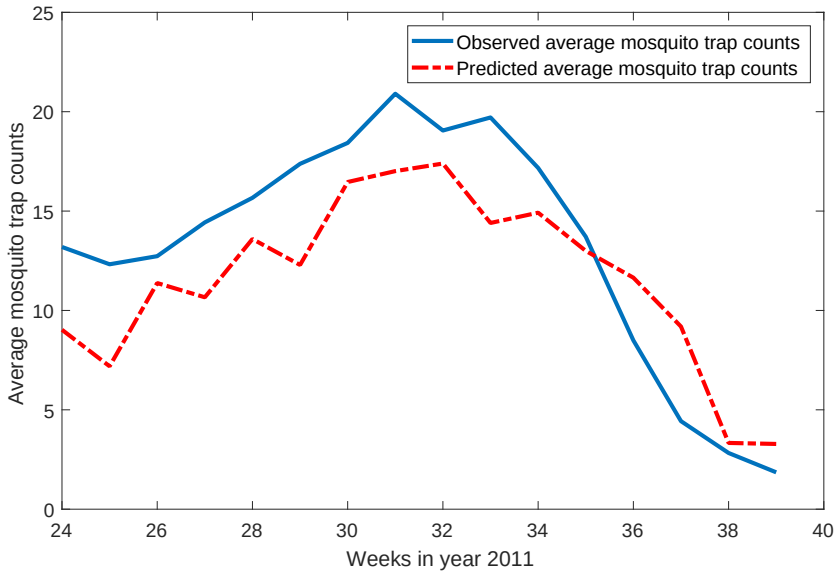

Figure 2.2: Observed *Culex* mosquito average trap counts and predicted *Culex* mosquito average trap counts in Peel Region in 2011.

Usually, the CDC light trap counts of *Culex* mosquitoes from the surveillance program can serve as a reflection of abundance of mosquitoes in the surrounding area of a trap. But for the modeling purpose we need to estimate the total number of mosquitoes in the area. We use $\overline{N}_M(t)$ from model (2.4) to estimate the total number of *Culex* mosquitoes $N_M(t)$ in Peel Region. Let ss_1 be the trap effective area and ss_0 be the area of Peel Region. We define the mosquito trap efficiency $\omega(T_t, P_t)$ as the portion of captured mosquito to the total number of mosquito in the trap effective area (T_t is the daily mean temperature on day t and P_t is the

precipitation on day t). So we have the following relationship,

$$\frac{N_M(t)}{ss_0}\omega(T_t, P_t) = \frac{\overline{N}_M(t)}{ss_1}. \tag{2.7}$$

When the temperature and precipitation are suitable for seeking of blood meals of mosquitoes, more mosquitoes can then be tapped, the proportional constant also depends on the weather conditions. If we let $\omega(T_t, P_t)$.be the constant depending on the daily temperature and precipitation, then we can have

$$N_M(t) = \frac{ss_0}{ss_1}\frac{1}{\omega(T_t, P_t)}\overline{N}_M(t). \tag{2.8}$$

2.3 The WNV epidemic model without impact of weather

We adopt the models of Bowman et al. (2005), Wonham et al. (2004) and Fan et al. (2010) to incorporate the effect of temperature and precipitation on the transmission of WNV. However, we first look at the model without considering weather conditions.

There are two health states for mosquitoes, which includes susceptible mosquitoes $M_s(t)$ and infected mosquitoes $M_i(t)$. The total number of mosquitoes is denoted by $N_M(t) = M_s(t) + M_i(t)$. There are three compartments for birds including susceptible birds $B_s(t)$, infected birds $B_i(t)$, and recovered birds $B_r(t)$. The total bird population is $N_B(t) = B_s(t) + B_i(t) + B_r(t)$. For human population, we consider three compartments which are susceptible humans $H_s(t)$, infected humans $H_i(t)$, and

recovered humans $H_r(t)$. Let $N_H(t) = H_s(t) + H_i(t) + H_r(t)$ be the total number of human population. Based on the available models (Bowman et al. 2005, Fan et al. 2010, Wonham et al. 2004), if we do not consider the impact of weather and ignore human demographics and death due to WNV infection, we can have the following model,

$$\begin{cases} \frac{dM_s(t)}{dt} &= r_m(N_M(t))N_M(t) - \frac{\kappa\beta_m M_s(t)B_i(t)}{N_B(t)+N_H(t)} - d_m M_s(t), \\ \frac{dM_i(t)}{dt} &= \frac{\kappa\beta_m M_s(t)B_i(t)}{N_B(t)+N_H(t)} - d_m M_i(t), \\ \frac{dB_s(t)}{dt} &= -\frac{\kappa\beta_b M_i(t)B_s(t)}{N_B(t)+N_H(t)}, \\ \frac{dB_i(t)}{dt} &= \frac{\kappa\beta_b M_i(t)B_s(t)}{N_B(t)+N_H(t)} - (\mu_b + v_b)B_i(t), \\ \frac{dB_r(t)}{dt} &= v_b B_i(t), \\ \frac{dH_s(t)}{dt} &= -\frac{\kappa\beta_h M_i(t)H_s(t)}{N_B(t)+N_H(t)}, \\ \frac{dH_i(t)}{dt} &= \frac{\kappa\beta_h M_i(t)H_s(t)}{N_B(t)+N_H(t)} - v_h H_i(t), \\ \frac{dH_r(t)}{dt} &= v_h H_i(t). \end{cases} \tag{2.9}$$

Comparing with the models in Bowman et al. (2005), Fan et al. (2010), here $r_m(N_M(t))$ is the mosquito per capita reproduction rate which is a function of the total number of adult mosquitoes $N_M(t)$. Usually people assume the reproduction function satisfy the following conditions (Cooke et al. 1999):

- $r_m(N_M) > 0$;
- $r_m(N_M)$ is continuously differentiable with $r'_m(N_M) < 0$; (2.10)

- $r_m(0^+) > d_m > r_m(\infty)$,

where d_m is natural death rate of mosquito.

From the first two equations of model (2.9), we have the total mosquito population satisfies

$$\frac{dN_M(t)}{dt} = r_m(N_M(t))N_M(t) - d_m N_M(t). \tag{2.11}$$

The nontrivial solutions of model 2.11 approach $r_m^{-1}(d_m)$ as $t \to \infty$ when $r_m(N_M(t))$ satisfies the conditions 2.10. An example is shown in Figure 2.3.

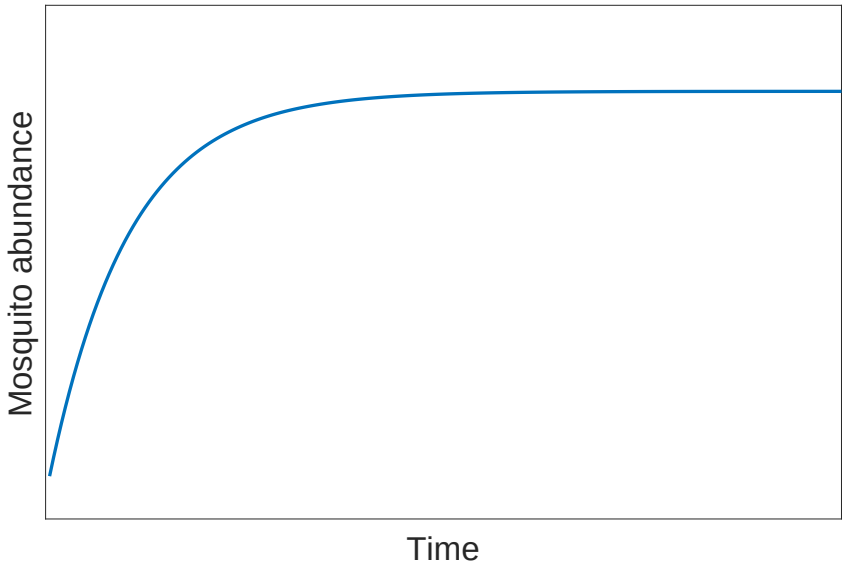

Figure 2.3: Mosquito abundance under model (2.11).

However, there is a peak in the surveillance data shown in Figure 2.1. In addition, depending on the weather conditions of each year, the peak value and peak time of

average mosquito count data vary, thus the mosquito population in model (2.11) can not capture the real surveillance data. This leads us to employ the statistical mosquito population model to describe the mosquito population.

For host birds, without the presence of WNV or other avian diseases, the total population of birds in one area is assumed to be constant in our study as the natural birth and death are balanced without the virus (Fan et al. 2010).

We also assume that in a region like Peel, the total human population remains constant in one mosquito season, the mosquito season usually is from middle of June to the end of September.

For other parameters, we have μ_b as the WNV induced per capita mortality rate of birds. Let κ be the mosquito biting rate per unit of time. Suppose β_m is the transmission probability from birds to mosquitoes per mosquito bite. Assume β_b is the WNV transmission probability from mosquitoes to birds bite by infectious mosquitoes and β_h is the WNV transmission probability from mosquitoes to humans per bite by infectious mosquitoes. Let ν_b and ν_h represent the per capita recovery rate of infected birds and humans, respectively. The time unit in this study is day. These parameters are summarized in Table 2.2.

Parameter	Description	Mean (range)	Source
β_m	WNV transmission probability from birds to mosquitoes	$0.69\ (0.23 - 1)$	Wonham et al. (2006)
β_b	WNV transmission probability from mosquitoes to birds	$0.88\ (0.80 - 1.00)$	Wonham et al. (2004)
β_h	WNV transmission probability from mosquitoes to humans	0.88	C. Bowman and Zhu (2005)
κ	mosquito biting rate per unit of time	$0.09\ (0.03 - 1.16)$	Wonham et al. (2004)
μ_b	WNV induced per capita mortality rate of birds	$0.143\ (0.125 - 0.200)$	Wonham et al. (2004)
ν_b	per capita recovery rate of infected birds	$0.15\ (0.01 - 0.3)$	Abdelrazec et al. (2013), Komar et al. (2003)
ν_h	per capita recovery rate of infected humans	0.17	Bowman et al. (2005)
d_m	adult per capita mosquito mortality rate	$0.029\ (0.016 - 0.07)$	Wonham et al. (2004)

Table 2.2: Parameters used in model (2.9).

For compartmental models of disease transmission, the basic reproduction number R_0 measures the expected number of secondary cases produced, in a completely

susceptible population, by a typical infected individual during its entire period of infectiousness (Diekmann et al. 1990). This number is a measurement of the infection power of the virus in both the host and vector population.

In equation 2.3, solving $r_m(N_M(t))N_M(t) - d_m N_M(t) = 0$ gives the equilibrium solution. Based on the conditions of the reproduction function stated above in (2.10), it is not difficult to conclude that $r_m(N_M) = d_m$ has a unique positive solution, and we denote it as N_M^*. The total number of human population is a constant N_H^*. Some of the dynamical modeling studies directly or indirectly assume that the total mosquito population remains constant (Cruz-Pacheco et al. 2005). When the total mosquitoes remains constant in the compartmental system, we then have a reduced model (2.9) as following,

$$\begin{aligned}
\frac{dM_i(t)}{dt} &= \frac{\kappa\beta_m(N_M^* - M_i(t))B_i(t)}{N_B(t) + N_H^*} - d_m M_i(t),\\
\frac{dB_s(t)}{dt} &= -\frac{\kappa\beta_b M_i(t)B_s(t)}{N_B(t) + N_H^*},\\
\frac{dB_i(t)}{dt} &= \frac{\kappa\beta_b M_i(t)B_s(t)}{N_B(t) + N_H^*} - (\mu_b + v_b)B_i(t),\\
\frac{dB_r(t)}{dt} &= v_b B_i(t),\\
\frac{dH_i(t)}{dt} &= \frac{\kappa\beta_h M_i(t)(N_H^* - H_i(t) - H_r(t))}{N_B(t) + N_H^*} - v_h H_i(t),\\
\frac{dH_r(t)}{dt} &= v_h H_i(t).
\end{aligned} \tag{2.12}$$

It is not difficult to verify that model (2.12) has a disease-free equilibrium (DFE).

We obtain the following by letting its right-hand side be zero,

$$E_0 :(M_i^*, B_s^*, B_i^*, B_r^*, H_i^*, H_r^*) = (0, B_s^*, 0, B_r^*, 0, H_r^*), \tag{2.13}$$

where B_s^*, B_r^* and H_r^* are any positive constants and $N_b^* = B_s^* + B_r^*$ is the initial total number of birds. Note that model (2.12) has an infinite number of equilibria defined by the initial state of the model.

To calculate the basic reproduction number R_0, we follow van den Driessche and Watmough (2002). We use vector notation to rewrite the equations. The infections appear in terms of the difference between the rate of appearance of new infections and the rate of transfer out by all other processes,

$$\frac{d}{dt}\begin{bmatrix} M_i(t) \\ B_i(t) \\ H_i(t) \end{bmatrix} = f - v = \begin{bmatrix} \frac{\kappa\beta_m(N_M^* - M_i(t))B_i(t)}{N_B(t)+N_H^*} \\ \frac{\kappa\beta_b M_i(t)B_s(t)}{N_B(t)+N_H^*} \\ \frac{\kappa\beta_h M_i(t)(N_H^* - H_i(t) - H_r(t))}{N_B(t)+N_H^*} \end{bmatrix} - \begin{bmatrix} d_m M_i(t) \\ (\mu_b + v_b)B_i(t) \\ v_h H_i(t) \end{bmatrix}, \tag{2.14}$$

the corresponding Jacobian matrices, $\mathcal{F}$ and $\mathcal{V}$, describe the linearization of this reduced system about the DFE,

$$\mathcal{F} = \begin{bmatrix} 0 & \frac{\kappa\beta_m N_M^*}{N_B^*+N_H^*} & 0 \\ \frac{\kappa\beta_b B_s^*}{N_B^*+N_H^*} & 0 & 0 \\ \frac{\kappa\beta_h(N_H^* - H_r^*)}{N_B^*+N_H^*} & 0 & 0 \end{bmatrix}, \mathcal{V} = \begin{bmatrix} d_m & 0 & 0 \\ 0 & \mu_b + \nu_b & 0 \\ 0 & 0 & \nu_h \end{bmatrix}, \tag{2.15}$$

and R_0 is the dominant eigenvalue of $\mathcal{F}\mathcal{V}^{-1}$ (van den Driessche and Watmough 2002):

$$R_0 = \sqrt{\frac{\kappa^2 \beta_m \beta_b M_s^* B_s^*}{(N_B^* + N_H^*)^2(\mu_b + \nu_b) d_m}} = \sqrt{\frac{\kappa \beta_m M_s^*}{(\mu_b + \nu_b)(N_B^* + N_H^*)} \frac{\kappa \beta_b B_s^*}{d_m (N_B^* + N_H^*)}}. \quad (2.16)$$

One can verify that in model (2.9), depending on the initial state and other transmission related parameters, the disease free equilibrium E_0 is locally asymptotically stable if $R_0 < 1$, and unstable if $R_0 > 1$.

From the expression (2.16) for R_0 near the DFE, each infective bird produces $\frac{\kappa \beta_m M_s^*}{(\mu_b + \nu_b)(N_B^* + N_H^*)}$ infectious mosquitoes over its expected infectious period. Similarly, each virus carrying mosquito produces $\frac{\kappa \beta_b B_s^*}{(N_B^* + N_H^*) d_m}$ new infected birds over its expected infectious period. The geometric mean gives the expected number of new infections that a single infective (mosquito or bird) can produce when introduced into a susceptible population. Note that as humans are dead-end hosts, it affects R_0 through the total number of human population N_H^* which share the biting of mosquitoes with other hosts.

2.4 Hybrid model for WNV transmission

Before we integrate the statistical model for *Culex* mosquito abundance and the compartmental model for WNV transmission. We consider the effect of mosquito biting preference and effect of weather conditions on mosquito biting rate and mortality rate.

2.4.1 Mosquito biting preference

Besides birds and humans, *Culex* mosquitoes also feed on non-human mammals such as horses, dogs, cats, squirrels, deer, and etc. These non-human mammals hosts divert infectious mosquitoes away from humans (Hamer et al. 2009), and therefore reduce the risk of human infection. For almost all the available compartmental models for the transmission of WNV, a major assumption is that mosquitoes have no host feeding preference and express opportunistic feeding behavior (Bowman et al. 2005, Thomas and Urena 2001, Wonham et al. 2004). We only consider three types of hosts including birds, humans and non-human mammals. If we denote $N_A(t)$ as the total number of non-human mammals at time t, one way to split the number of mosquito bites on birds, humans and non-human mammals would be $N_B(t) : N_H(t) : N_A(t)$ proportionally. However, many studies have shown that *Culex* do have host seeking and biting preference, which means that *Culex* would feed preferentially on selected hosts (Hamer et al. 2009, Kilpatrick et al. 2006, Lura et al. 2012, Rizzoli et al. 2015).

In the studies of modeling the predator-prey interactions, the similar problem to mosquito host feeding preference is called selective predation. It occurs when the relative frequencies of prey types in a predator's diet differ from the relative frequencies in the environment (Chesson 1978). Based on the study of Murdoch

(1969), Manly (1974) suggest a model to describe the probability of individuals being selected one-by-one from a population consisting of two or more different classes of individuals. The probability that next individual is chosen from the ith class is

$$p_i n_i / \sum_{j=1}^{J} p_j n_j, \qquad i = 1, 2, \cdots, J, \tag{2.17}$$

where the population contains n_j individuals in the jth class ($j = 1, 2, \cdots, J$), p_i is the probability that an individual is selected from the ith class when the selection process has a choice of an equal number of individuals in each of the J classes.

Sota and Mogi (1989) also develop a similar model for *Culex* mosquito biting preference. Based on the findings of Manly (1974) and Sota and Mogi (1989), we assume that for each mosquito bite, the probability of biting birds, human and non-human mammals are p_1, p_2 and p_3 respectively when there are equal number of birds, human and non-human mammals, and we have $p_1 + p_2 + p_3 = 1$. The distribution of the feeding probability (preference) on birds, human and non-human mammals becomes $p_1 N_B(t) : p_2 N_H(t) : p_3 N_A$.

2.4.2 Effect of temperature and precipitation on mosquito daily mortality rate and biting rate

The adult mosquito daily mortality rate is affected by both temperature and precipitation (Brady et al. 2013, Jones et al. 2012a, Reisen 1995, Rubel et al. 2008, Yang et al. 2009). We denote it as $d_m(T, P)$, where T is the daily mean temperature with unit C° and P is daily precipitation with unit millimeter (mm) per day. We assume the effects of temperature and precipitation on $d_m(T, P)$ are independent. We first introduce the temperature dependent mosquito mortality rate. Then we introduce the impact of precipitation on adult mosquito survival rate. Finally, we get the mosquito mortality rate based on temperature and precipitation.

In many studies about the relationship between adult mosquito mortality rate and temperature (Brady et al. 2013, Rubel et al. 2008, Yang et al. 2009), we observe that the mortality is high when the temperature is high or low while a medium temperature would lead to low mortality rate. So for adult mosquitoes, we assume that there is an optimal temperature T_{opt} at which the mosquitoes have the lowest mortality rate. Mortality rate will increase when temperature is above T_{opt} or lower than T_{opt}. Based on the above assumption, in a suitable range of temperature $[T_{min},\ T_{max}]$, the simplest form of the temperature dependent mosquito mortality rate can be written as following,

$$f_1(T) = a_1(T - T_{opt})^2 + a_0, \tag{2.18}$$

where a_0 and a_1 are constant parameters, T_{opt} is the optimal temperature for adult female mosquitoes to survive.

Besides temperature, another weather factor that affects mosquito surviving and biting behavior is precipitation (rainfall) (Dickerson et al. 2012, Jones et al. 2012a). We denote *Culex* mosquito daily survival rate as $s_m(T, P)$, $s_m(T, P) = 1 - d_m(T, P)$. Since the effects of temperature and precipitation on survival rate are independent, we have $s_m(T, P) = f_2(T)g_2(P)$, where $f_2(T)$ is the adult mosquito daily survival rate based on temperature ($f_2(T) = 1 - f_1(T)$). And $g_2(P)$ is the effect of precipitation on adult mosquito daily survival rate. Jones et al. (2012a) indicate that mosquito daily survival rate is negatively affected by rainfall, and their results suggest that $g_2(P) = exp(-\alpha P)$. The daily survival rate can be close to 0 if daily precipitation P is large enough based on the results of Jones et al. (2012a).

However, Dickerson et al. (2012) show that heavy falling rain cannot kill a flying mosquito. They performed raindrop impact experiments on mosquitoes, and they found that the mosquito is so lightweight that the resulting force imparted upon it is low, this enables a mosquito to survive flying in the rain. Mosquitoes may experience life-threatening impacts only when flying very low to the ground.

Based on the experiments conducted by Dickerson et al. (2012), we can get the conclusion that the effect of rainfall on adult mosquito daily survival rate should be small and therefore $g_2(P)$ should be close to 1, which is contrary to the results of Jones et al. (2012a).

To combine the results of Jones et al. (2012a) and Dickerson et al. (2012), we introduce parameter C_1, $0 \leq C_p \leq 1$. We get a new rainfall effect on mosquito daily survival rate $g_2^*(P)$ as following,

$$g_2^*(P) = (1 - C_1)exp(-\alpha P) + C_1. \tag{2.19}$$

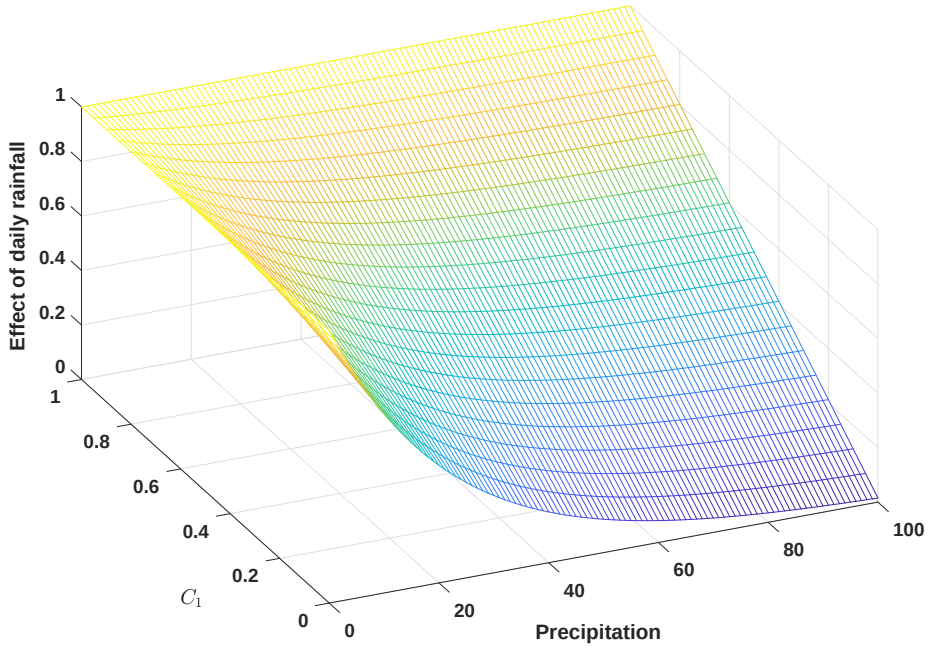

Figure 2.4: Effect of rainfall on mosquito survival rate with different C_1.

Figure 2.4 shows the effect of rainfall $g_2^*(P)$ with different values of P. When $C_1 = 0$, $g_2^*(P) = g_2(P) = exp(-\alpha P)$, $g_2^*(P)$ becomes the effect defined by Jones et al. (2012a). When $C_1 = 1$, $g_2^*(P) = 1$, $g_2^*(P)$ becomes the effect found by Dickerson et al. (2012), which is that a flying mosquito can not be killed by the falling rain (no effect). When $0 < C_1 < 1$, $g_2^*(P)$ is a combination of the results of Jones et al. (2012a) and Dickerson et al. (2012). So we have

$$\begin{aligned} s_m(T,P) &= f_2(T)g_2^*(P) \\ &= (1 - f_1(T)) * ((1 - C_1)exp(-\alpha P) + C_1) \\ &= (1 - (a_1(T - T_{opt})^2 + a_0)) * ((1 - C_1)exp(-\alpha P) + C_1), \end{aligned}$$

and

$$\begin{aligned} d_m(T,P) &= 1 - s(T,P) \\ &= 1 - (1 - (a_1(T - T_{opt})^2 + a_0)) * ((1 - C_1)exp(-\alpha P) + C_1). \end{aligned}$$

Figure 2.5 shows the effects of temperature and precipitation on daily mortality rate of adult mosquitoes.

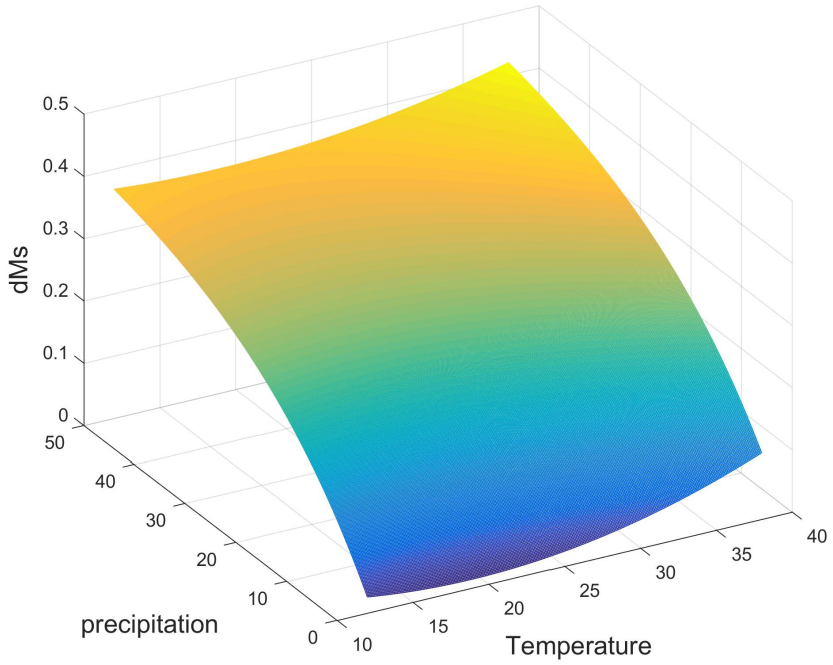

Figure 2.5: The effects of temperature and precipitation on daily adult mosquito mortality rate.

We also assume the effects of temperature and rainfall on the biting rate of adult mosquito are independent. Let $\kappa(T, P) = f_3(T)g_3(P)$, where $f_3(T)$ is the adult mosquito biting rate based on temperature, and $g_3(P)$ is the effect of rainfall on mosquito biting rate. The temperature dependent biting rate is used by Reisen et al. (1992b) and Rubel et al. (2008), where they fit the biting rate to the reciprocal of

the duration of the mosquito gonotrophic cycle, which is given as

$$f_3(T) = \frac{0.344}{1 + 1.231 \exp(-0.184(T - 20))}. \tag{2.20}$$

Considering rainfall can affect mosquito flight (Dickerson et al. 2012) and therefore reduce the host seeking ability of mosquito, we assume rainfall has an adverse effect on mosquito biting rate. We assume $g_3(P)$ is similar to $g_2^*(T, P)$, but with a different limit C_2, so we can have $g_3(P) = (1 - C_2)exp(-\alpha P) + C_2$, and we get

$$\kappa(T, P) = \frac{0.344}{1 + 1.231 exp(-0.184(T - 20))}((1 - C_2)exp(-\alpha P) + C_2). \tag{2.21}$$

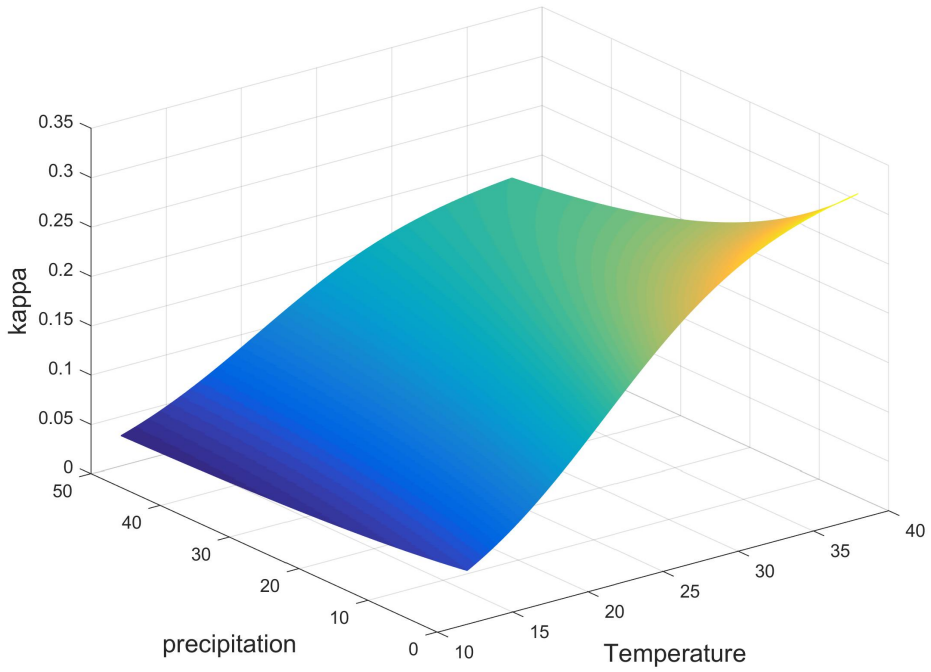

Figure 2.6: The effects of temperature and precipitation on mosquito biting rate.

Figure 2.6 shows the effects of temperature and precipitation on mosquito biting rate.

For the total number of mosquitoes $N_M(t)$ in Peel Region. Reisen et al. (1992a, 1991) present that the range of $Culex$ mosquito flight distance per day is from 0.6 km to 1 km. In the study of Tsuda et al. (2008), they show that $Culex$ mosquitoes can travel $470m$ on average for one day. Assume $Culex$ mosquito flight distance per day is dr, so the trap effective area is $ss_1 = \pi(dr)^2\ km^2$. From the 2011 Canadian Census (Canada 2012), the area of Peel Region ss_0 is 1254 km^2, so we let $\gamma = \frac{ss_0}{ss_1} = \frac{1254}{\pi(dr)^2}$. We will estimate γ as an parameter in the following section. We have

$$N_M(t) = \frac{ss_0}{ss_1}\frac{1}{\omega(T,P)}\overline{N}_M(t) = \frac{\gamma}{\omega(T,P)}\overline{N}_M(t). \tag{2.22}$$

For the mosquito trap efficiency ω in equation (2.8), we use similar effects of temperature and precipitation on the biting rate $\kappa(T,P)$ since the biting rate can be treated as a measurement of mosquito activeness. Many studies have shown that the overall recapture rate is about 0.01 (Ciota et al. 2012, Tsuda et al. 2008). Thus we assume that ω is in the range $(0.009, 0.011)$, and modify $\kappa(T,P)$ to get the following results,

$$\omega(T,P) = 0.009 + \frac{0.002}{1 + 1.231exp(-0.184(T-20))}((1-C_2)exp(-\alpha P) + C_2). \tag{2.23}$$

Based on above discussion, we adapt model (2.12) and get the following model,

$$\begin{aligned}
\frac{dM_i(t)}{dt} &= \frac{\kappa(T_t,P_t)\beta_m(N_M(t)-M_i(t))p_1B_i(t)}{p_1N_B(t)+p_2N_H^*+p_3N_A} - d_m(T_t,P_t)M_i(t),\\
\frac{dB_s(t)}{dt} &= -\frac{\kappa(T_t,P_t)\beta_bM_i(t)p_1B_s(t)}{p_1N_B(t)+p_2N_H^*+p_3N_A},\\
\frac{dB_i(t)}{dt} &= \frac{\kappa(T_t,P_t)\beta_bM_i(t)p_1B_s(t)}{p_1N_B(t)+p_2N_H^*+p_3N_A} - (\mu_b+v_b)B_i(t),\\
\frac{dB_r(t)}{dt} &= v_bB_i(t),\\
\frac{dH_i(t)}{dt} &= \frac{\kappa(T_t,P_t)\beta_hM_i(t)p_2(N_H^*-H_i(t)-H_r(t))}{p_1N_B(t)+p_2N_H^*+p_3N_A} - v_hH_i(t),\\
\frac{dH_r(t)}{dt} &= v_hH_i(t).
\end{aligned} \tag{2.24}$$

2.5 Parameter estimation and numerical simulations

In this section, we first give the details about initial conditions of our model and estimate the unknown parameters by grid search algorithm. Then we show the impact of different weather patterns on our model.

2.5.1 Initial conditions

The mosquito surveillance program in Peel Region usually starts from week 24 and finishes at week 40 of each year, so the statistical model for *Culex* mosquito abundance is accuracy in this period. Our model simulation period should be the similar range. Therefore our model simulation starts from June 1 each year and ends on

October 15 each year.

Culex mosquito abundance $N_M(t)$ in our model (2.24) is from equation (2.22), and $\overline{N}_M(t)$ in equation (2.22) is from equation (2.4). The initial number of infected *Culex* mosquito is still unknown. Although here may be some mosquitoes which get the WNV from vertical transmission, the portion of vertical transmission is very small. We are interested in the effects of different weather patterns on the WNV transmission, thus we assume that there is a very small portion of *Culex* mosquitoes ($M_i(1) = 2000$, about 0.01% to 0.1% of the total mosquito population) get infected at the beginning of our model simulation.

Based upon the average bird density in Ontario being $657/100ha$ ($1ha = 0.01$ km^2) (Kennedy et al. 1999), we estimate that the total number of birds in Peel Region is $N_B(1) = 657*1254 = 823878$. Furthermore, assuming 0.01% infected birds existing at the beginning of each mosquito season (June), we have $B_s(1) = 0.9999 * N_B(1)$, $B_i(1) = 0.0001 * N_B(1)$ and $B_r(1) = 0$.

Based on the population in Peel region (Canada 2011 Census) and assumption that no human gets infected at the beginning of each mosquito season, we get $H_s(1) = 1296814$, $H_i(1) = 0$ and $H_r(1) = 0$.

2.5.2 Parameter estimation

Although we can find most of our parameters in the model through references, there are still a few parameters that we cannot find in the references. We need to decide the values of the unknown parameters.

Since the reported human case is a portion of the total infected human case, we focus on making our modeled $H_i(t)$ fit the trend of reported human cases. We use Pearson correlation coefficient (Pearson 1896) as the measurement of our model. It is a measure of the dependence between two variables. We assume $\tilde{H}_i(t_j)$ as the number of reported human cases at time t_j, $1 \leq j \leq n$ (suppose we have n records of human cases reported). We can have our target function defined as the correlation coefficient of $H_i(t)$ and $\tilde{H}_i(t_j)$, which is defined as following:

$$\rho(H_i, \widetilde{H}_i) = \frac{\sum_{j=1}^{n}(H_i(t_j) - \overline{H}_i)(\widetilde{H}_i(t_j) - \overline{\widetilde{H}}_i)}{\sqrt{\sum_{j=1}^{n}(H_i(t_j) - \overline{H}_i)^2}\sqrt{\sum_{j=1}^{n}(\widetilde{H}_i(t_j) - \overline{\widetilde{H}}_i)^2}}, \tag{2.25}$$

where

$$\overline{H}_i = \frac{1}{n}\sum_{j=1}^{n} H_i(t_j), \tag{2.26}$$

$$\overline{\widetilde{H}}_i = \frac{1}{n}\sum_{j=1}^{n} \widetilde{H}_i(t_j). \tag{2.27}$$

Denote θ to be the unknown parameter set in model 2.24, then the modeled human infections $H_i(t)$ is depended on θ and we can write it as $H_i(t|\theta)$. We have the estimated unknown parameters as $\hat{\theta}$ which maximize the $\rho(H_i(t|\theta), \widetilde{H_i})$,

$$\hat{\theta} = \arg\max_{\theta} \rho(H_i(t|\theta), \widetilde{H_i}). \tag{2.28}$$

We estimate parameters through the grid search algorithm used in Gong et al. (2010). We first set the range and search step size for each unknown parameter. Then for each combination of the possible unknown parameters we get a set of parameter values, we run our model based on each set of possible parameters and record the associated $\rho(H_i(t|\theta), \widetilde{H_i})$. Our estimated parameters $\hat{\theta}$ is the corresponding set of the parameters which maximize $\rho(H_i(t|\theta), \widetilde{H_i})$.

As in our model, we have $\theta = (p_1,\ p_2,\ C_1,\ C_2,\ \gamma)$ with $p_3 = 1 - p_1 - p_2$, $p_1 > 0$, $p_2 > 0$, $p_3 > 0$. The possible range of $C_1,\ C_2$ and γ are $0 \leq C_1 \leq 1$, $0 \leq C_2 \leq 1$ and $1500 \leq \gamma \leq 3500$. Since *Culex* mosquitoes prefer birds and nonhuman mammals than human Hamer et al. (2009), we have $p_1 >= p_2$ and $p_3 >= p_2$. With above constraint and step size as 0.05, we have the possible combinations of p_1 and p_2 shown in Figure 2.7,

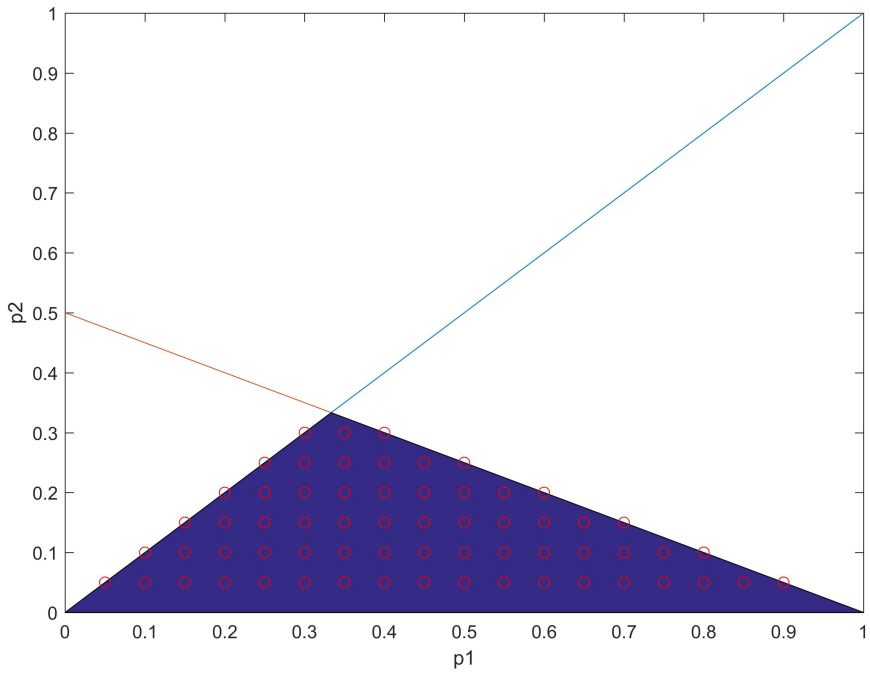

Figure 2.7: Possible values of p_1 and p_2 marked in red circle.

With step size for $(p_1,\ p_2,\ C_1,\ C_2,\ \gamma)$ as $(0.05,\ 0.05,\ 0.05,\ 0.05,\ 200)$, we run our model with all the possible combinations of p_1, p_2 C_1, C_2 and γ. Comparing with the reported human cases in year 2002, 2003, 2005 and 2011, the correlation coefficient reach maximum $\rho(H_i, \widetilde{H}_i) = 0.7732$ when $p_1 = 0.9$, $p_2 = 0.05$ $C_1 = 0.1$, $C_2 = 0.9$, and $\gamma = 3100$, so we get our estimated unknown parameters as $\hat{\theta} = (\hat{p_1},\ \hat{p_2},\ \hat{C_1},\ \hat{C_2},\ \hat{\gamma}) = (0.9750,\ 0.01,\ 0.2,\ 0.025,\ 3100)$ and $\hat{p_3} = 1 - \hat{p_1} - \hat{p_2} = 0.015$.

The parameters in model (2.24) are summarized in Table 2.3.

Parameter	Description	Value	Source
p_1	*Culex* mosquito host seeking preference on birds	0.9750	Estimated
p_2	*Culex* mosquito host seeking preference on humans	0.01	Estimated
p_3	*Culex* mosquito host seeking preference on other non-human mammals	0.015	Estimated
a_1	parameter in mosquito daily mortality rate	0.00025	Rubel et al. (2008)
a_0	parameter in mosquito daily mortality rate	0.0142	Rubel et al. (2008)
T_{opt}	optimal temperature for mosquito with lowest daily mortality rate	18.8	Rubel et al. (2008)
C_1	weight of no effect from precipitation in mosquito daily mortality rate	0.2	Estimated
C_2	weight of no effect from precipitation in mosquito daily biting rate	0.025	Estimated
γ	$\frac{ss_0}{ss_1}$	3100	Estimated
α	parameter in mosquito mortality rate and biting rate	0.042	Jones et al. (2012a)

Table 2.3: Parameters used in model (2.24).

The advantage of this method is that it can search all the possible combination of the unknown parameters and get a global optimal result. The drawback is that the computation expensive would increase rapidly when the number of estimated parameters increases.

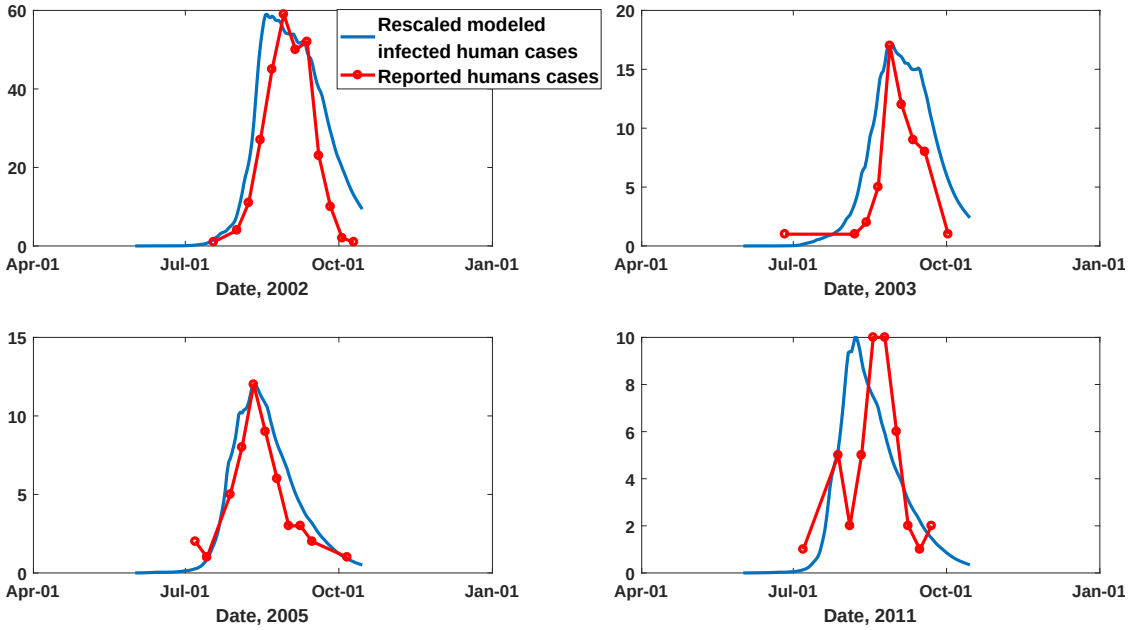

Figure 2.8: Comparison of rescaled modeled infected human cases and reported human cases for year 2002, 2003, 2005, and 2011.

The comparison of our modeled infection human cases and the reported human cases is shown in Figure 2.8. Since we are interested in the ability of our model to catch the trend of reported human cases, we rescale the modeled human infection cases to make it more comparable in the figures. Figure 2.8 also shows that our model captures the trend of reported human cases very well.

2.5.3 Weather patterns

To explore the impact of weather conditions on the transmission dynamics of WNV, we carried out numerical simulations under different weather patterns, i.e., different combinations of temperature and precipitation in Peel Region. We considered 5 basic types of weather patterns as illustrated conceptually in Figure 2.9.

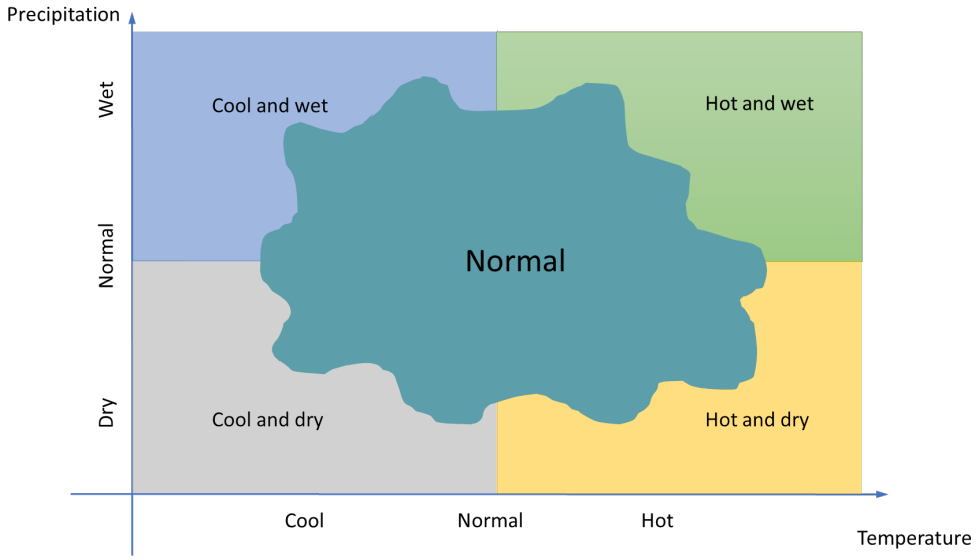

Figure 2.9: Different weather based on different combinations of temperature and precipitation, a conceptual sketch. Here as preliminary study, we consider 5 basic weather patterns.

We use a simple weather generator to obtain the different weather patterns. For daily mean temperature, we classify it into 3 categories as cool temperature, normal temperature and hot temperature. The normal daily mean temperature is defined as

the average daily mean temperature of last 30 years (weather data from the weather station at Pearson International Airport, Ontario, Canada, available from the website of Environment Canada, `http://climate.weather.gc.ca/index_e.html`). We then increase the normal daily mean temperature by 1.5 standard deviations for each day to reach the hot temperatures. Similarly, we decrease the daily mean temperature by 1.5 standard deviations from the normal temperature to represent cool temperatures.

For precipitation, we follow the method used in a computer simulation model called WGEN (Weather Generator) which is proposed by Richardson and Wright Richardson and Wright (1984). In WGEN, they use a first order Markov chain to generate the occurrence of wet or dry days. If a wet day is generated, the gamma distribution is employed to produce the precipitation amount.

If there is 0.02 mm of precipitation or more for a day, it is defined as a wet day. Otherwise, it is called a dry day. Through the first order Markov chain model, the probability of precipitation on a certain day is conditioned on the wet or dry status of the previous day. For month j, let $p_i^j(W|W)$ be the probability of a wet day on day i given a wet day on day $i-1$ (W denotes the wet day). $p_i^j(W|D)$ is the probability of a wet day on day i given a dry day on day $i-1$ (D denotes the dry day). Then

we have

$$p_i^j(D|W) = 1 - p_i^j(W|W), \tag{2.29}$$

$$p_i^j(D|D) = 1 - p_i^j(W|D), \tag{2.30}$$

where $p_i^j(D|W)$ is the probability of a dry day i given a wet day $i-1$, $p_i^j(D|D)$ is the probability of a dry day i given a dry day on previous day $i-1$.

If day i on month j is a wet day, let the precipitation amount be pr_i^j, pr_i^j would follow a Gamma distribution, $pr_i^j \backsim Gamma(\alpha_j, \beta_j)$. In WGEN, $p_i^j(W|W)$, $p_i^J(W|D)$, α_j and β_j are constants for a given month, but are varied from month to month.

In our simulation for different weather patterns, we consider the period is from June to September, we only need to generate the precipitation scenarios for these four months. First, we use historical precipitation of last 30 years for these 4 months to estimate the precipitation parameters of each month ($p_i^j(W|W)$, $p_i^J(W|D)$, α_j and β_j). Then we apply the first order Markov chain model (with parameters $p_i^j(W|W)$ and $p_i^J(W|D)$ for each month) to determine the wet or dry status of each day (the first day of each month is assumed to be dry). Finally, the Gamma distribution (with parameters α_j and β_j) is used to generate the precipitation amount for each wet day of each month. These precipitation scenarios are treated as the precipitation scenarios for the normal weather in our work.

For the wet weather scenarios, $\alpha_j^w = \alpha_j$ and $\beta_j^w = \beta_j * 1.3$ are used as new

Gamma distribution parameters to generate the amount of precipitation for each wet day. Similarly, for the dry weather scenarios, $\alpha_j^d = \alpha_j$ and $\beta_j^w = \beta_j * 0.7$ are as new Gamma distribution parameters to generate the precipitation amount.

For each weather pattern, since the precipitation is randomly generated, we run the simulation for 500 times and take the average as the simulation results for that weather pattern. Figure 2.10 and Figure 2.11 show the average simulation results under different weather patterns. Figure 2.11 shows the rescaled cool weather simulation results in Figure 2.10.

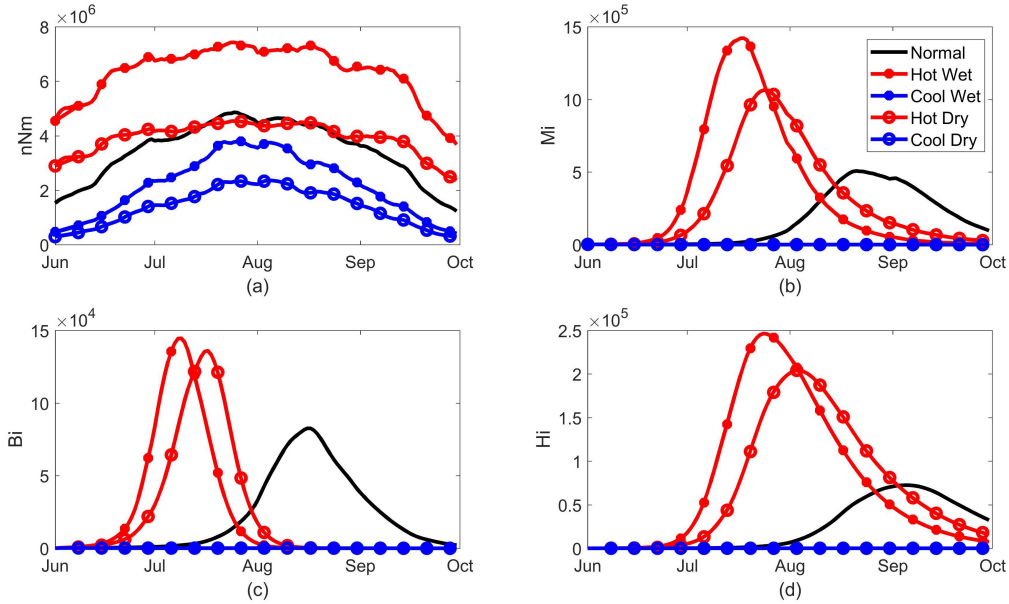

Figure 2.10: Simulation results under different weather patterns. Hot weather would lead to more infections while cool weather leads less infections. When temperature is high, wet weather causes more infections.

Compared to normal weather, there are more infected birds, infected mosquitoes, and infected humans under hot wet weather and hot dry weather. When temperature is high, the wet weather would lead to more infections (birds, mosquitoes, and humans) than the dry weather. On the contrary, less infections appear under cool wet and cool dry weather patterns compared with normal weather, where the number of infections in cool wet weather is less than that in cool dry weather.

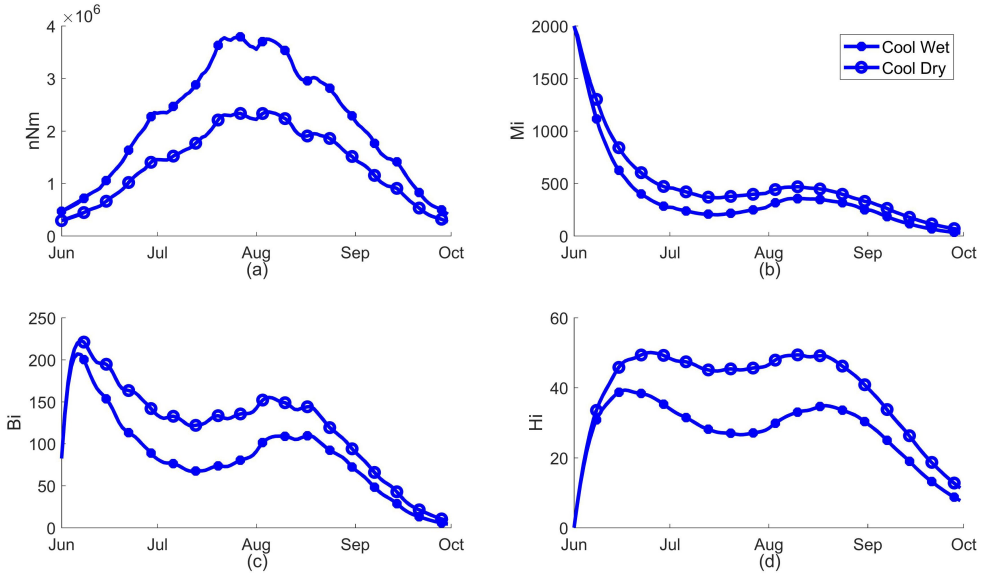

Figure 2.11: Simulation results under different weather patterns. Hot weather would lead to more infections while cool weather leads to less infections. When temperature is low, wet weather causes less infections.

For hot wet weather, the number of infected birds and infected mosquitoes reach a peak around the middle of July, after that the infected humans reach a peak around

late July. Thus the peak of infected humans occurs on account of more infected birds and infected mosquitoes.

Based on the simulation results in Figure 2.10 and Figure 2.11, we can conclude that the effect of temperature on WNV transmission is more significant than that of precipitation. Higher temperature can enhance the development of mosquitoes and the transmission of WNV, while cool temperatures cause opposite results.

2.6 Conclusion and Discussion

In this chapter, we incorporate the effect of weather factors into modeling the transmission of WNV. First, a weather driven statistical model is employed to describe the *Culex* mosquito abundance. Then we integrate the statistical model with the compartmental WNV transmission model, where we also take into account the impact of mosquito host seeking preference and effect of weather on mosquito biting rate and mortality rate. In the last, we estimate some parameters of our model and compare simulations results under different weather patterns.

Based on the simulation results of our model, we find that weather factors (temperature and precipitation) are key factors to influence the WNV transmission. Particularly, temperature is more important than precipitation to affect WNV transmission. High temperature can lead to more infections, while low temperature would

cause less infection. The effects of precipitation are different when temperature is different. Wet weather could lead to more infections under high temperature, but would cause less infection under low temperature.

Based on our simulation, our model gets a good match to the trend of human infection cases in Peel Region. Our model can also be applied to other areas as long as sufficient mosquito surveillance data is available to train the statistical model. What's more, the method can be used to model other mosquito-borne diseases such as Zika, Dengue, and Malaria. Hence the model in our work can be regarded as a general model to study mosquito-borne diseases with the effect of weather conditions.

3 A temperature driven matrix population model for mosquitoes

3.1 Introduction

Mosquito life cycle is heavily affected by environmental conditions such as temperature, precipitation, photoperiod, etc. (Brady et al. 2013, Denlinger and Armbruster 2014, Jones et al. 2012b, Reisen 1995, Robich and Denlinger 2005, Rubel et al. 2008, Yang et al. 2009). However, most of the mosquito-borne diseases transmission models do not consider the weather impact on the mosquito population (Bowman et al. 2005, Lewis et al. 2006, Macdonald 1957, Ross 1911). Some of the models tried to consider the impact of temperature on mosquito population, but they only added a delay to represent mosquito mature process (Fan et al. 2010, Wan and Zhu 2012). Mosquitos have overwintering diapause to avoid unfavourable cold temperature in areas where the weather does not support year round development. But the overwintering dia-

pause has been either ignored or modelled too simplistically in the literature. For example, Ahumada et al. (2004) and Schaeffer et al. (2008) develop matrix mosquito population models which consider the effect of weather conditions. But they do not consider different behaviors of mosquitoes in different seasons. Although Lončarić and Hackenberger (2013) present a stage and age structured mosquito population model including effect of weather conditions, they simply assume that the overwintering diapause mosquito population remains constant.

In order to better describe the mosquito behaviors of the whole year, we first separate the year into breeding season and overwintering period. For *Culex* female diapause mosquitoes in Southern Ontario in late fall and early winter, the unfavorite environmental condition is an alert for the pre-diapause mosquito to start diapause (Denlinger and Armbruster 2014). But the mosquitoes will not start diapause immediately even when the weather condition has changed significantly.

To define the breeding season and overwintering period, we choose two thresholds for the temperature and photoperiod. When both temperature and photoperiod are above the thresholds for a certain number of days, we say that the breeding season starts. After the start of the breeding season, when both temperature and photoperiod are below the thresholds for the certain number of days, we say that the overwintering period starts. We define a mosquito year as the combination of the

breeding season and the following overwintering period. We emphasize that the two periods are determined adaptively according to weather condition of one particular year.

We then build a matrix population model for each period respectively. We believe that our method of separating the year into two periods is more reasonable and realistic in comparison to that in Lončarić and Hackenberger (2013).

In this chapter, Section 3.2 describes the two periods and mosquito year. The models for the two periods of the mosquito year and the properties are given in Section 3.3. In Section 3.4, we present the simulation results. The discussion and conclusion are in Section 3.5.

3.2 *Culex pipiens/restuans* mosquito breeding season and the overwintering period

Affected mainly by temperature and photoperiod, mosquito behaviors (including reproduction, development, and biting) are different during different periods of year. In the summer time, the weather remains warm and the length of day is relatively long, therefore mosquitoes are most active in biting and reproduction. In late summer and fall, the female mosquito can have the ability to enter the overwintering diapause when they experience low temperature and shorter day length in their fourth

larval instar and early pupa stage. They accumulate more fat reserves than those non-diapause adult female mosquitoes and will not lay eggs until they terminate overwintering diapause in the next spring Robich and Denlinger (2005). In winter, only these adult female diapause mosquitoes can enter the overwintering diapause. Their development is halted or greatly retarded, and stress tolerance increases. In the following spring, when temperature becomes higher and the photoperiod is longer enough, the diapause adult female mosquitoes terminate the overwintering diapause and start to reproduce Denlinger and Armbruster (2014), Robich and Denlinger (2005).

To build a mosquito population model over a whole year, we divide the year into two periods, say breeding season (including late spring, summer and early fall) and overwintering period (including late fall, winter and early spring). The studies in Denlinger and Armbruster Denlinger and Armbruster (2014), Sanburg and Larsen Sanburg and Larsen (1973) have shown that temperature and photoperiod have an interactive effect to induce and terminate the mosquito overwinter diapause. Thus we use temperature and photoperiod to determine the mosquito periods of the year.

The mosquito breeding season and the overwintering period vary from different years based on the temperature and photoperiod. Let t_y^b be the start date of the

breeding season in year y, then we have

$$t_y^b = \min \{y^s \leq t \leq y^e | (\sum_{\tau=t-p^*}^{t-1} \mathbb{I}^d_{[T^*,\ \infty)}(T_\tau)\ \mathbb{I}^d_{[P^{p^*},\ \infty)}(P_\tau^p)) = p^*\}, \tag{3.1}$$

where y^s and y^e represent the first and last day of year y, T^* and P^{p^*} are the threshold temperature and photoperiod for *Culex* female diapause mosquitoes to feel the alert to start the breeding season or overwintering period, T_τ is the daily mean temperature on date τ and P_τ^p is the photoperiod on date τ. p^* is the certain number of days that both the temperature and photoperiod have to remain below (above) T^* and P^{p*} to start the overwintering period (breeding season). $\mathbb{I}^d_{[T^*,\ \infty)}(T_\tau)$ is the indicator function evaluating if $T_\tau \in [T^*,\ \infty)$.

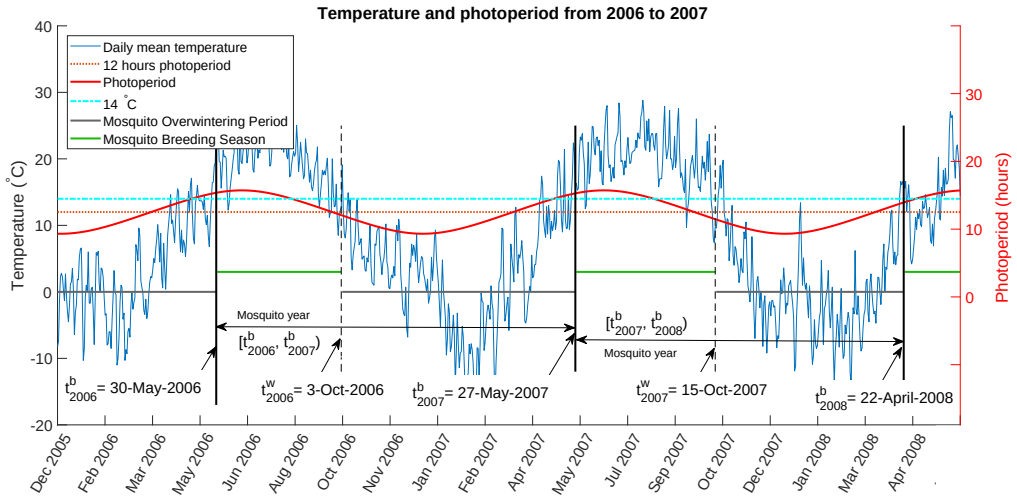

Figure 3.1: Temperature, photoperiod and mosquito year of 2006 and 2007.

Let t_y^w be the start date of the overwintering period in year y, we have

$$t_y^w = \min \{t_y^b < t \leq y^e | (\sum_{\tau=t-p^*}^{t-1} \mathbb{I}^d_{(-\infty,\ T^*)}(T_\tau)\ \mathbb{I}^d_{(-\infty,\ P^{p^*})}(P_\tau^p)) = p^*\}. \tag{3.2}$$

For year y, the breeding season is $[t_y^b,\ t_y^w)$, the ovrwintering period is $[t_y^w,\ t_{y+1}^b)$. We call the period of $[t_y^b,\ t_{y+1}^b)$ the mosquito year of y.

The breeding season, the overwintering period, and mosquito year for the year of 2006 and 2007 in Peel Region are shown in Figure 3.1.

3.3 Age and stage structured model for *Culex pipiens/restuans* mosquito population

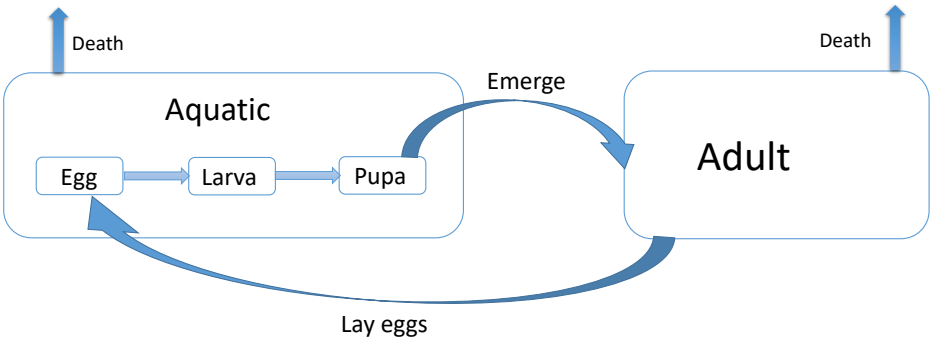

Figure 3.2: Basic diagram for the model.

The mosquito stages of eggs, larva and pupa are largely aquatic and all need to accumulate enough heat to develop into the next stage. So we treat these 3 stages as one stage called aquatic.

As shown in many studies, the adult female *Culex pipiens/restuans* mosquitoes who receive short day length during their larva stage will be the diapause adult female *Culex pipiens/restuans* mosquitoes, which would not lay eggs till the next spring. We consider this important fact in our model, and divide the adult female mosquitoes into non-diapause adult female mosquitoes and diapause adult female mosquitoes. The structure of our model is shown in Figure 3.3.

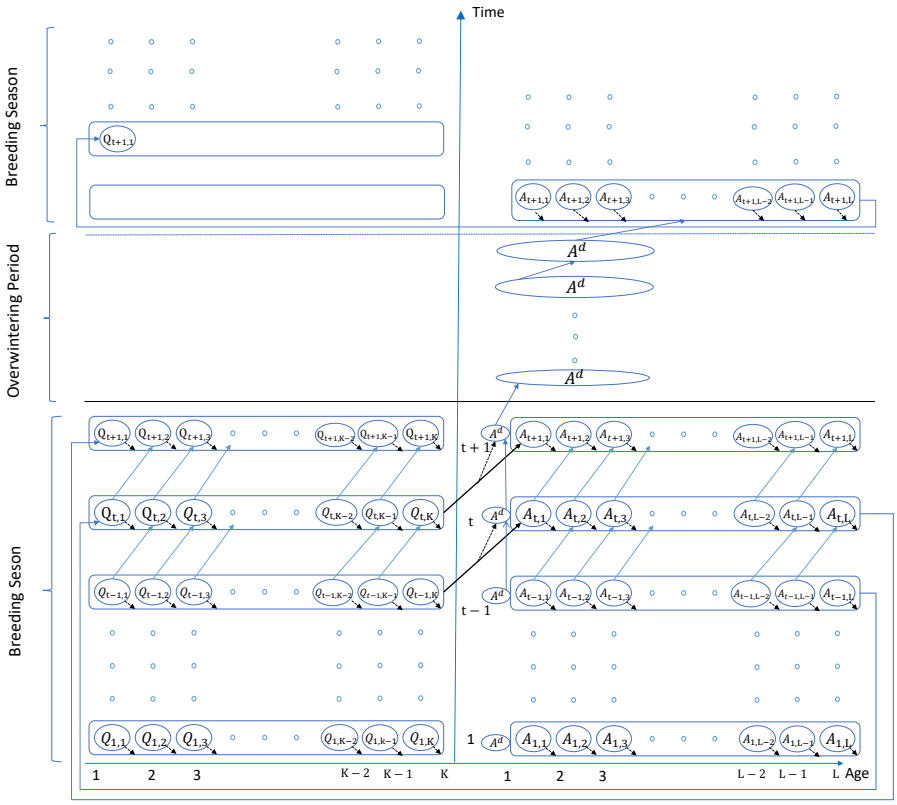

Figure 3.3: Structure of our matrix population model.

3.3.1 Model for mosquito breeding season

Symbol	Definition
$A_{t,i}$	The number of i days old non-diapause adult female mosquitoes on date t
$A^d_{t,i}$	The number of i days old diapause adult female mosquitoes on date t
$Q_{t,j}$	The number of j days old aquatics on date t
$g^c_{t,j}$	The accumulated growing degree days for j days old aquatic mosquitoes until date t
$\mu^a_{t,i}$	Daily mortality rate of i days old adult female mosquito on date t
$\mu^q_{t,j}$	Daily mortality rate of j days old aquatic mosquito on date t
$\mu^{\mathcal{W}}(T_t)$	Daily mortality rate of diapause adult female mosquito on date t
$f_{t,i}$	Number of eggs that one i days old adult female mosquito lays on date t
p^*	The certain number of days that both the temperature and photoperiod have to remain below (above) T^* and P^{p*} to start the mosquito overwintering period (breeding season)
P^{p*}	Threshold photoperiod for mosquito diapause
T_b	Base temperature to accumulate degree days
T^*	Threshold temperature for mosquito diapause
t_d	The accumulated degree days the aquatic mosquito needs to emergence
$\delta_{t,i}$	Indicator if the i day old non-diapause adult female mosquitoes can lay eggs on date t
T_t	Daily mean temperature on date t
t_p	Time between two ovipositions
t	Date
L	Maximum age of adult female mosquitoes
i	Age of adult female mosquitoes ($1 \leq i \leq L$)
K	Maximum age of aquatic mosquitoes
j	Age of aquatics ($1 \leq j \leq K$)
$\mathbb{I}^d_B(x)$	Indicator function, equals to 1 when $x \in B$, otherwise equals to 0

Table 3.1: Symbols used in model (3.3).

The symbols used in our model are summarized in Table 3.1. We have our model for the breeding season as following

$$M_{t+1} = P_t \; M_t. \tag{3.3}$$

As shown in the model structure in Figure 3.3, we divide mosquito population in the breeding season into three parts. So we have $M_t = (Q_t, A_t, A_t^d)^T$, where $A_t = (A_{t,1}, A_{t,2}, \ldots, A_{t,L})^T$, $Q_t = (Q_{t,1}, Q_{t,2}, \ldots, Q_{t,K})^T$, and $A_t^d = (A_{t,1}^d, A_{t,2}^d, \ldots, A_{t,L}^d)^T$.

The transition matrix P_t has the following form,

$$P_t = \begin{pmatrix} V_t & Z_t & \mathbf{0} \\ \mathcal{W}_t & U_t & \mathbf{0} \\ \mathcal{W}_t^d & \mathbf{0} & U_t \end{pmatrix}. \tag{3.4}$$

In the transition matrix, we have V_t, U_t, and U_t to represent the daily survival transition of Q_t, A_t, and A_t^d respectively. We use $\mathcal{W}_t$ and $\mathcal{W}_t^d$ to describe the aquatic mosquitoes emerging to non-diapause adult female mosquitoes and diapause adult female mosquitoes respectively. The reproduction of non-diapause adult female mosquitoes is described by Z_t.

$$U_t = \begin{pmatrix} 0 & 0 & 0 & \cdots & 0 \\ 1-\mu^a_{t,1} & 0 & 0 & \cdots & 0 \\ 0 & 1-\mu^a_{t,2} & 0 & \cdots & 0 \\ \vdots & \vdots & \vdots & \ddots & 0 \\ 0 & 0 & \cdots & 1-\mu^a_{t,L-1} & 0 \end{pmatrix}_{L\times L} . \tag{3.5}$$

$$V_t = \begin{pmatrix} 0 & 0 & 0 & \cdots & 0 \\ 1-\mu^q_{t,1} & 0 & 0 & \cdots & 0 \\ 0 & 1-\mu^q_{t,2} & 0 & \cdots & 0 \\ \vdots & \vdots & \vdots & \ddots & 0 \\ 0 & 0 & \cdots & 1-\mu^q_{t,K-1} & 0 \end{pmatrix}_{K\times K} . \tag{3.6}$$

$$\mathcal{W}_t = \begin{pmatrix} 0 & \omega_{t,2} & \cdots & \omega_{t,K} \\ 0 & 0 & \cdots & 0 \\ \vdots & \vdots & \ddots & \vdots \\ 0 & 0 & \cdots & 0 \end{pmatrix}_{L\times K} , \tag{3.7}$$

where $\omega_{t,j} = \mathbb{I}^d_{[t_d,\ \infty)}(g^c_{t,j})\ \mathbb{I}^d_{[0,\ t_d)}(g^c_{t-1,j-1})\ (1-\pi(P^p_t)),\ 2 \le j \le K$, $\mathbb{I}^d_{[t_d,\ \infty)}(g^c_{t,j})$ is the

indicator function evaluating if $g^c_{t,j} \in [t_d,\ \infty)$.

$$\mathcal{W}^d_t = \begin{pmatrix} 0 & \omega^d_{t,2} & \cdots & \omega^d_{t,K} \\ 0 & 0 & \cdots & 0 \\ \vdots & \vdots & \ddots & \vdots \\ 0 & 0 & \cdots & 0 \end{pmatrix}_{L\times K}, \tag{3.8}$$

where $\omega^d_{t,j} = \mathbb{I}^d_{[t_d,\ \infty)}(g^c_{t,j})\mathbb{I}^d_{[0,\ t_d)}(g^c_{t-1,j-1})\pi(P^p_t), 2 \le j \le K$.

$$Z_t = \begin{pmatrix} f^*_{t,1} & f^*_{t,2} & \cdots & f^*_{t,L} \\ 0 & 0 & \cdots & 0 \\ \vdots & \vdots & \ddots & \vdots \\ 0 & 0 & \cdots & 0 \end{pmatrix}_{K\times L}, \tag{3.9}$$

where $f^*_{t,i} = f_{t,i}\delta_{t,i}$ $(1 \le i \le L)$.

3.3.1.1 Effect of heat accumulation

Let $g^c_{t,j}$ be the accumulated growing degree days for j days old aquatic mosquitoes on date t. 1 day old aquatic mosquito have 0 growing degree day, we have

$$\begin{cases} g^c_{t,1} = 0, \\ g^c_{t+1,j+1} = g^c_{t,j} + (T_t - T_b)\mathbb{I}^d_{(T_b,\ \infty)}(T_t), \quad 1 \le j \le K-1. \end{cases} \tag{3.10}$$

We use $\mathbb{I}^d_{[t_d,\ \infty)}(g^c_{t,j})$ as the indicator of wether the j days old aquatic mosquitoes accumulate enough GDDs to develop into adult mosquitoes on date t. If the indicator

$\mathbb{I}^d_{[t_d,\ \infty)}(g^c_{t,j}) = 1$ for $Q_{t,j}$ on date t, it will also equals to 1 on date $t+1$ for $Q_{t+1,j+1}$, however these aquatic mosquitoes already developed into adult mosquitoes on date t. To avoid this possible multiple counting, we use $\mathbb{I}^d_{[0,\ t_d)}(g^c_{t-1,j-1})$ as the indicator to ensure that the aquatic mosquitoes will be counted only once. Thus for $\mathcal{W}_t$ and $\mathcal{W}^d_t$, we get

$$\omega_{t,j} = \mathbb{I}^d_{[t_d,\ \infty)}(g^c_{t,j})\mathbb{I}^d_{[0,\ t_d)}(g^c_{t-1,j-1})(1-\pi(P^p_t))(2 \le j \le K),$$

$$\omega^d_{t,j} = \mathbb{I}^d_{[t_d,\ \infty)}(g^c_{t,j})\mathbb{I}^d_{[0,\ t_d)}(g^c_{t-1,j-1})\pi(P^p_t)(2 \le j \le K).$$

3.3.1.2 Mosquito reproduction

Let $\delta_{t,i}$ be the indicator to show if the i days old adult female mosquitoes will lay eggs on date t. We assume the time between two ovipositions is constant, denote it as t_p and assume it to be $t_p = 7$ days. Thus the non-diapause adult female mosquitos will lay eggs every t_p days, and we have $\delta_{t,i} = 1$ when $i \equiv\ 0\ (mod\ t_p)$, otherwise $\delta_{t,i} = 0$, where $i \equiv\ 0\ (mod\ t_p)$ means that i is congruent to 0 modulo t_p. Let $f_{t,i}$ be the number of eggs laid by one i days old adult female mosquito on date t. Thus the number of eggs laid by all i days old adult female mosquitoes on date t is $f_{t,i}\delta_{t,i}A_{t,i}$, and we have $f^*_{t,i} = f_{t,i}\delta_{t,i}$ in Z_t.

3.3.2 Model for the overwintering period

Lončarić and Hackenberger (2013) assume that mosquitoes will diapause in winter without death. However this assumption is not realistic because that the temperature has effect on the mortality rate of the diapause adult female mosquitoes (Bradshaw and Holzapfel 1977). Let daily mortality rate of diapause adult female mosquitoes be $\mu^W(T)$ in mosquito overwintering period, where T is daily mean temperature. Our model for overwintering period has the following form:

$$\begin{cases} A^d_{t+1} = P^d_t A^d_t, \\ Q_t = 0, \end{cases} \tag{3.11}$$

where

$$P^d_t = \left(\ I_L * (1 - \mu^{\mathcal{W}}(T_t)) \ \right)_{(L \times L)}, \tag{3.12}$$

where I_L is the $L \times L$ identity matrix.

3.3.3 Integration of the two models for the breeding season and the overwintering period

To integrate the breeding season model and the overwintering period model, we use the number of diapause adult female mosquitoes A^d on the last day of the breeding season as the initial condition for diapause adult female mosquitoes of the overwintering period model. When the breeding season starts, all the diapause adult

female mosquitoes terminate diapause. We use the number of diapause adult female mosquitoes A^d on the last day of the overwintering period as initial condition of non-diapause adult female mosquitos for the breeding season. The initial condition for aquatic mosquitoes are set to be zeros as shown in Figure 3.3.

3.3.4 Properties of the model

Compared with the original Leslie age-structured population models (Leslie 1945, 1948), our model (3.3) is a more general structured model. Firstly, our projection matrix P_t depends on time (temperature). Secondly, we have two stages (including three classes) based on age structure, while original Leslie matrix population model is only age-structured.

It is difficult to analyze the properties of the model since our projection matrix P_t is time dependent. Therefore we assume the temperature is constant all the time. We only study the theoretical properties for the breeding season and assume that there is no diapause adult female mosquitos ($\pi(P_t^p) = 0$). We also suppose the mortality rate of adult female mosquitos and aquatic mosquito are constants. Based on the study of Cushing and Zhou (1994), we calculate the net reproductive value and use it as a critical to justify the stability of our model.

Since we assume there is no A_t^d, we have model (3.3) reduced to

$$M_{t+1}^s = P_t^s M_t^s, \tag{3.13}$$

where

$$M_t^s = \begin{pmatrix} Q_t \\ \\ A_t \end{pmatrix}, \tag{3.14}$$

and

$$P_t^s = \begin{pmatrix} V_t & Z_t \\ \\ \mathcal{W}_t & U_t \end{pmatrix}. \tag{3.15}$$

If the temperature is set to be constant $T_t = \overline{T}$, then $g_{n,j}^c = (\overline{T} - T_l)(j-1)$. We then have

$$\mathbb{I}^d_{[t_d,\ \infty)}(g_{t,j}^c)\mathbb{I}^d_{[0,\ t_d)}(g_{n-1,j-1}^c) = \begin{cases} 1, & \text{if } j = j^* = \lceil \frac{T_d}{\overline{T}-T_b} \rceil, \\ \\ 0, & \text{otherwise,} \end{cases}$$

where $\lceil x \rceil$ is the smallest integer not less than x. This will lead to a simplified form of $\mathcal{W}_t$ as $\mathcal{W}$. Let $\mu_{t,i}^a \equiv \mu^a$, $\mu_{t,j}^q \equiv \mu^q$. We assume $s^a = 1 - \mu^q$, $s^q = 1 - \mu^q$. After assuming $f_{t,i}\delta_{t,i} = f_i$, we have simplified forms of U_t, V_t, and Z_t as U, V, and Z respectively.

$$U = \begin{pmatrix} 0 & 0 & 0 & \cdots & 0 \\ s^a & 0 & 0 & \cdots & 0 \\ 0 & s^a & 0 & \cdots & 0 \\ \vdots & \vdots & \vdots & \ddots & 0 \\ 0 & 0 & \cdots & s^a & 0 \end{pmatrix}_{L\times L}, V = \begin{pmatrix} 0 & 0 & 0 & \cdots & 0 \\ s^q & 0 & 0 & \cdots & 0 \\ 0 & s^q & 0 & \cdots & 0 \\ \vdots & \vdots & \vdots & \ddots & 0 \\ 0 & 0 & \cdots & s^q & 0 \end{pmatrix}_{K\times K},$$

$$\mathcal{W} = \begin{pmatrix} 0 & 0 & \cdots & 0 & 1 & 0 & \cdots & 0 \\ 0 & 0 & \cdots & 0 & 0 & 0 & \cdots & 0 \\ \vdots & \vdots & \ddots & \vdots & \vdots & \vdots & \vdots & \vdots \\ 0 & 0 & \cdots & 0 & 0 & 0 & \cdots & 0 \end{pmatrix}_{L\times K}, Z = \begin{pmatrix} f_1 & f_2 & f_3 & \cdots & f_{L-1} & f_L \\ 0 & 0 & 0 & \cdots & 0 & 0 \\ \vdots & \vdots & \vdots & \ddots & \vdots & \vdots \\ 0 & 0 & 0 & \cdots & 0 & 0 \end{pmatrix}_{K\times L}.$$

Then P_t^s in model (3.13) becomes

$$P^s = \begin{pmatrix} V & Z \\ \mathcal{W} & U \end{pmatrix}. \tag{3.16}$$

Let

$$\mathfrak{F} = \begin{pmatrix} \mathbf{0} & Z \\ \mathbf{0} & \mathbf{0} \end{pmatrix} \text{ and } \mathfrak{S} = \begin{pmatrix} V & \mathbf{0} \\ \mathcal{W} & U \end{pmatrix}. \tag{3.17}$$

We then have $P^s = \mathfrak{S} + \mathfrak{F}$.

Let $c_{1(K+k)}$ be the cofactor of the $1(K+k)^{th}$ entry in $I - \mathfrak{S}$, we have

$$\mathbf{y} = \begin{pmatrix} c_{11} \\ c_{12} \\ c_{13} \\ \vdots \\ c_{1K} \\ c_{1(K+1)} \\ c_{1(K+2)} \\ c_{1(K+3)} \\ \vdots \\ c_{1(K+L)} \end{pmatrix} = \begin{pmatrix} 1 \\ s^q \\ (s^q)^2 \\ \vdots \\ (s^q)^{K-1} \\ (s^q)^{j^*-1} \\ s^a(s^q)^{j^*-1} \\ (s^a)^2(s^q)^{j^*-1} \\ \vdots \\ (s^a)^{L-1}(s^q)^{j^*-1} \end{pmatrix}, \tag{3.18}$$

Since each element of $\mathbf{y}$ is positive, according to Cushing and Zhou (1994), we then have the net reproductive value as

$$n = \frac{1}{\det(I - \mathfrak{S})} \sum_{k=1}^{L} f_k c_{1(K+k)} = \sum_{k=1}^{L} f_k (s^a)^{k-1} (s^q)^{j^*-1}. \tag{3.19}$$

Based on the results in Cushing and Zhou (1994), the trivial equilibrium $M^* = \mathbf{0}$ of the model is asymptotically stable (respectively unstable) if and only if $n < 1$ (respectively $n > 1$). If $n = 1$ then there exist a family of positive equilibria $M^* = c\mathbf{y}$ where c is an arbitrary positive constant.

3.4 Simulation

In order to validate our model, we carry out simulation based on the weather condition of Peel Region of Southern Ontario. We estimate some of the parameters through comparing with real observed mosquito data. Then we performance simulation studies under different weather conditions.

3.4.1 Initial setting and assumptions about the model

The simulation starts from January 1st, 2003, and we assume that January 1st is in mosquito winter. We let $L = 30$ and $K = 90$ in our simulations. We have $A^d_{1,i} = 31 - i$, $i = 1 \cdots 30$, as the initial condition for the adult *Culex* mosquitoes.

Low temperature in winter will lead to a high death rate for diapause adult female mosquito. We assume daily mortality rate for adult female mosquito in the overwintering period to be $\mu^{\mathcal{W}}(T) = exp(\frac{-10000}{(T-25)^2+1}) + 0.00125$.

Based on the fact that the portion of diapause is dependent on day length (Rubel et al. 2008). The portion of diapause adult female mosquito based on day length is as following:

$$\pi(P^p_t) = \frac{1}{1 + 1775.7 * \exp 1.559(P^p_t - 18.177)}, \tag{3.20}$$

For the daily mortality rate of adult female mosquitoes $\mu^a_{t,i}$ and aquatic mosquitoes $\mu^q_{t,i}$ in our model. We assume the mosquito daily mortality is only affected by daily

mean temperature. According to Reisen (1995), Rubel et al. (2008), we let

$$\mu^a_{t,i} = \mu^a(T_t) = 0.00025T_t^2 - 0.0094T_t + 0.10257, \tag{3.21}$$

and

$$\mu^q_{t,i} = \mu^q(T_t) = 10\mu^a(T_t) = 0.0025T_t^2 - 0.094T_t + 1.0257. \tag{3.22}$$

We also assume the number of eggs that one i day old adult female mosquito lays on date t is same and therefore we have $f_{t,i} = f$.

We use weather data of Peel Region, Ontario, Canada from 2003 to 2012. For normal weather, we use the average of 30 years daily mean temperature in Peel Region, Ontario, Canada (years from 1980 to 1991 and 1994 to 2011). For hot weather, we add 0.5 standard deviation to the average of 30 years daily mean temperature. For cool weather, we subtract 0.5 std from the average of 30 years daily mean temperature.

3.4.2 Parameter estimation

Although we set most of our parameters from the references, there are still a few parameters that need to be estimated. We use the grid search algorithm to estimate the unknown parameters.

We use the Pearson correlation coefficient as the lost function. It is defined as

following,

$$\rho^y(A_t, A_t^o) = \frac{\sum_{t \in TD^y} (A_t - \overline{A_t})(A_t^o - \overline{A_t^o})}{\sqrt{\sum_{t \in D^y} (A_t - \overline{A_t})^2} \sqrt{\sum_{t \in D^y} (A_t^o - \overline{A_t^o})^2}}, \tag{3.23}$$

where $\overline{A_t} = \frac{1}{N} \sum_{t \in D^y} A_t$, and $\overline{A_t^o} = \frac{1}{N} \sum_{t \in D^y} A_t^o$, N is the total times of mosquito observation. The CDC traps attract mosquitoes through the mosquito bitting behaviors, therefore we assume the trapped mosquitoes are all non-diapause adult female mosquitoes and use it to match A_t in our model. A_t^o is the observed average trapped mosquito count on date t. D^y is the dates set of mosquito observation date in year y.

We denote $\theta = (f, T_d, T_b, T^*, P^{p*}, p^*)$ as the unknown parameter set and $\hat{\theta}$ as the estimation of the unknown parameters. We use the average of $\rho^y(A_t, A_t^o)$ from year 2003 to year 2011 as our target function. Then $\hat{\theta}$ is defined to be

$$\hat{\theta} = \arg\max_{\theta} \rho(A_t(\theta), A_t^o), \tag{3.24}$$

where $\rho(A_t, A_t^o) = \frac{1}{9} \sum_{y=2003}^{2011} \rho^y(A_t, A_t^o)$. We use the grid search algorithm used in (Gong et al. 2010) and then find the estimation of the unknown parameters.

As in our model, based on available study, we have our parameter search range, step size, and estimated values shown in Table 3.2, with maximum value of $\rho(A_t(\theta), A_t^o)$ as 0.8056,

Parameter	Search interval	Step size	Estimated value
t_d	$[130, 230]$	20	170
T_b	$[5, 11]$	1.5	9.5
f	$[50, 200]$	20	50
P^{p*}	$[11, 15]$	1	12
T^*	$[11, 14]$	1	12
$p*$	$[5, 15]$	2	5

Table 3.2: Estimated parameters, search range, step size, and estimated values.

3.4.3 Simulation results and discussion

First, we perform the simulation studies under different weather patterns. Then we compared the simulated mosquito count with the observed data in Peel Region, Ontario, for 2004 and 2010.

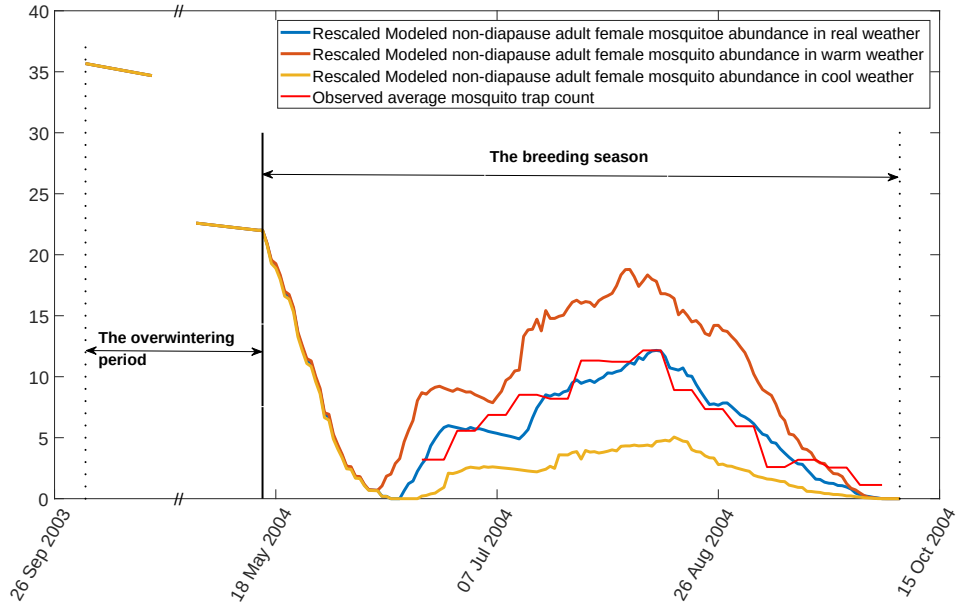

Figure 3.4: Simulation under different weather pattern based on weather conditions in year 2004. The modeled mosquito abundance under different weather conditions are rescaled with the same factor.

We compare our model in real temperature, warm temperature, and cool temperature in the breeding season. We use the year 2004 as an example. To get the warm temperature of each day in the breeding season, we add 0.5 standard deviation of the last 30 years daily mean temperature to the observed daily mean temperature. To get the cool temperature of each day in the breeding season, we subtract 0.5 standard deviation of the last 30 years daily mean temperature from the observed daily mean temperature. We use the real temperature in the overwintering period

for different simulations. Thus for the three simulations, the modeled diapause adult female mosquito abundance in the overwintering period are same with same initial conditions. As shown in Figure 3.4, warm temperature in the breeding season can lead to an early and high peak of the non-diapause adult female mosquito abundance compared with the cool temperature. The peak time and peak value of the mosquito abundance in the real temperature are in between that in the warm temperature and that in the cool temperature.

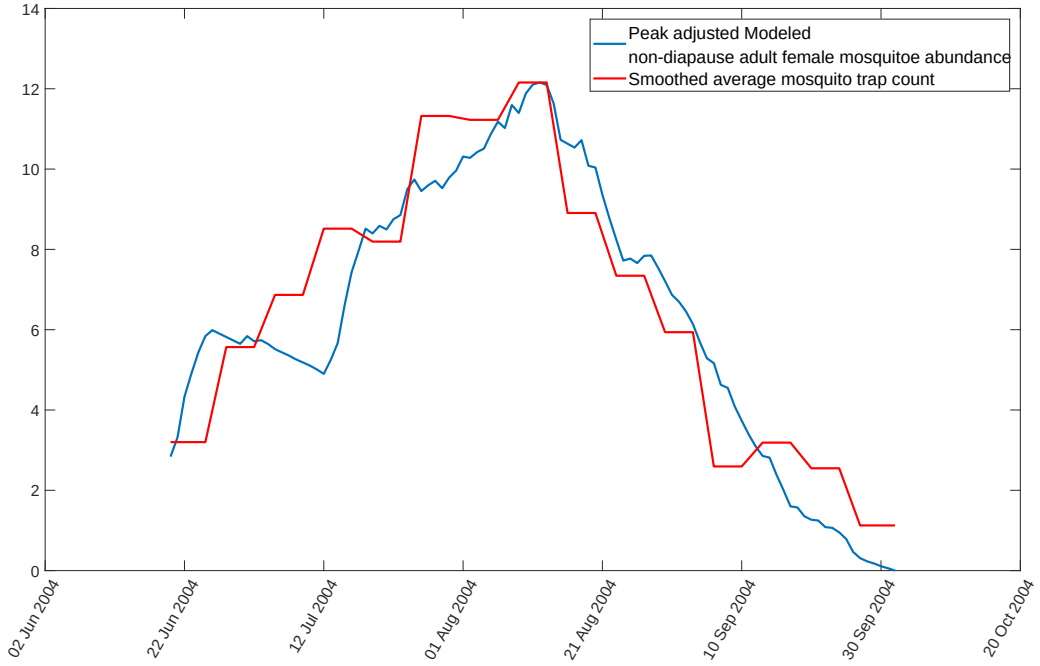

Figure 3.5: Simulation result in year 2004.

The rescaled modeled non-diapause adult female mosquito abundance compared with average mosquito trap count of year 2004 and 2010 in Peel Region are shown

in Figure 3.5 and Figure 3.6 respectively. The red line represents smoothed average mosquito trap count in Peel Region. The blue line represents the rescaled simulated mosquito abundance. Our model capture the trend of the surveillance mosquito data very well with average correlation coefficient to be 0.8056 from year 2003 to year 2011.

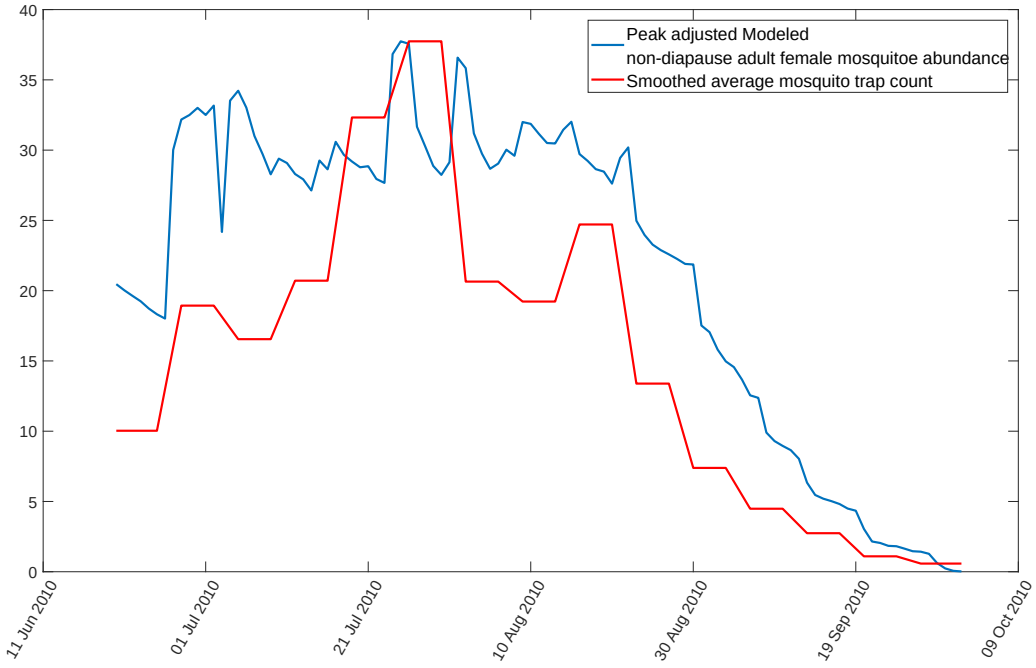

Figure 3.6: Simulation result in year 2010.

3.5 Discussion and conclusion

We study the effect of mosquito overwintering diapause by dividing the whole year into two periods. Compared with previous models, we use a more realistic method

to separate the year into the breeding season and the overwintering period. For the overwintering period, we consider the effect of temperature on diapause adult female mosquito mortality rate. Simulation results show that our model can capture the trend of observed average mosquito count very well. When we run our model under different weather conditions, it indicates that high temperature could lead to more mosquitoes with early peak while low temperature would cause fewer mosquitoes with later peak. We also study the theoretical properties of our model in breeding season by assuming there is no diapause adult female mosquitoes and temperature remains constant.

4 Hidden dimension method for spatio-temporal modeling of mosquito abundance

4.1 Introduction

Wang et al. (2011) use a generalized linear model to study the effect of temperature and precipitation on mosquito abundance. Many factors have impacts on mosquito abundance other than temperature and precipitation. These factors include land use conditions, elevation, humidity, and photoperiod at each trap. Some of these factors are usually missing, or simply unobservable. We also do not know the exact mechanism details of how some of these factors affect mosquito abundance. In this chapter, we study the spatio-temporal distribution of mosquito abundance by using hidden dimension method to estimate the collective impact of all the unobservable information for each trap except for daily weather conditions. The method is applied to mosquito surveillance data in Peel Region, Ontario, Canada. The results demon-

strate that the method significantly improves the modeling accuracy. Simulation results also confirm that the method can significantly improve the GLM fitting accuracy. In addition, we compare the method with Generalized Linear Mixed Models (GLMM). Simulation results show there are more improvements from our method than the GLMM. We also derive the condition when the MSE of GLM including missing information would be smaller compared to GLM without missing information.

Modeling spatio-temporal environmental processes remains a challenging task due to the complexity and intrinsic uncertainty of these processes. One significant challenge is to build a suitable model using limited information or data. Wang et al. (2011) build a mosquito abundance model for average mosquito abundance from 31 traps in Peel Region, Ontario, Canada. By using temperature and precipitation as factors, their model works well for the averaged mosquito counts in the region. However the model does not work well if it is used to model the mosquito count for each of the 31 traps. This may be due to the lack of information about the landscape or other unobservable information of each trap.

This phenomenon is quite common in scientific studies and can be viewed mathematically as modeling in a submanifold of the space in which all variables reside on. In physics, dimension expansion is used to explain the complex phenomenon in

three-dimensional space (Seiberg and Witten 1999, Witten 1995). Bornn et al. (2012) propose a novel method for modeling nonstationary processes through dimension expansion by projecting the geographic plane into higher dimensional space. This method relaxes the often common but untenable assumption that the underlying processes are stationary as discussed in Cressie and Cassie (1993). Dimension expansion is achieved by examining the theoretical variogram in a transformed higher dimension. Their method is justified by a fundamental result from Perrin and Meiring (2003) that a nonstationary random field in $\mathcal{R}^d$ can always be represented as a second-order stationary process in $\mathcal{R}^{2d}$.

In this chapter, we apply the hidden dimension method to model the spatio-temporal distribution of mosquito population by utilizing a loss function. Simulation results from application of the method to model mosquito abundance demonstrate that significant improvements in prediction can be achieved by modifying the classical GLM through dimension expansion. The outcome from realistic simulation studies which mimic mosquito patterns in reality also confirms that such improvements are indeed achievable and significant.

We believe that the method is a valuable modeling tool to understand environmental processes when collected samples do not contain all important relevant information. The current method, therefore, provides practitioners a way to evaluate

and assess the collective impact of unobservable information, and to efficiently improve model accuracy. For example, landscape or other geographical information is known to play a very important role in understanding the inhomogeneous spread of mosquitoes. However, this information might not be available for a given site. The model can take these missing factors into account by examining the fitting errors and provide a site-specific estimation of the collective impact on mosquito patterns for a given site. These local improvements, in turn, will significantly improve the accuracy of statistical models for spatio-temporal environmental processes.

At first glance, our model might seem to be similar to GLMM. However, they are different. The GLMM, which considers random effects by categories, is an improvement of the GLM. GLMM usually assumes random effect follows a normal distribution with zero mean, while in our approach, we do not have any assumption on the missing information. Both our method and the GLMM have smaller model error compared to regular GLM. We also compare the results of our method to the GLMM when applied to real data and the simulation data. It shows that our approach has a smaller error than the GLMM.

This chapter is organized as follows. We describe hidden dimension method by Bornn et al. (2012) in the rest of this section. In Section 4.2, we present the methodology of dimension expansion for spatio-temporal processes, and the method is applied

to mosquito abundance of Peel Region, Ontario, Canada. Results of simulation studies are presented in Section 4.3. In Section 4.4, we derive the condition that when the MSE of GLM with missing information is smaller than that without missing information, we also verify the conditions by simulations. We provide a discussion in Section 4.5.

4.1.1 Hidden dimension method

Bornn et al. (2012) develop a method to modeling nonstationary spatial fields by expanding the geographic plane into higher dimensional spaces. $\{Y(x) : x \in S\}, (S \in R^k)$ is a spatial process. If $Y(x)$ is stationary, the variogram model $2\gamma(x_r, x_s) = E(|Y(x_r) - Y(x_s)|^2)$ can become stationary variogram $\gamma_\phi(h)$, where $h = x_r - x_s$ is the different vector between locations and ϕ is the set of parameters. We assume $Y(x)$ is nonstationary, and $\gamma_\phi(h)$ will be a misspecification. The aim of the method is to find a higher dimension $S' \in R^{k+j}$, where $j > 0$, S is a subset of S' and $[x, z] \in S'$. In other words, they add extra dimensions $z_1, \cdots, z_s$ to observed location $x_1, \cdots, x_s$, which makes $Y([x, z])$ stationary with variogram model $\gamma_\phi([x_r, z_r], [x_s, z_s])$.

To get the hidden dimensions $z_1, \cdots, z_s$, they propose

$$\hat{\phi}, Z = \arg\min_{\phi, Z'} \sum_{r<s} (v^*_{rs} - \gamma_\phi(\bar{d_{rs}}([X, Z'])))^2, \tag{4.1}$$

where υ^*_{rs} is the estimated spatial dispersion between r and s, it can be

$$\upsilon^* = \frac{1}{\tau}\sum_{\tau}|Y(x_r) - Y(x_s)|^2,$$

where $\tau > 1$ is the multiple observations of the system.

Bornn et al. (2012) modify 4.1 by adding a group lasso penalty term on Z. The object function becomes

$$\hat{\phi}, Z = \arg\min_{\phi, Z'}\sum_{r<s}(\upsilon^*_{rs} - \gamma_\phi(\bar{d_{rs}}([X, Z'])))^2 + \lambda_1\sum_{k=1}^{p}\|Z'_{.,k}\|_1, \tag{4.2}$$

where $Z'_{.,k}$ is the kth column of Z'. For the variogram, they use the following exponential variogram,

$$\gamma_\phi(x_r, x_s) = \phi_1(1 - exp(-\|x_r - x_s\|/\phi_2)) + \phi_3,$$

where $\phi_1,\ \phi_2,\ \phi_3$ are parameters.

4.1.2 Current mosquito model

We use mosquito data from 2006 to 2012 from the 30 traps in Peel Region, Ontario (We ignore one trap since it missed the mosquito data in the year 2006). The raw data, however, are very noisy due to various uncontrollable factors. Therefore, we apply the three weeks moving average method to smooth the raw data to study the trends. This technique is well accepted in the literature since the smoothed data are more robust than the raw data.

We use the reanalysis data of ERA-Interim (Dee and National Center for Atmospheric Research Staff (Eds) 2017, Dee et al. 2011) with high spatial resolution ($0.125° \times 0.125°$, $\sim$ 10 km) as the historical weather data (daily mean temperature and daily total precipitation) in Peel Region. As shown in Figure 4.1, there are 13 grid points in and very close to Peel Region in ERA-Interim. So we use an interpolating thin-plate spline to interpolate each of the weather observation, add observations of temperature and precipitation from $n = 13$ sites to the 30 mosquito trap locations. The thin-plate spline (TPS) method, introduced by Duchon (1976, 1977), was first applied to weather data by Wahba and Wendelberger (1980). Many researchers have shown that it is an accurate, operationally straightforward and computationally efficient solution to the problem of spatial interpolation of weather data (Hutchinson 1995, Tait et al. 2006). What's more, in a comparison of different interpolation methods conducted by Jarvis and Stuart (2001), TPS achieved the best accuracy compared with ordinary kriging and inverse distance weighting method.

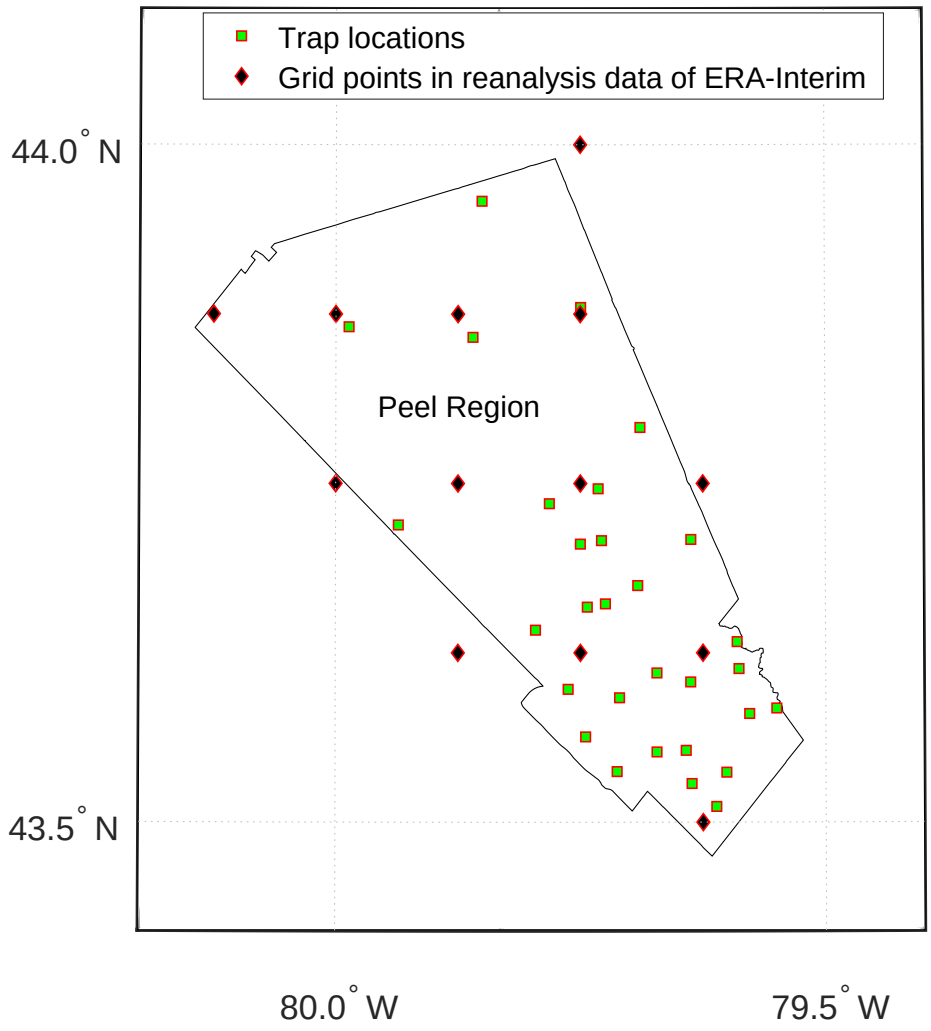

Figure 4.1: Trap locations in Peel Region and grid points in ERA-Interim.

When applying the model 2.3 on average *Culex* mosquito trap count in Peel Region from 2006 to 2012, we use deviance as a statistic to compare different models with combinations of $ddm_t^{[n]}$s and $ppm_t^{[m]}$s. We find that the model with $ddm_t^{[12]}$ and

$ppm_t^{[42]}$ achieves the lowest deviance (smaller deviance represents a better model) in all 3600 models, so we will use $ddm_t^{[12]}$ and $ppm_t^{[42]}$ in this study.

4.2 Our missing information method

4.2.1 Modeling through dimension expansion

Let $\{y_1, \cdots, y_n\}$ be n independent observations of a response, where y_i is treated as a realization of a random variable Y_i. Assume that the observations follow a distribution in exponential family with the following density function,

$$f(y_i) = exp\left\{\frac{y_i\theta_i - b(\theta_i)}{a_i(\phi)} + c(y_i, \phi)\right\}, \tag{4.3}$$

where θ_i and ϕ are parameters, $a_i(\phi)$, $b(\theta_i)$ and $c(y_i, \phi)$ are known functions. $a_i(\phi)$ has following form,

$$a_i(\phi) = \frac{\phi}{p_i}, \tag{4.4}$$

where p_i is a known prior weight. If Y_i has a distribution in the exponential family, it has mean and variance

$$E(Y_i) = \mu_i = b'(\theta_i); \quad Var(Y_i) = \sigma_i^2 = b''(\theta_i)a_i(\phi).$$

For GLM (Nelder and Baker 1972), one defines a link function $g(\mu_i) = \eta_i$ which describes how the mean $E(Y_i) = \mu_i$ depends on the linear predictor. Therefore the

generalized linear model with spatio-temporal setting can be defined as

$$\begin{aligned} E(Y_{k,t}) &= \mu_{k,t}, \\ g(\mu_{k,t}) &= \eta_{k,t}, \\ \eta_{k,t} &= \beta_0 + \beta_1 x^1_{k,t} + \cdots + \beta_p x^p_{k,t}, \end{aligned} \tag{4.5}$$

where k in $Y_{k,t}$ is location index ($1 \leq k \leq K$) and t is time index ($1 \leq t \leq T$). Let $\mathbf{x^j} = (x^j_{k,t})_{K \times T}$ be the matrix corresponding to jth predictor, $1 \leq j \leq p$.

When confronted by incomplete information, we assume that the collection of all independent variables includes $\mathbf{x^1},\ \mathbf{x^2}, \cdots,\ \mathbf{x^p},\ \mathbf{u^1}, \cdots,\ \mathbf{u^m}$. We can only observe $\mathbf{x^1},\ \mathbf{x^2}, \cdots,\ \mathbf{x^p}$, while $\mathbf{u^1}, \cdots,\ \mathbf{u^m}$ are not observable.

So we construct a new linear predictor in GLM as following,

$$\widehat{\eta}_{k,t} = \beta_0 + \beta_1 x^1_{k,t} + \cdots + \beta_p x^p_{k,t} + z_k, \tag{4.6}$$

where z_k represents the collective impact of all unobserved information $u^1_{k,t}, \cdots,\ u^m_{k,t}$ for location k.

In order to find z_k, it is desirable to have the new predicted output $g^{-1}(\widehat{\eta}_{k,t})$ to be as close as possible to observations $y_{k,t}$. The closeness, however, can be arbitrarily defined. Denote the loss function by $\psi(y_{k,t}, \widehat{\eta}_{k,t})$. The collective impacts z_k can then be estimated by the following:

$$\mathbf{z} = \arg\min_{\mathbf{z}} \sum_{k,t} \psi(y_{k,t}, \widehat{\eta}_{k,t}), \tag{4.7}$$

where $\mathbf{z} = (z_1, z_2, \cdots, z_K)^T$.

It is clear that the estimated z_k's depend on the chosen loss function. With the purpose of improving model prediction accuracy, we want the distance of observations $y_{k,t}$ and predicted output $g^{-1}(\widehat{\eta}_{k,t})$ to be as small as possible, so we choose the loss function in this study as follows:

$$\psi(y_{k,t}, \widehat{\eta}_{k,t}) = |y_{k,t} - g^{-1}(\widehat{\eta}_{k,t})|. \tag{4.8}$$

4.2.2 Application on mosquito modeling

Model 2.3 is for average mosquito abundance in Peel Region, Ontario, Canada. We adjust it and construct a model for mosquito abundance of each trap in Peel Region. There are 30 traps with available data, so we have $K = 30$. From 2006 to 2012, we take mosquito data from week 25 to week 39. For each year, we use one model to study mosquito abundance, so we have $T = 15$ and get the following Gamma GLM for mosquito abundance of each trap for a certain year,

$$\begin{aligned} E(\rho_{k,t}) =& \mu_{k,t}, \\ g(\mu_{k,t}) =& log(\mu_{k,t}) = \eta_{k,t}, \\ \eta_{k,t} =& \beta_0 + \beta_1 \ (ddm_{k,t}^{[12]})^2 + \beta_2 \ ddm_{k,t}^{[12]} + \beta_3 \ (ppm_{k,t}^{[42]})^2 \\ &+ \beta_4 \ ppm_{k,t}^{[42]} + \beta_5 \ ddm_{k,t}^{[12]} \ ppm_{k,t}^{[42]}, \end{aligned} \tag{4.9}$$

where $\rho_{k,t}$ is the captured mosquito number of trap k at week t, $1 \leq k \leq 30,\ 1 \leq t \leq 15$, we assume $\rho_{k,t} \sim Gamma(\alpha, \beta)$. $ddm_{k,t}^{[12]}$ is 12 days of arithmetic means of daily growing degree-day before mosquito collection of week t at trap k, $ppm_{k,t}^{[42]}$ is 42 days of arithmetic means of daily precipitation before mosquito collection of week t at trap k. We add the interaction term of $ddm_{k,t}^{[12]}\ ppm_{k,t}^{[42]}$ since we believe interaction of temperature and precipitation also has an impact on mosquito abundance.

Model 2.3 works well for average mosquito abundance of Peel Region, but for mosquito abundance in each trap, the model defined by equation (4.9) has large error compared with surveillance data. For simplicity, we call the model defined by equation (4.9) the partial model. To improve the accuracy of the partial model and have a better understanding of the spatial distribution of mosquito population, we apply our method. We assume that missing information for trap k can be represented by one variable z_k, so we get a new linear predictor $\widehat{\eta}_{k,t}$, and the model with dimension expansion for one year can be defined as follows,

$$\begin{aligned} E(\rho_{k,t}) =& \mu_{k,t}, \\ g(\mu_{k,t}) =& log(\mu_{k,t}) = \widehat{\eta}_{k,t}, \\ \widehat{\eta}_{k,t} =& \beta_0 + \beta_1\ (ddm_{k,t}^{[12]})^2 + \beta_2\ ddm_{k,t}^{[12]} + \beta_3\ (ppm_{k,t}^{[12]})^2 \\ &+ \beta_4\ ppm_{k,t}^{[42]} + \beta_5\ ddm_{k,t}^{[12]}\ ppm_{k,t}^{[42]} + z_k, \end{aligned} \tag{4.10}$$

where $\mathbf{z} = (z_1,\ z_2, \cdots,\ z_k)'$ can be estimated by

$$\mathbf{z} = \arg\min_{\mathbf{z}} \sum_{k,t} |y_{k,t} - g^{-1}(\widehat{\eta}_{k,t})|, \tag{4.11}$$

$y_{k,t}$ is the observed number of mosquito caught in trap k at week t for the year, $\mathbf{z}$ is estimated for each year so it could be different for different years.

Traps have different land use types. In general, land use is categorized into three types: built environment, green land, and open area. We use built environment proportion in $1km$ radio of each trap as land use information for the trap. Then we introduce the model with land use information for each year which is defined as:

$$\begin{aligned} E(\rho_{k,t}) =& \mu_{k,t}, \\ g(\mu_{k,t}) =& log(\mu_{k,t}) = \widetilde{\eta}_{k,t}, \\ \widetilde{\eta}_{k,t} =& \beta_0 + \beta_1\ (ddm_{k,t}^{[12]})^2 + \beta_2\ ddm_{k,t}^{[12]} + \beta_3\ (ppm_{k,t}^{[42]})^2 \\ &+ \beta_4\ ppm_{k,t}^{[42]} + \beta_5\ ddm_{k,t}^{[12]}\ ppm_{k,t}^{[42]} + \beta_6 l_k. \end{aligned} \tag{4.12}$$

where l_k is the built environment proportion for trap k.

We calculate errors of modeled mosquito abundance from 2006 to 2012 and show them in Table 4.1.

Year	E_0 (Partial model)	E_1 (Model with land)	E_2 (GLMM)	E_3 (Dimension)
2006	146.03	140.03 (0.04)	94.57 (0.35)	89.00 (0.39)
2007	229.05	214.32 (0.06)	126.95 (0.45)	125.01 (0.45)
2008	458.79	438.13 (0.05)	241.22 (0.47)	232.84 (0.49)
2009	488.60	485.57 (0.01)	259.58 (0.47)	237.79 (0.51)
2010	408.50	406.75 (0.00)	206.35 (0.49)	189.62 (0.54)
2011	323.28	314.76 (0.03)	167.42 (0.48)	153.41 (0.53)
2012	425.75	407.01 (0.04)	208.64 (0.51)	189.94 (0.55)

Table 4.1: Comparison of fitting accuracy of different models. NOTE: The numbers in bracket after E_1 is the proportion of absolute error reduced compared with absolute error of the partial model, which is $(E_0 - E_1)/E_0$. Similar for the numbers in the bracket after E_2 and E_3, they are $(E_0 - E_2)/E_0$ and $(E_0 - E_3)/E_0$.

In Table 4.1, we have $E_0 = \frac{1}{T}\sum_{k,t} |\hat{y}_{k,t} - y_{k,t}|$ for each year, $y_{k,t}$ is observed mosquito abundance in trap k at week t, where $\hat{y}_{k,t}$ is modeled mosquito abundance of trap k at week t from the partial model. $E_1 = \frac{1}{T}\sum_{k,t} |\hat{y}^{[1]}_{k,t} - y_{k,t}|$, where $\hat{y}^{[1]}_{k,t}$ is modeled mosquito abundance in trap k at week t from the model with land use information. $E_2 = \frac{1}{T}\sum_{k,t} |\hat{y}^{[2]}_{k,t} - y_{k,t}|$, in which $\hat{y}^{[2]}_{k,t}$ is modeled mosquito abundance in trap k at week t from the GLMM. $E_3 = \frac{1}{T}\sum_{k,t} |\hat{y}^{[3]}_{k,t} - y_{k,t}|$, where $\hat{y}^{[3]}_{k,t}$ is modeled mosquito abundance in trap k at week t from the model with dimension expansion.

Table 4.1 shows that the average absolute error of the model with dimension expansion is significantly less than that of the partial model (E_3 is almost half of E_0 for each year). This demonstrates the benefit of using the dimension expansion

method compared with the original model (the partial model). Compared with GLMM, our method can lead to more improvement (E_3 is less than E_2). Figures 4.2 to 4.8 show the observed mosquito abundance and modeled mosquito abundance for the 30 traps from the year 2006 to the year 2012. In Figure 4.2 to 4.8 between week 25 and week 39, the blue line shows the observed mosquito abundance, the dashed black line presents modeled mosquito abundance by the partial model. The green line represents modeled mosquito abundance from the model with dimension expansion. The pink line is modeled mosquito abundance from GLMM and the red line shows modeled mosquito abundance from the model with land use information.

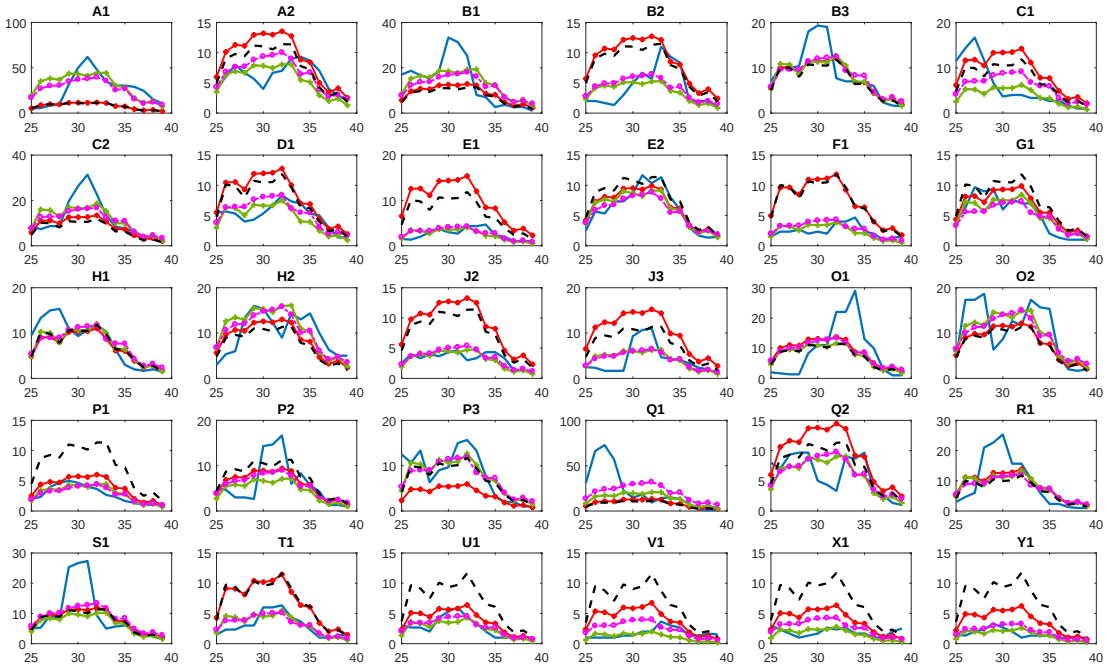

Figure 4.2: Observed mosquito trap counts (blue) and modeled mosquito trap counts of each trap for the year 2006. The modeled mosquito trap counts by the partial model is described by the dashed black line, modeled mosquito trap counts from the model with dimension expansion is represented by the green line, modeled mosquito trap counts from the model with land use information is in the red line, modeled mosquito trap counts from GLMM is presented by the pink line.

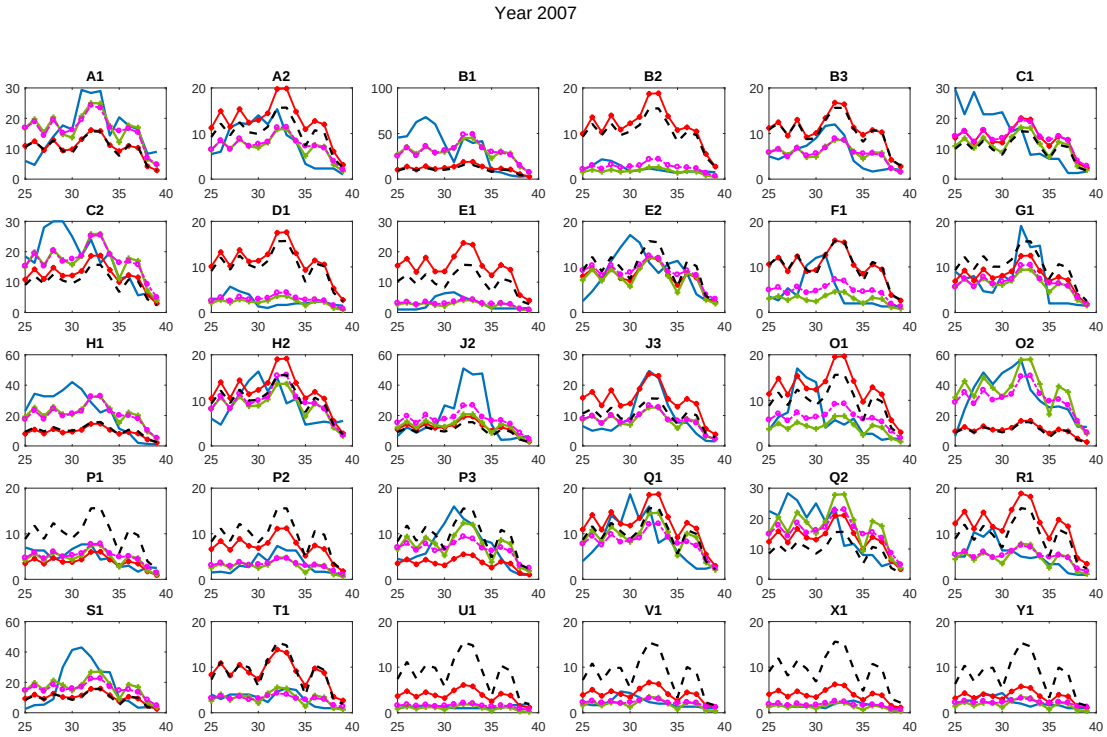

Figure 4.3: Observed mosquito trap counts (blue) and modeled mosquito trap counts of each trap for year 2007.

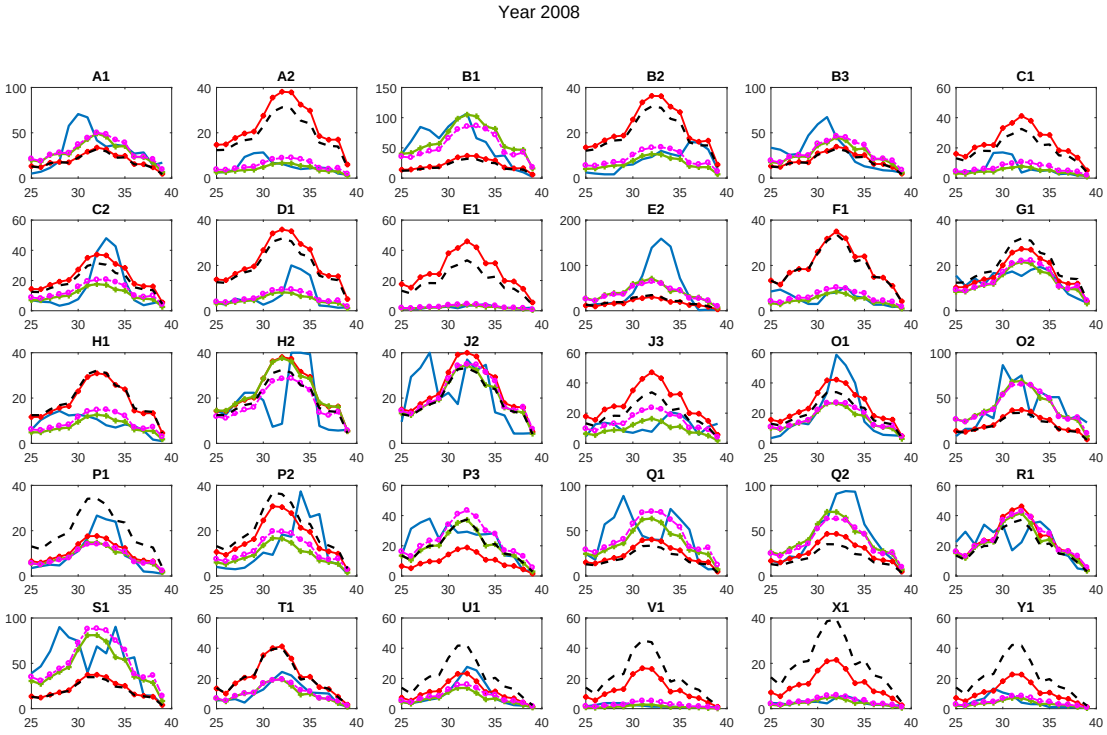

Figure 4.4: Observed mosquito trap counts (blue) and modeled mosquito trap counts of each trap for year 2008.

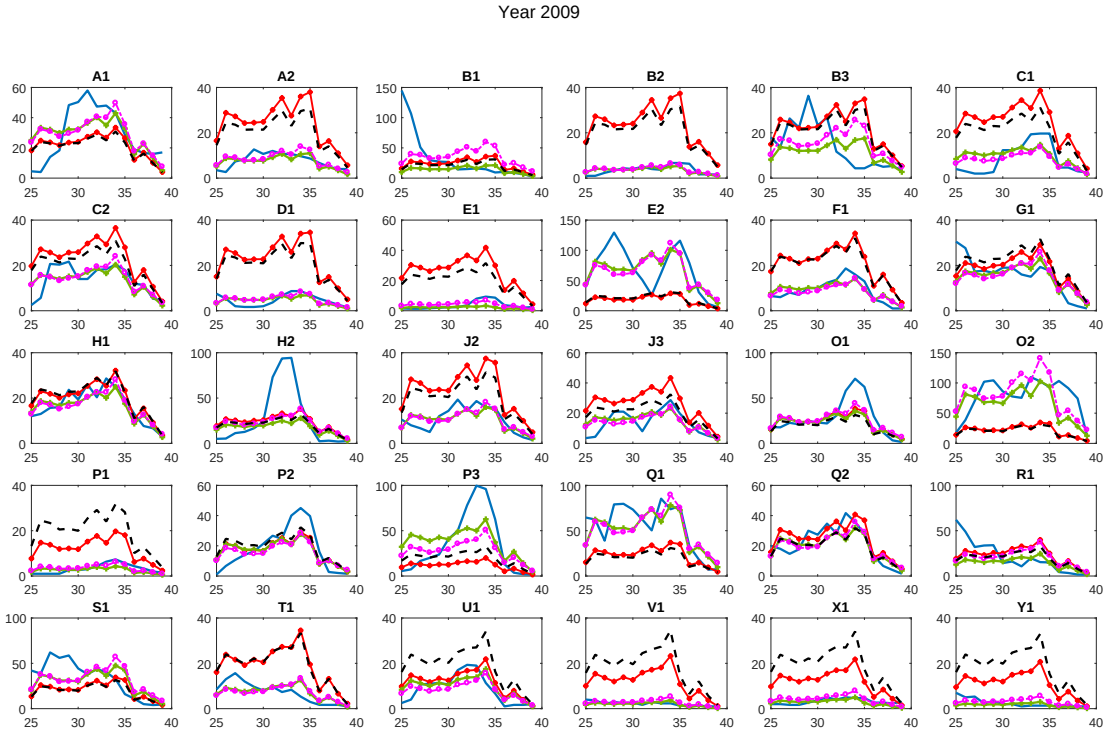

Figure 4.5: Observed mosquito trap counts (blue) and modeled mosquito trap counts of each trap for year 2009.

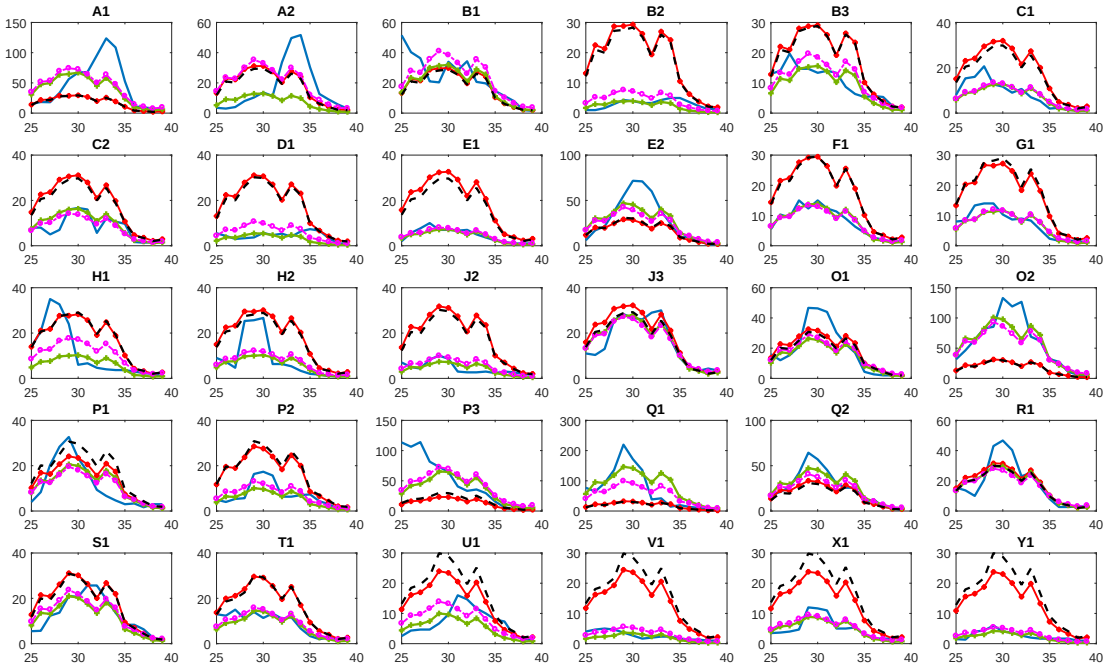

Figure 4.6: Observed mosquito trap counts (blue) and modeled mosquito trap counts of each trap for year 2010.

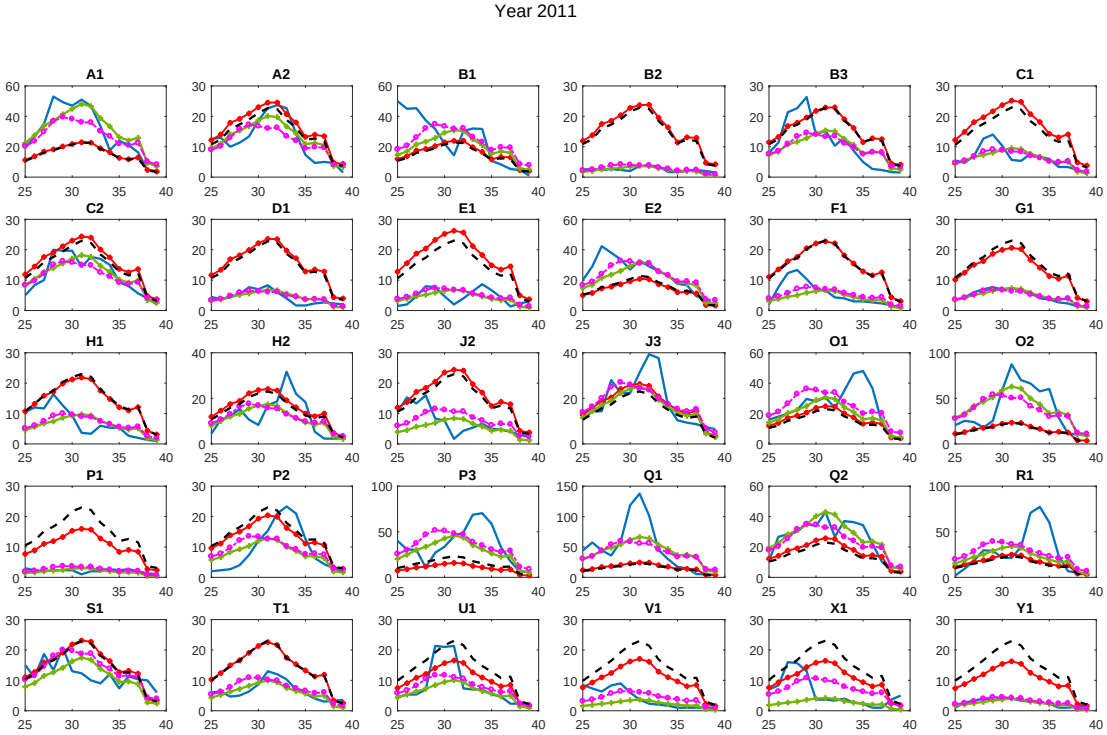

Figure 4.7: Observed mosquito trap counts (blue) and modeled mosquito trap counts of each trap for year 2011.

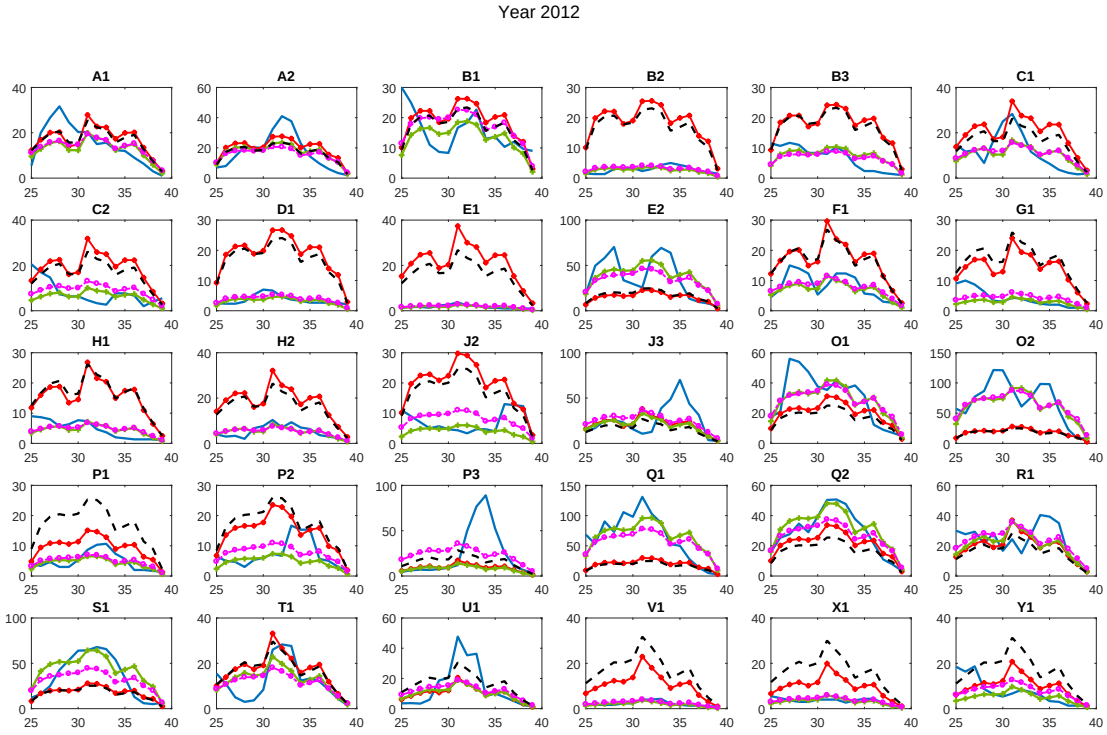

Figure 4.8: Observed mosquito trap counts (blue) and modeled mosquito trap counts of each trap for year 2012.

In general, our method works well across all 30 traps in Peel region. However, the magnitude of improvement varies from one spatial location to the next. The histogram of average error reductions from 2006 to 2012 for each trap is shown in Figure 4.9.

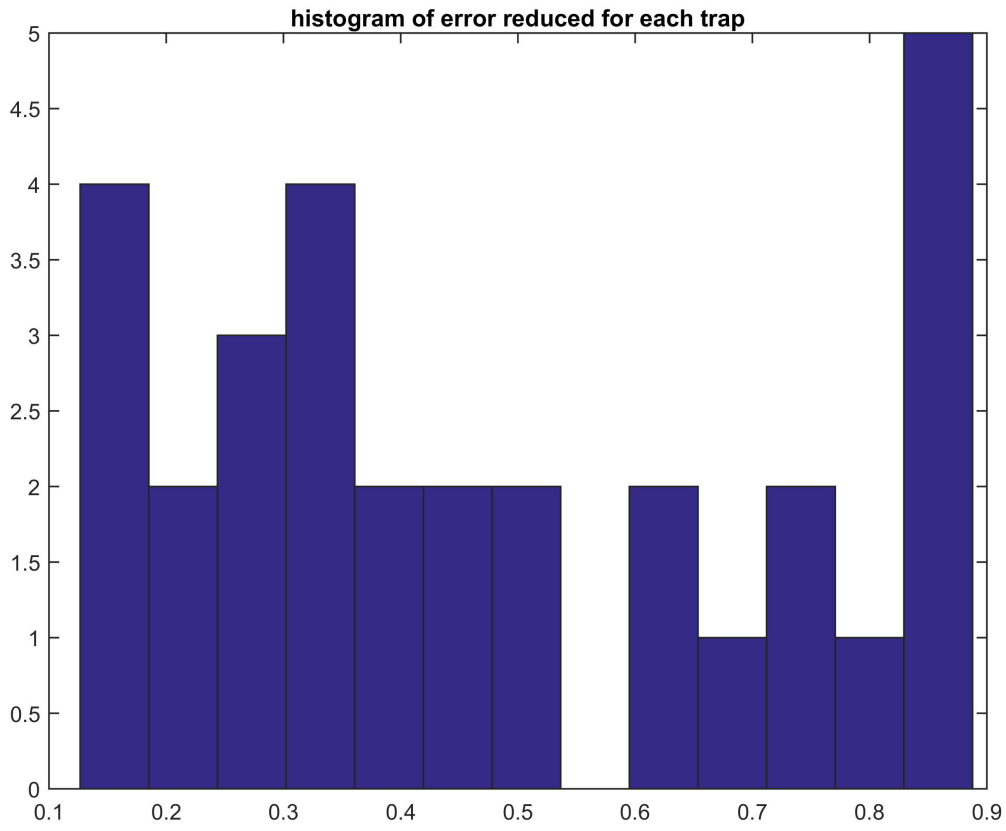

Figure 4.9: Histogram of average error reduced by our method for each trap.

There is a gap at 0.6 which naturally divides the 30 traps into two sub-groups. We call the upper group the high improvement group with 11 traps and the other one the low improvement group with 19 traps.

Figure 4.10 shows the locations of traps of the two groups and identification of group memberships in Peel Region of Ontario, Canada.

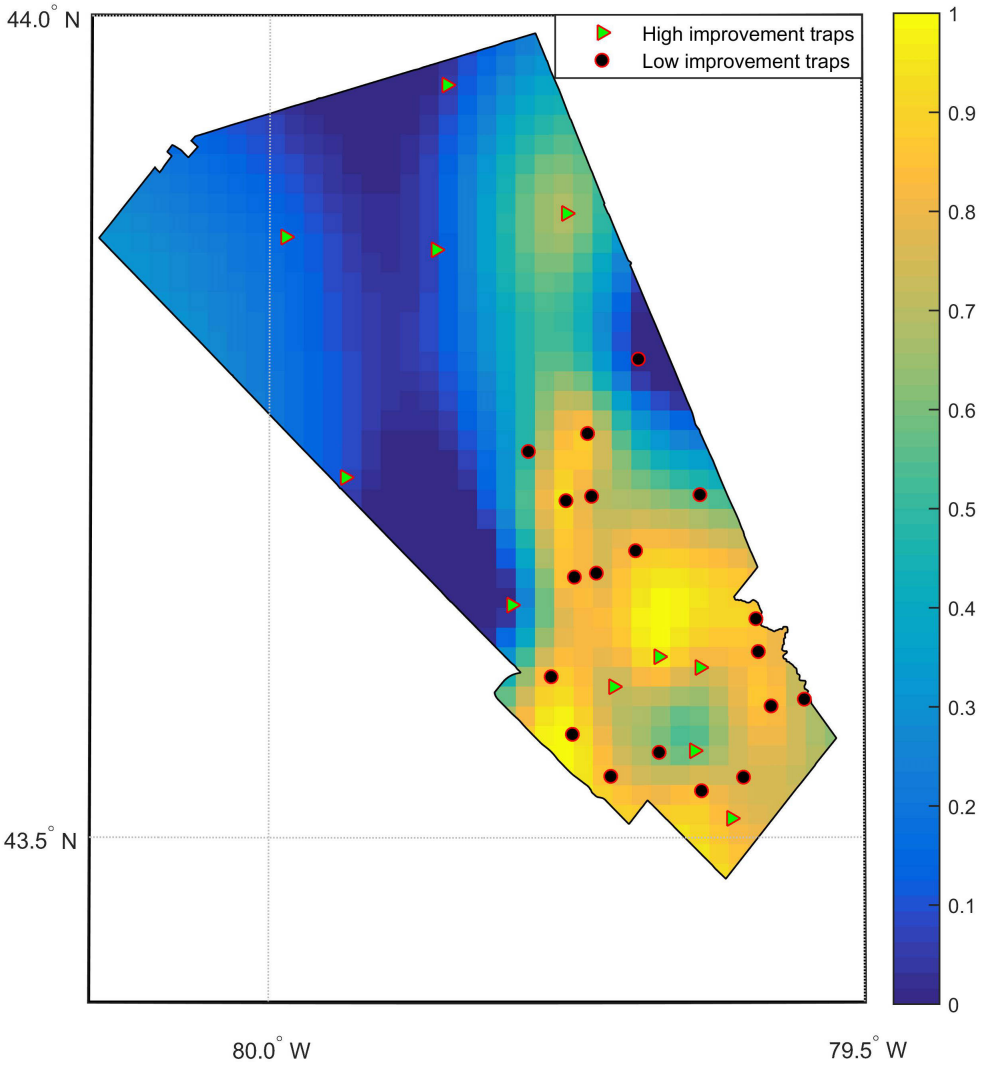

Figure 4.10: Locations of traps in the two groups and the proportion of built environment in Peel Region.

As shown in Figure 4.10, the high improvement traps tend to locate in the low built environment locations while low improvement traps tend to be in high built

areas. Proportions of built environment are relatively low in the high improvement group (with mean 0.4473), in comparison with those in the low improvement group (with mean 0.7532). To confirm the built environment proportion differences, we do a permutation test with the null hypothesis that the land use data (built environment proportion l_k) of traps in high improvement group and low improvement group are from populations with the same mean. The test gives a p value of 0.0056 which rejects the null hypothesis and indicates that the differences are significant. This shows that mosquitoes in the low built environment area have different patterns compared with mosquitoes in high built environment area. The partial model works well in an urban area with more buildings. Our method could significantly improve the partial model in areas with more green land and open areas.

To better understand the different performance of the two groups, we also compare the missing information z_k found in high improvement group to that found in low improvement group. We combine all the values across the 7 years of observation period to make the comparison (we have $7 * 11 = 77$ $z_k's$ for high improvement traps and $7 * 19 = 133$ $z_k's$ for low improvement traps).

We perform a permutation test with the null hypothesis that the $z_k's$ found for traps in high improvement group and low improvement group are from populations with the same mean. The permutation test shows a significant difference between

$z_k's$ found in the high improvement group and the low improvement group (with $p < 0.0001$). The missing information found for traps in high improvement group has negative value with mean -1.3524 (which is significantly different from 0 with $p < 0.0001$ from permutation test), which indicates that the partial model tends to over-estimate for the traps in high improvement group.

4.3 Simulation and Application

In this section, we evaluate the performance of our proposed method by numerical simulations. In the first simulation, we assume the model with land use information is the true model, and use the output of it to generate simulated mosquito abundance from a gamma distribution. Then we use the generated mosquito abundance and observed historical *ddm* and *ppm* to fit a partial model by pretending that the land use information is not known. In comparisons, we apply the model with dimension expansion and GLMM. Absolute errors are used for comparison purposes and find significant improvements using the model with dimension expansion and GLMM, but there are more improvements from the model with dimension expansion than the GLMM as shown in the simulation, which indicates that our method can lead more improvements than the GLMM.

It is also well known that a regression model will have a better fit even if one

unrelated variable is added. In the second simulation study, we assume that land use information has no impact on the mosquito abundance. Therefore a GLM with only *ddm* and *ppm* now becomes the correct model. We then compare the performance of the model with dimension expansion and the model with only *ddm* and *ppm*, and observe comparable performance. This indicates that the dimension expansion approach will not add unnecessary dimension when there is none. Furthermore, this justifies the observed improvement in the first simulation study.

4.3.1 Simulation study with land use information in the true Model

We recall the model with land use information, defined as follows:

$$
\begin{aligned}
E(\rho_{k,t}) =& \mu_{k,t}, \\
g(\mu_{k,t}) =& log(\mu_{k,t}) = \widetilde{\eta}_{k,t}, \\
\widetilde{\eta}_{k,t} =& \beta_0 + \beta_1 \ (ddm_{k,t}^{[12]})^2 + \beta_2 \ ddm_{k,t}^{[12]} + \beta_3 \ (ppm_{k,t}^{[42]})^2 + \beta_4 \ ppm_{k,t}^{[42]} \\
& + \beta_5 \ ddm_{k,t}^{[12]} \ ppm_{k,t}^{[42]} + \beta_6 l_k.
\end{aligned}
$$

In this simulation study, firstly, we use a Gamma distribution to randomly generate new mosquito abundance, the scale parameter of the Gamma distribution is $a = 1$ and shape parameter $b = \hat{y}_{k,t}^{[1]}$ is modeled mosquito abundance from the model with land use information (model (4.12), which is fitted using observed mosquito

abundance, *ddm*, *ppm* and land use data of Peel Region from 2006 to 2012). Then we use the generated mosquito abundance and corresponding *ddm*, *ppm* (Peel Region from 2006 to 2012) to fit the partial model (model(4.9)), GLMM and the model with dimension expansion (model (4.10)). Finally, we compare the absolute errors of the three models (the model with dimension expansion, GLMM, and the partial model). We also generated new mosquito abundance with larger variance but same mean (use $a = 1/2$, $b = 2 * \hat{y}_{k,t}^{[1]}$ to generate new mosquito abundance with variance 2 times as before, with $a = 1/5$, $b = 5 * \hat{y}_{k,t}^{[1]}$ to generate new mosquito abundance with variance 5 times as before) to compare the effect of noise and show the results in Table 4.2,

Year	$(\overline{E}_0 - \overline{E}_2^*)/\overline{E}_0$ (GLMM 1var/2var/5var)	$(\overline{E}_0 - \overline{E}_2)/\overline{E}_0$ (Dimension 1var/2var/5var)
2006	0.3876/0.2932/0.1912	0.4244/0.3446/0.2592
2007	0.5452/0.4461/0.3179	0.5218/0.4424/0.3379
2008	0.5391/0.4553/0.3328	0.5417/0.4723/0.3682
2009	0.4036/0.3406/0.2453	0.4306/0.3730/0.2870
2010	0.1614/0.1198/0.0755	0.2348/0.2096/0.1778
2011	0.3090/0.2257/0.1480	0.3494/0.2767/0.2063
2012	0.4459/0.3633/0.2524	0.4589/0.3862/0.2872

Table 4.2: Average percentage of errors reduced, our method and GLMM, with different variance, 1var/2var/5var. NOTE: We repeat the simulation 200 times for each year. $\overline{E}_0$ is mean absolute error of the partial model, $\overline{E}_2$ is mean absolute error of the model with dimension expansion. $\overline{E}_2^*$ is mean absolute error of the GLMM.

Based on information in Table 4.2, our method can reduce error by 0.23 to 0.54 on average. This indicates that our model can find the missing information and significantly improve the model. With original variance, there is only one year that GLMM reduces more error than our method (the year 2007, 0.5452 compare with 0.5218). While with five times of the original variance, our method reduces more errors than GLMM for all the years. This shows that when we increase the variance/noise, our method has more power than the GLMM to reduce the error.

4.3.2 Simulation study without land use information in the true Model

First, we randomly generate new mosquito abundance from a Gamma distribution. The scale parameter of the Gamma distribution is $a = 1$. The shape parameter $b = \hat{y}_{k,t}$ is modeled mosquito abundance from the partial model (the model is fitted using observed *ddm*, *ppm* and mosquito abundance of Peel Region from 2006 to 2012). We then use the generated mosquito abundance and corresponding *ddm*, *ppm* (Peel Region from 2006 to 2012) to fit the partial model and the model with dimension expansion. Then we compare the absolute errors of the two models. Table 4.2 shows the simulation results,

Year	2006	2007	2008	2009	2010	2011	2012
$(\overline{E}_0 - \overline{E}_2)/\overline{E}_0$	0.0659	0.0628	0.0624	0.0599	0.0672	0.0596	0.0612

Table 4.3: Average percentage of errors reduced by our method. NOTE: We repeat the simulation 200 times for each year. $\overline{E}_0$ is mean absolute error of the partial model, $\overline{E}_2$ is mean absolute error of the model with dimension expansion.

As shown in Table 4.3, our method can only reduce the error by $0.0596 - 0.0672$. This indicates that the absolute errors of the partial model and that of the model with dimension expansion are similar. Therefore it shows that the missing information found through our dimension expansion method is necessary when there is missing information, and if there is no missing information, the dimension expansion method

does not add any unrelated information.

4.4 Theory results

In this section, we show the condition when the GLM with missing information has smaller MSE compared with GLM without missing information. Suppose we have the following fitting GLM as the model without missing information,

$$\begin{aligned} \mathrm{E}(\mathbf{y}) &= \boldsymbol{\mu}, \\ g(\boldsymbol{\mu}) &= \boldsymbol{\eta}, \\ \boldsymbol{\eta} &= \mathbf{X}\boldsymbol{\beta}_0, \end{aligned} \tag{4.13}$$

where $\boldsymbol{y}_{n\times 1}$ is the n observations, with $\boldsymbol{\mu}$ as the expection, g is the link function, $\boldsymbol{\eta}$ is the linear predictor, $\boldsymbol{X}_{n\times p}$ is the design matrix, and the $p \times 1$ coefficient is $\boldsymbol{\beta}_0$.

We have the following model as the truth model with missing inofrmation,

$$\begin{aligned} \mathrm{E}(\mathbf{y}) &= \boldsymbol{\mu}_T, \\ g(\boldsymbol{\mu}_T) &= \boldsymbol{\eta}_T, \\ \boldsymbol{\eta}_T &= \mathbf{X}\boldsymbol{\beta}_0 + \mathbf{x}_u\beta_u, \\ &= (\mathbf{X}, \mathbf{x}_u) * \begin{pmatrix} \boldsymbol{\beta}_0 \\ \beta_u \end{pmatrix}, \\ &= \widetilde{\mathbf{X}} * \boldsymbol{\beta}_T, \end{aligned} \tag{4.14}$$

where $\mathbf{x}_u$ is the hidden unobserved dimension $(n \times 1)$, and β_u is the corresponding coefficient, $\widetilde{\mathbf{X}} = (\mathbf{X}, \mathbf{x}_u)$, and $\boldsymbol{\beta}_T = \binom{\boldsymbol{\beta}_0}{\beta_u}$. We have $\mathrm{MSE}(\hat{\boldsymbol{\mu}}) = \mathrm{E}[(\hat{\boldsymbol{\mu}} - \boldsymbol{\mu}_T)^2]$ for the fitting model and $\mathrm{MSE}(\hat{\boldsymbol{\mu}}_T) = \mathrm{E}[(\hat{\boldsymbol{\mu}}_T - \boldsymbol{\mu}_T)^2]$ for the truth model. We define $M_1 = \frac{1}{n}\mathrm{tr}(\mathrm{MSE}(\hat{\boldsymbol{\mu}}))$ and $M_2 = \frac{1}{n}\mathrm{tr}(\mathrm{MSE}(\hat{\boldsymbol{\mu}}_T))$, and show that under certain conditions, $M_2 < M_1$.

For $\mathrm{MSE}(\hat{\boldsymbol{\mu}})$, we use the similar method in Adewale and Xu (2010) with different setting. Let

$$\mathbf{b} = \frac{\mathbf{X}^T(\boldsymbol{\mu}_T - \boldsymbol{\mu})}{n * a(\phi)}, \tag{4.15}$$

$$\omega_i = \frac{\partial \mu_i / \partial \eta_i}{a(\phi)},\ \omega_{\mathrm{T},i} = \frac{\mathrm{Var}_T(y_i)}{a^2(\phi)}, \tag{4.16}$$

where μ_i is the i-th element of $\boldsymbol{\mu}$ and η_i is the i-th element of $\boldsymbol{\eta}$, y_i is the i-th element of $\mathbf{y}$. Define W and W_T as the diagonal matrix with diagonal elements ω_i and $\omega_{\mathrm{T},i}$ respectively. And define

$$\mathbf{H}_n = \frac{1}{n}\mathbf{X}^T W \mathbf{X},$$
$$\widetilde{\mathbf{H}}_n = \frac{1}{n}\mathbf{X}^T W_T \mathbf{X},$$

we have the following results,

Lemma 4.4.1. *For generalized linear models with canonical link function, the MLE $\widetilde{\boldsymbol{\beta}}$ of $\boldsymbol{\beta}_0$ from the fitting model has the following asymptotic bias and asymptotic*

covariance matrix,

$$\text{Bias}(\widehat{\boldsymbol{\beta}}) = \text{E}(\widehat{\boldsymbol{\beta}} - \boldsymbol{\beta}_0) = \mathbf{H}_n^{-1}\mathbf{b} + o(n^{-1/2}), \tag{4.17}$$

$$\text{Cov}(\sqrt{n}(\widehat{\boldsymbol{\beta}} - \boldsymbol{\beta}_0)) = \mathbf{H}_n^{-1}\widetilde{\mathbf{H}}_n\mathbf{H}_n^{-1} + o(1). \tag{4.18}$$

Theorem 4.4.2. *For GLM with canonical link, if* $W \approx W_T$ *and* $\beta_u^2 < (\mathbf{x}_u^T W_T \mathbf{x}_u - \mathbf{x}_u^T W_T \mathbf{X}(\mathbf{X}^T W_T \mathbf{X})^{-1}\mathbf{X}^T W_T \mathbf{x}_u)^{-1}$*, then* $M_1 < M_2$*.*

For GLM with non-canonical link, we focus on the log-gamma GLM since our method is based it. Define

$$\mathbb{H}_n = \frac{1}{n\phi}\mathbf{X}^T\Delta_{\boldsymbol{y}}\mathbf{X} = -\frac{1}{n}\frac{\partial^2 l_n(\boldsymbol{\beta})}{\partial\boldsymbol{\beta}\partial\boldsymbol{\beta}^T}, \tag{4.19}$$

$$\tilde{\mathbf{b}} = \frac{1}{n\phi}\mathbf{X}^T\Delta(\boldsymbol{\mu}_T - \boldsymbol{\mu}), \tag{4.20}$$

and

$$\widetilde{\mathbb{H}}_n = \frac{1}{n^2}\mathbf{X}^T\Delta\mathbf{W}_T\Delta\mathbf{X}, \tag{4.21}$$

where $\Delta_{\boldsymbol{y}} = diag\{\frac{y_i}{\exp(\mathbf{x}_i^T\boldsymbol{\beta}_0)}\}$ and $\Delta = diag\{\frac{1}{\exp(\mathbf{x}_i^T\boldsymbol{\beta}_0)}\}$. We have the following lemma,

Lemma 4.4.3. *For log-gamma GLM with normalized covariate, the MLE* $\widetilde{\boldsymbol{\beta}}$ *of* $\boldsymbol{\beta}_0$ *from the fitting model has the following asymptotic bias and asymptotic covariance*

matrix,

$$\text{Bias}(\widehat{\boldsymbol{\beta}}) = \text{E}(\widehat{\boldsymbol{\beta}} - \boldsymbol{\beta}_0) = \mathbb{H}_n^{-1}\tilde{\mathbf{b}} + o(n^{-1/2}), \tag{4.22}$$

$$\text{Cov}(\sqrt{n}(\widehat{\boldsymbol{\beta}} - \boldsymbol{\beta}_0)) = \mathbb{H}_n^{-1}\widetilde{\mathbb{H}}_n\mathbb{H}_n^{-1} + o(1). \tag{4.23}$$

We define condition $S0$ as following,

Condition S0:

- $x_u^T\beta_u$ is small, which indicates that $\phi\Delta W_T\Delta \approx I$.
- $\Delta_{\boldsymbol{y}} \approx I$.

Theorem 4.4.4. *For log-gamma GLM with normalized covariate, if condition $S0$ holds, and $\beta_u^2 < \phi(\mathbf{x}_u^T W_T \mathbf{x}_u - \mathbf{x}_u^T W_T \mathbf{X}(\mathbf{X}^T W_T \mathbf{X})^{-1}\mathbf{X}^T W_T \mathbf{x}_u)^{-1}$, then $M_1 < M_2$.*

4.4.1 Proofs

We show the proof of lemma 4.4.1, 4.4.2, 4.4.3, and 4.4.4 in this section. Based on the similar idea used in Adewale and Xu (2010), but with different setting, proof of the lemma 4.4.1 is as following,

Proof. Under the conditions in Fahrmexr (1990), $\hat{\boldsymbol{\beta}}$ exists and consist. We also have

$$\frac{\partial l_n(\boldsymbol{\beta})}{\partial \boldsymbol{\beta}} = \sum_{i=1}^{n} \frac{\partial l_i(\boldsymbol{\beta})}{\partial \boldsymbol{\beta}}$$

$$
\begin{aligned}
&= \sum_{i=1}^{n} \frac{\partial l_i}{\partial \theta_i} \frac{\partial \theta_i}{\partial \mu_i} \frac{\partial \mu_i}{\partial \eta_i} \frac{\partial \eta_i}{\partial \boldsymbol{\beta}} \\
&= \sum_{i=1}^{n} \frac{(y_i - \mu_i)}{var(y_i)} \mathbf{x}_i \frac{\partial \mu_i}{\partial \eta_i} \\
&= \sum_{i=1}^{n} \frac{(y_i - \mu_i)}{a(\phi)} \mathbf{x}_i,
\end{aligned}
$$

$$
\begin{aligned}
-\frac{\partial^2 l_n(\boldsymbol{\beta})}{\partial \boldsymbol{\beta} \partial \boldsymbol{\beta}^T} &= -\sum_{i=1}^{n} \frac{1}{a(\phi)} \mathbf{x}_i \frac{\partial (y_i - \mu_i)}{\boldsymbol{\beta}^T} \\
&= -\sum_{i=1}^{n} \frac{1}{a(\phi)} \mathbf{x}_i \frac{\partial (-\mu_i)}{\partial \eta_i} \frac{\partial \eta_i}{\partial \boldsymbol{\beta}^T} \\
&= \sum_{i=1}^{n} \omega_i \mathbf{x}_i \mathbf{x}_i^T \\
&= \mathbf{X}^T W \mathbf{X}.
\end{aligned}
$$

So the Taylor expansion of $\partial l_n(\boldsymbol{\beta})/\partial \beta_j$ around $\boldsymbol{\beta}_0$ would be

$$
\begin{aligned}
\frac{\partial l_n(\boldsymbol{\beta})}{\partial \beta_j} =& \frac{\partial l_n(\boldsymbol{\beta}_0)}{\partial \beta_j} + \sum_{k=1}^{p} (\beta_k - \beta_{0,k}) \frac{\partial^2 l_n(\boldsymbol{\beta})}{\partial \beta_j \partial \beta_k} \\
&+ \frac{1}{2} \sum_{k=1}^{p} \sum_{l=1}^{p} (\beta_k - \beta_{0,k})(\beta_l - \beta_{0,l}) \frac{\partial^3 l_n(\boldsymbol{\beta}_*)}{\partial \beta_j \partial \beta_k \partial \beta_l},
\end{aligned}
$$

where β_j and $\beta_{0,j}$ are the j-th element of $\boldsymbol{\beta}$ and $\boldsymbol{\beta}_0$, $\boldsymbol{\beta}_*$ is a point in the line between $\boldsymbol{\beta}$ and $\boldsymbol{\beta}_0$. If we replace $\boldsymbol{\beta}$ by $\hat{\boldsymbol{\beta}}$ in the above expression, we get,

$$
\begin{aligned}
0 = \frac{\partial l_n(\hat{\boldsymbol{\beta}})}{\partial \beta_j} =& \frac{\partial l_n(\boldsymbol{\beta}_0)}{\partial \beta_j} + \sum_{k=1}^{p} (\hat{\beta}_k - \beta_{0,k}) \frac{\partial^2 l_n(\boldsymbol{\beta})}{\partial \beta_j \partial \beta_k} \\
&+ \frac{1}{2} \sum_{k=1}^{p} \sum_{l=1}^{p} (\hat{\beta}_k - \beta_{0,k})(\hat{\beta}_l - \beta_{0,l}) \frac{\partial^3 l_n(\boldsymbol{\beta}_*)}{\partial \beta_j \partial \beta_k \partial \beta_l},
\end{aligned}
$$

so we have

$$\sqrt{n}\sum_{k=1}^{p}(\hat{\beta}_k - \beta_{0,k})[\frac{1}{n}\frac{\partial^2 l_n(\boldsymbol{\beta})}{\partial\beta_j\partial\beta_k} + \frac{1}{2n}\sum_{l=1}^{p}(\hat{\beta}_l - \beta_{0,l})\frac{\partial^3 l_n(\boldsymbol{\beta}_*)}{\partial\beta_j\partial\beta_k\partial\beta_l}] = -\frac{1}{\sqrt{n}}\frac{\partial l_n(\boldsymbol{\beta}_0)}{\partial\beta_j}.$$

Since $\boldsymbol{\beta}$ is weakly consist and the third derivatives $\frac{\partial^3 l_n(\boldsymbol{\beta}_*)}{\partial\beta_j\partial\beta_k\partial\beta_l}$ are bounded by Kredler (1986), we have

$$\frac{1}{2n}\sum_{l=1}^{p}(\hat{\beta}_l - \beta_{0,l})\frac{\partial^3 l_n(\boldsymbol{\beta}_*)}{\partial\beta_j\partial\beta_k\partial\beta_l} \xrightarrow{p} 0,$$

so

$$\frac{1}{n}\frac{\partial^2 l_n(\boldsymbol{\beta})}{\partial\beta_j\partial\beta_k} + \frac{1}{2n}\sum_{l=1}^{p}(\hat{\beta}_l - \beta_{0,l})\frac{\partial^3 l_n(\boldsymbol{\beta}_*)}{\partial\beta_j\partial\beta_k\partial\beta_l} \xrightarrow{p} -H_{j,k},$$

so we have

$$\sqrt{n}\sum_{k=1}^{p}H_{j,k}(\hat{\beta}_k - \beta_{0,k}) \xrightarrow{p} \frac{1}{\sqrt{n}}\frac{\partial l_n(\boldsymbol{\beta}_0)}{\partial\beta_j},$$

which is

$$\mathbf{H}_n\sqrt{n}(\hat{\boldsymbol{\beta}} - \boldsymbol{\beta}_0) \xrightarrow{p} \frac{1}{\sqrt{n}}\frac{\partial l_n(\boldsymbol{\beta}_0)}{\partial\boldsymbol{\beta}},$$

so we get

$$\sqrt{n}(\hat{\boldsymbol{\beta}} - \boldsymbol{\beta}_0) \xrightarrow{p} \mathbf{H}_n^{-1}\frac{1}{\sqrt{n}}\frac{\partial l_n(\boldsymbol{\beta}_0)}{\partial\boldsymbol{\beta}}.$$

By the central limit theorem for independent not identically distributed random variables, we have that $\frac{1}{\sqrt{n}}\frac{\partial l_n(\boldsymbol{\beta}_0)}{\partial\boldsymbol{\beta}}$ has a multivarate normal limit distribution with

asymptotic mean

$$\frac{1}{\sqrt{n}}\sum_{i=1}^{n}\frac{E(y_i-\mu_i)}{a(\phi)}\mathbf{x}_i=\sqrt{n}\mathbf{b},$$

and asymptotic covariance matrix

$$\widetilde{\mathbf{H}}_n=\frac{1}{n}\mathbf{X}^T W_T\mathbf{X}.$$

Also we get that $\sqrt{n}(\hat{\boldsymbol{\beta}}-\boldsymbol{\beta}_0)$ is $AN(\sqrt{n}\mathbf{H}_n^{-1}\mathbf{b},\ \mathbf{H}_n^{-1}\widetilde{\mathbf{H}}_n\mathbf{H}_n)$. □

Proof of theory 4.4.2.

Proof. To calculate $\text{Bias}(\hat{\boldsymbol{\mu}})=\text{E}(\hat{\boldsymbol{\mu}})-\boldsymbol{\mu}_T$, we expand $\hat{\mu}_i$ around η_T by Taylor expansion and get

$$\begin{aligned}\hat{\mu}_i=h(\hat{\eta}_i)&\approx h(\eta_{\text{T},i})+(\hat{\eta}_i-\eta_{\text{T},i})\frac{\partial h(\eta_{\text{T},i})}{\partial\eta_i}\\&=\mu_{\text{T},i}+(\hat{\eta}_i-\eta_{\text{T},i})\frac{\partial h(\eta_{\text{T},i})}{\partial\eta_i},\end{aligned}\tag{4.24}$$

take expectation on both sides and get

$$\begin{aligned}\text{E}(\hat{\mu}_i)&\approx\mu_{\text{T},i}+\text{E}(\hat{\eta}_i-\eta_{\text{T},i})\frac{\partial h(\eta_{\text{T},i})}{\partial\eta_i},\\\text{Bias}(\hat{\mu}_i)&\approx\text{Bias}(\hat{\eta}_i)\frac{\partial h(\eta_{\text{T},i})}{\partial\eta_i},\end{aligned}$$

which indicates that

$$\text{Bias}(\hat{\boldsymbol{\mu}})\approx\mathbf{D}(\boldsymbol{\eta})\,\text{Bias}(\hat{\boldsymbol{\eta}}),$$

where $\mathbf{D}(\boldsymbol{\eta})$ is a diagonal matrix with diagonal element as $\frac{\partial h(\eta_{\mathrm{T},i})}{\partial \eta_i}$, $\mathbf{D}(\boldsymbol{\eta}) = diag\{\frac{\partial h(\eta_{\mathrm{T},i})}{\partial \eta_i}\}$, and $\frac{\partial h(\eta_{\mathrm{T},i})}{\partial \eta_i} = \frac{\partial h(\eta)}{\partial \eta} \mid_{\eta=\eta_{\mathrm{T},i}}$.

We can also get the variance of $\hat{\mu}_i$ from 4.24 as following,

$$\mathrm{Var}(\hat{\mu}_i) \approx \mathrm{Var}(\hat{\eta}_i)(\frac{\partial h(\eta_{\mathrm{T},i})}{\partial \eta_i})^2,$$

and the following matrix form,

$$\mathrm{Var}(\hat{\boldsymbol{\mu}}) \approx \mathbf{D}(\boldsymbol{\eta}_T)\,\mathrm{Var}(\boldsymbol{\eta})\mathbf{D}(\boldsymbol{\eta}_T).$$

For $\mathrm{Bias}(\hat{\eta}_i)$, we have the following

$$\begin{aligned}
\mathrm{Bias}(\hat{\eta}_i) &= \mathrm{E}(\hat{\eta}_i) - \eta_{\mathrm{T},i} \\
&= \mathrm{E}(\mathbf{x}_i^T\hat{\boldsymbol{\beta}}) - (\mathbf{x}_i^T\hat{\boldsymbol{\beta}}_0 + \mathbf{x}_{u,i}\beta_u) \\
&= \mathbf{x}_i^T(\mathrm{E}(\hat{\boldsymbol{\beta}}) - \hat{\boldsymbol{\beta}}_0) - \mathbf{x}_{u,i}\beta_u \\
&= \mathbf{x}_i^T\,\mathrm{Bias}(\hat{\boldsymbol{\beta}}) - \mathbf{x}_{u,i}\beta_u.
\end{aligned}$$

So we get the matrix form of $Bias(\boldsymbol{\eta})$ as

$$\mathrm{Bias}(\boldsymbol{\eta}) = \mathbf{X}\,\mathrm{Bias}(\hat{\boldsymbol{\beta}}) - \mathbf{x}_u\beta_u.$$

Since $\hat{\eta}_i = \mathbf{x}_i^T\hat{\boldsymbol{\beta}}$, we get

$$\mathrm{Var}(\hat{\eta}_i) = \mathbf{x}_i^T\,\mathrm{Var}(\hat{\boldsymbol{\beta}})\mathbf{x}_i$$

and

$$\mathrm{Var}(\hat{\boldsymbol{\eta}}) = \mathbf{X}\,\mathrm{Var}(\hat{\boldsymbol{\beta}})\mathbf{X}^T.$$

Since

$$\begin{aligned}\mu_{\mathrm{T},i} = h(\eta_{\mathrm{T},i}) &\approx h(\eta_i) + (\eta_{\mathrm{T},i} - \eta_i)\frac{\partial h(\eta_i)}{\partial \eta_i} \\ &= \mu_i + \frac{\partial h(\eta_i)}{\partial \eta_i}\mathbf{x}_{u,i}\beta_u,\end{aligned}$$

we have

$$\mu_{\mathrm{T},i} - \mu_i \approx \frac{\partial h(\eta_i)}{\partial \eta_i}\mathbf{x}_{u,i}\beta_u,$$

notice that $\frac{\partial h(\eta_i)}{\partial \eta_i} = a(\phi)\frac{\partial \mu_i/\partial \eta_i}{a(\phi)} = a(\phi)\omega_i$ and $\frac{1}{a(\phi)}\mathbf{D}(\boldsymbol{\eta}) = W$, we get

$$\begin{aligned}\boldsymbol{\mu}_{\mathrm{T}} - \boldsymbol{\mu} &\approx \mathbf{D}(\boldsymbol{\eta})\mathbf{x}_u\beta_u \\ &= a(\phi)W\mathbf{x}_u\beta_u.\end{aligned}$$

So by 4.4.1, we have

$$\begin{aligned}\mathrm{Bias}(\hat{\boldsymbol{\beta}}) &\approx \mathbf{H}_n^{-1}\mathbf{b} \\ &= (\frac{1}{n}\mathbf{X}^T W\mathbf{X})^{-1}\frac{\mathbf{X}^T(\boldsymbol{\mu}_{\mathrm{T}} - \boldsymbol{\mu})}{na(\phi)} \\ &\approx (\frac{1}{n}\mathbf{X}^T W\mathbf{X})^{-1}\frac{\mathbf{X}^T a(\phi)W\mathbf{x}_u\beta_u}{na(\phi)}\end{aligned}$$

$$= (\mathbf{X}^T W \mathbf{X})^{-1} \mathbf{X}^T W \mathbf{x}_u \beta_u.$$

We also get

$$\begin{aligned}\mathrm{Var}(\hat{\boldsymbol{\beta}}) &\approx \frac{1}{n} \mathbf{H}_n^{-1} \widetilde{\mathbf{H}}_n \mathbf{H}_n^{-1} \\ &= (\mathbf{X}^T W \mathbf{X})^{-1} \mathbf{X}^T W_T \mathbf{X} (\mathbf{X}^T W \mathbf{X})^{-1}.\end{aligned}$$

So for $\mathrm{MSE}(\hat{\boldsymbol{\mu}})$, we have

$$\begin{aligned}&\mathrm{MSE}(\hat{\boldsymbol{\mu}}) = \mathrm{Var}(\hat{\boldsymbol{\mu}}) + \mathrm{Bias}(\hat{\boldsymbol{\mu}}) \, \mathrm{Bias}^T(\hat{\boldsymbol{\mu}}) \\ \approx &\mathbf{D}(\boldsymbol{\eta}_T) \, \mathrm{Var}(\boldsymbol{\eta}) \mathbf{D}(\boldsymbol{\eta}_T) + \mathbf{D}(\boldsymbol{\eta}_T) \, \mathrm{Bias}(\hat{\boldsymbol{\eta}}) \, \mathrm{Bias}^T(\hat{\boldsymbol{\eta}}) \mathbf{D}(\boldsymbol{\eta}_T) \\ = &\mathbf{D}(\boldsymbol{\eta}_T) \mathbf{X} \, \mathrm{Var}(\hat{\boldsymbol{\beta}}) \mathbf{X}^T \mathbf{D}(\boldsymbol{\eta}_T) \\ &+ \mathbf{D}(\boldsymbol{\eta}_T) (\mathbf{X} \, \mathrm{Bias}(\hat{\boldsymbol{\beta}}) - \mathbf{x}_u \beta_u) (\mathbf{X} \, \mathrm{Bias}(\hat{\boldsymbol{\beta}}) - \mathbf{x}_u \beta_u)^T \mathbf{D}(\boldsymbol{\eta}_T) \\ \approx &\mathbf{D}(\boldsymbol{\eta}_T) \mathbf{X} (\mathbf{X}^T W \mathbf{X})^{-1} \mathbf{X}^T W_T \mathbf{X} (\mathbf{X}^T W \mathbf{X})^{-1} \mathbf{X}^T \mathbf{D}(\boldsymbol{\eta}_T) \\ &+ \mathbf{D}(\boldsymbol{\eta}_T) (\mathbf{X} (\mathbf{X}^T W \mathbf{X})^{-1} \mathbf{X}^T W \mathbf{x}_u \beta_u - \mathbf{x}_u \beta_u) \\ &\cdot (\mathbf{X} (\mathbf{X}^T W \mathbf{X})^{-1} \mathbf{X}^T W \mathbf{x}_u \beta_u - \mathbf{x}_u \beta_u)^T \mathbf{D}(\boldsymbol{\eta}_T) \\ = &\mathbf{D}(\boldsymbol{\eta}_T) \mathbf{X} (\mathbf{X}^T W \mathbf{X})^{-1} \mathbf{X}^T W_T \mathbf{X} (\mathbf{X}^T W \mathbf{X})^{-1} \mathbf{X}^T \mathbf{D}(\boldsymbol{\eta}_T) \\ &+ \mathbf{D}(\boldsymbol{\eta}_T) (\mathbf{X} (\mathbf{X}^T W \mathbf{X})^{-1} \mathbf{X}^T W - \mathbf{I}) \mathbf{x}_u \beta_u [(\mathbf{X} (\mathbf{X}^T W \mathbf{X})^{-1} \mathbf{X}^T W - \mathbf{I}) \mathbf{x}_u \beta_u]^T \mathbf{D}(\boldsymbol{\eta}_T) \\ = &\mathbf{D}(\boldsymbol{\eta}_T) \mathbf{X} (\mathbf{X}^T W \mathbf{X})^{-1} \mathbf{X}^T W_T \mathbf{X} (\mathbf{X}^T W \mathbf{X})^{-1} \mathbf{X}^T \mathbf{D}(\boldsymbol{\eta}_T) \\ &+ \mathbf{D}(\boldsymbol{\eta}_T) (\mathbf{X} (\mathbf{X}^T W \mathbf{X})^{-1} \mathbf{X}^T W - \mathbf{I}) \mathbf{x}_u \beta_u \beta_u \mathbf{x}_u^T (W \mathbf{X} (\mathbf{X}^T W \mathbf{X})^{-1} \mathbf{X}^T - \mathbf{I}) \mathbf{D}(\boldsymbol{\eta}_T).\end{aligned}$$

For $\mathrm{MSE}(\hat{\boldsymbol{\mu}}_T)$, it is unbiased and we have

$$
\begin{aligned}
&\mathrm{MSE}(\hat{\boldsymbol{\mu}}_T) = \mathrm{Var}(\hat{\boldsymbol{\mu}}_T) \\
\approx &\mathbf{D}(\boldsymbol{\eta}_T)\,\mathrm{Var}(\hat{\boldsymbol{\eta}}_T)\mathbf{D}(\boldsymbol{\eta}_T) \\
= &\mathbf{D}(\boldsymbol{\eta}_T)\widetilde{\mathbf{X}}\,\mathrm{Var}(\hat{\boldsymbol{\beta}}_T)\widetilde{\mathbf{X}}^T\mathbf{D}(\boldsymbol{\eta}_T) \\
= &\mathbf{D}(\boldsymbol{\eta}_T)(\mathbf{X}, \mathbf{x}_u)(\widetilde{\mathbf{X}}^T W_T \widetilde{\mathbf{X}})^{-1}\begin{pmatrix}\mathbf{X}^T \\ \mathbf{x}_u^T\end{pmatrix}\mathbf{D}(\boldsymbol{\eta}_T) \\
= &\mathbf{D}(\boldsymbol{\eta}_T)(\mathbf{X}, \mathbf{x}_u)(\begin{pmatrix}\mathbf{X}^T \\ \mathbf{x}_u^T\end{pmatrix} W_T(\mathbf{X}, \mathbf{x}_u))^{-1}\begin{pmatrix}\mathbf{X}^T \\ \mathbf{x}_u^T\end{pmatrix}\mathbf{D}(\boldsymbol{\eta}_T) \\
= &\mathbf{D}(\boldsymbol{\eta}_T)(\mathbf{X}, \mathbf{x}_u)\begin{pmatrix}\mathbf{X}^T W_T \mathbf{X} & \mathbf{X}^T W_T \mathbf{x}_u \\ \mathbf{x}_u^T W_T \mathbf{X} & \mathbf{x}_u^T W_T \mathbf{x}_u\end{pmatrix}^{-1}\begin{pmatrix}\mathbf{X}^T \\ \mathbf{x}_u^T\end{pmatrix}\mathbf{D}(\boldsymbol{\eta}_T) \\
= &\mathbf{D}(\boldsymbol{\eta}_T)\{\mathbf{X}[(\mathbf{X}^T W_T \mathbf{X})^{-1} + (\mathbf{X}^T W_T \mathbf{X})^{-1}\mathbf{X}^T W_T \mathbf{x}_u \\
&\quad \cdot (\mathbf{x}_u^T W_T \mathbf{x}_u - \mathbf{x}_u^T W_T \mathbf{X}(\mathbf{X}^T W_T \mathbf{X})^{-1}\mathbf{X}^T W_T \mathbf{x}_u)^{-1}\mathbf{x}_u^T W_T \mathbf{X}(\mathbf{X}^T W_T \mathbf{X})^{-1}]\mathbf{X}^T \\
&\quad + \mathbf{x}_u[-(\mathbf{x}_u^T W_T \mathbf{x}_u - \mathbf{x}_u^T W_T \mathbf{X}(\mathbf{X}^T W_T \mathbf{X})^{-1}\mathbf{X}^T W_T \mathbf{x}_u)^{-1}\mathbf{x}_u^T W_T \mathbf{X}(\mathbf{X}^T W_T \mathbf{X})^{-1}]\mathbf{X}^T \\
&\quad + \mathbf{X}[-(\mathbf{X}^T W_T \mathbf{X})^{-1}\mathbf{X}^T W_T \mathbf{x}_u(\mathbf{x}_u^T W_T \mathbf{x}_u - \mathbf{x}_u^T W_T \mathbf{X}(\mathbf{X}^T W_T \mathbf{X})^{-1}\mathbf{X}^T W_T \mathbf{x}_u)^{-1}]\mathbf{x}_u^T \\
&\quad + \mathbf{x}_u(\mathbf{x}_u^T W_T \mathbf{x}_u - \mathbf{x}_u^T W_T \mathbf{X}(\mathbf{X}^T W_T \mathbf{X})^{-1}\mathbf{X}^T W_T \mathbf{x}_u)^{-1}\mathbf{x}_u^T\}\mathbf{D}(\boldsymbol{\eta}_T) \\
= &\mathbf{D}(\boldsymbol{\eta}_T)\mathbf{X}(\mathbf{X}^T W_T \mathbf{X})^{-1}\mathbf{X}^T\mathbf{D}(\boldsymbol{\eta}_T) \\
&\quad + \mathbf{D}(\boldsymbol{\eta}_T)(\mathbf{X}(\mathbf{X}^T W_T \mathbf{X})^{-1}\mathbf{X}^T W_T - \mathbf{I})\mathbf{x}_u \\
&\quad \cdot (\mathbf{x}_u^T W_T \mathbf{x}_u - \mathbf{x}_u^T W_T \mathbf{X}(\mathbf{X}^T W_T \mathbf{X})^{-1}\mathbf{X}^T W_T \mathbf{x}_u)^{-1} \\
&\quad \cdot \mathbf{x}_u^T(\mathbf{X}(W_T \mathbf{X}^T W_T \mathbf{X})^{-1}\mathbf{X}^T - \mathbf{I})\mathbf{D}(\boldsymbol{\eta}_T).
\end{aligned}
$$

If we assume that $W \approx W_T$ then the only difference of MSE($\hat{\boldsymbol{\mu}}_T$) and MSE($\hat{\boldsymbol{\mu}}$) in the second term of the expression as following,

$$\beta_u \beta_u$$

and

$$(\mathbf{x}_u^T W_T \mathbf{x}_u - \mathbf{x}_u^T W_T \mathbf{X} (\mathbf{X}^T W_T \mathbf{X})^{-1} \mathbf{X}^T W_T \mathbf{x}_u)^{-1}.$$

When $\beta_u^2 < (\mathbf{x}_u^T W_T \mathbf{x}_u - \mathbf{x}_u^T W_T \mathbf{X} (\mathbf{X}^T W_T \mathbf{X})^{-1} \mathbf{X}^T W_T \mathbf{x}_u)^{-1}$, each element of MSE($\hat{\boldsymbol{\mu}}_T$) would be smaller than MSE($\hat{\boldsymbol{\mu}}$), and thus we have $M_1 < M_2$. □

Proof of lemma 4.4.3.

Proof. For log-gamma GLM, we use similar idea used in the proof of lemma 4.4.1 and have the log likelihood function of the fitting model defined as following,

$$l_n(\boldsymbol{\beta}) = \sum_{i=1}^{n} \frac{y_i / \exp(\mathbf{x}_i^T \boldsymbol{\beta}) + \mathbf{x}_i^T \boldsymbol{\beta}}{-\phi} + \frac{\phi + 1}{\phi} \ln(y_i) - \frac{\ln(\phi)}{\phi} - \ln \Gamma(\frac{1}{\phi}),$$

where $\Gamma(z) = \int_0^\infty x^{z-1} e^{-x} dx$.

With $\theta_i = 1/\mu_i$, we have

$$\begin{aligned} \frac{\partial l_n(\boldsymbol{\beta})}{\partial \boldsymbol{\beta}} &= \sum_{i=1}^{n} -\frac{1}{\phi} \{ y_i (-1) \frac{1}{\exp^2(\mathbf{x}_i^T \boldsymbol{\beta})} \exp(\mathbf{x}_i^T \boldsymbol{\beta}) \mathbf{x}_i + \mathbf{x}_i \} \\ &= \sum_{i=1}^{n} \frac{1}{\phi} \{ \frac{y_i}{\exp(\mathbf{x}_i^T \boldsymbol{\beta})} \mathbf{x}_i - \mathbf{x}_i \}, \end{aligned}$$

and

$$\frac{\partial^2 l_n(\boldsymbol{\beta})}{\partial\boldsymbol{\beta}\partial\boldsymbol{\beta}^T} = \frac{1}{\phi}\sum_{i=1}^{n} y_i(-1)\frac{1}{\exp^2(\mathbf{x}_i^T\boldsymbol{\beta})}\exp(\mathbf{x}_i^T\boldsymbol{\beta})\mathbf{x}_i\mathbf{x}_i^T$$
$$= \frac{-1}{\phi}\sum_{i=1}^{n}\frac{y_i}{\exp(\mathbf{x}_i^T\boldsymbol{\beta})}\mathbf{x}_i\mathbf{x}_i^T.$$

For each β_j, we have

$$\frac{\partial l_n(\boldsymbol{\beta})}{\partial\beta_j} = \sum_{i=1}^{n} -\frac{1}{\phi}\{y_i(-1)\frac{1}{\exp^2(\mathbf{x}_i^T\boldsymbol{\beta})}\exp(\mathbf{x}_i^T\boldsymbol{\beta})\mathbf{x}_{ij} + \mathbf{x}_{ij}\}$$
$$= \sum_{i=1}^{n}\frac{1}{\phi}\{\frac{y_i x_{ij}}{\exp(\mathbf{x}_i^T\boldsymbol{\beta})} - x_{ij}\},$$

$$\frac{\partial^2 l_n(\boldsymbol{\beta})}{\partial\beta_j\partial\beta_k} = \frac{-1}{\phi}\sum_{i=1}^{n}\frac{y_i x_{ij}x_{ik}}{\exp(\mathbf{x}_i^T\boldsymbol{\beta})},$$

and

$$\frac{\partial^3 l_n(\boldsymbol{\beta})}{\partial\beta_j\partial\beta_k\partial\beta_l} = \frac{1}{\phi}\sum_{i=1}^{n}\frac{y_i x_{ij}x_{ik}x_{il}}{\exp(\mathbf{x}_i^T\boldsymbol{\beta})}.$$

Expansion of $\partial l_n(\boldsymbol{\beta})/\partial\beta_j$ around $\boldsymbol{\beta}_0$ gives

$$\frac{\partial l_n(\boldsymbol{\beta})}{\partial\beta_j} = \frac{\partial l_n(\boldsymbol{\beta}_0)}{\partial\beta_j} + \sum_{k=1}^{p}(\beta_k - \beta_{0,k})\frac{\partial^2 l_n(\boldsymbol{\beta}_0)}{\partial\beta_j\partial\beta_k} + \sum_{l=1}^{p}(\hat{\beta}_l - \beta_{0,l})\frac{\partial^3 l_n(\boldsymbol{\beta}_*)}{\partial\beta_j\partial\beta_k\partial\beta_l},$$

where $\boldsymbol{\beta}_*$ is a point on the line segment between $\boldsymbol{\beta}$ and $\boldsymbol{\beta}_0$. Comparing the second order derivative term and third order derivative term, since the corivate is normalized, the third order term is small compared with the second order term. So we can get the following,

$$\frac{\partial l_n(\boldsymbol{\beta})}{\partial \beta_j} \approx \frac{\partial l_n(\boldsymbol{\beta}_0)}{\partial \beta_j} + \sum_{k=1}^{p} (\beta_k - \beta_{0,k}) \frac{\partial^2 l_n(\boldsymbol{\beta}_0)}{\partial \beta_j \partial \beta_k}.$$

If we replace $\boldsymbol{\beta}$ by $\hat{\boldsymbol{\beta}}$, we get

$$\sqrt{n} \sum_{k=1}^{n} (\hat{\beta}_k - \beta_{0,k}) \frac{1}{n} \frac{\partial^2 l(\boldsymbol{\beta}_0)}{\partial \beta_j \partial \beta_k} \approx -\frac{1}{\sqrt{n}} \frac{\partial l(\boldsymbol{\beta}_0)}{\partial \beta_j}.$$

Define $\Delta_{\boldsymbol{y}} = diag\{\frac{y_i}{\exp(\mathbf{x}_i^T \boldsymbol{\beta}_0)}\}$, we define

$$\mathbb{H}_n = \frac{1}{n\phi} \mathbf{X}^T \Delta_{\boldsymbol{y}} \mathbf{X} = -\frac{1}{n} \frac{\partial^2 l_n(\boldsymbol{\beta})}{\partial \boldsymbol{\beta} \partial \boldsymbol{\beta}^T}.$$

So we have

$$\mathbb{H}_n \sqrt{n} (\hat{\boldsymbol{\beta}} - \boldsymbol{\beta}_0) \approx \frac{1}{\sqrt{n}} \frac{\partial l(\boldsymbol{\beta}_0)}{\partial \boldsymbol{\beta}}.$$

Furthermore, we define

$$\tilde{\mathbf{b}} = \frac{1}{n\phi} \mathbf{X}^T \Delta (\boldsymbol{\mu}_T - \boldsymbol{\mu}),$$

where $\Delta = diag\{\frac{1}{\exp(\mathbf{x}_i^T \boldsymbol{\beta}_0)}\}$.

Since

$$\frac{\partial l(\boldsymbol{\beta}_0)}{\partial \boldsymbol{\beta}} = \sum_{i=1}^{n} \frac{1}{\phi} \{\frac{y_i}{\exp(\mathbf{x}_i^T \boldsymbol{\beta}_0)} \mathbf{x}_i - \mathbf{x}_i\},$$

by the central limit theorem for independent not identically distributed random variables, we have that $\frac{1}{\sqrt{n}} \frac{\partial l_n(\boldsymbol{\beta}_0)}{\partial \boldsymbol{\beta}}$ has a multivarate normal limit distribution with asymptotic mean

$$\frac{1}{\sqrt{n}} \sum_{i=1}^{n} \frac{1}{\phi} \{\frac{\mathrm{E}(y_i)}{\exp(\mathbf{x}_i^T \boldsymbol{\beta}_0)} \mathbf{x}_i - \mathbf{x}_i\}$$

$$=\frac{1}{\sqrt{n}}\sum_{i=1}^{n}\frac{1}{\phi}\frac{\mu_{Ti}-\mu_i}{\exp(\mathbf{x}_i^T\boldsymbol{\beta}_0)}\mathbf{x}_i$$

$$=\sqrt{n}\tilde{\mathbf{b}}.$$

And the asymptotic variance,

$$\widetilde{\mathbb{H}}_n=\frac{1}{n^2}\mathbf{X}^T\Delta\mathbf{W}_T\Delta\mathbf{X}.$$

So we get

$$\mathbb{H}_n\sqrt{n}(\hat{\boldsymbol{\beta}}-\boldsymbol{\beta}_0)\longrightarrow N(\sqrt{n}\tilde{\mathbf{b}},\widetilde{\mathbb{H}}_n),$$

Also we get that $\sqrt{n}(\hat{\boldsymbol{\beta}}-\boldsymbol{\beta}_0)$ is $AN(\sqrt{n}\widetilde{\mathbb{H}}_n^{-1}\tilde{\mathbf{b}},\mathbb{H}_n^{-1}\widetilde{\mathbb{H}}_n\mathbb{H}_n)$. □

Proof of 4.4.4.

Proof. For MSE($\hat{\boldsymbol{\mu}}$), since,

$$\hat{\mu}_i=h(\hat{\eta}_i)\approx h(\eta_{T,i})+(\hat{\eta}_i-\eta_{T,i})\frac{\partial h(\eta_{T,i})}{\partial\eta_i},$$

we have

$$\text{Bias}(\hat{\mu}_i)\approx\text{Bias}(\hat{\eta}_i)\frac{\partial h(\eta_{T,i})}{\partial\eta_i},$$

and

$$\text{Bias}(\hat{\boldsymbol{\mu}})\approx\mathbf{D}(\boldsymbol{\eta}_T)\,\text{Bias}(\hat{\boldsymbol{\eta}}).$$

For the variance, we get

$$\mathrm{Var}(\hat{\boldsymbol{\mu}}) \approx \mathbf{D}(\boldsymbol{\eta}_T)\,\mathrm{Var}(\hat{\boldsymbol{\eta}})\mathbf{D}(\boldsymbol{\eta}_T).$$

And for $\hat{\boldsymbol{\eta}}$, we have

$$\begin{aligned}\mathrm{Bias}(\hat{\eta}_i) &= \mathrm{E}(\hat{\eta}_i) - \eta_{T,i} \\ &= \mathbf{x}_i^T\,\mathrm{E}(\hat{\boldsymbol{\beta}}) - (\mathbf{x}_i^T\boldsymbol{\beta}_0 + x_{u,i}\beta_u) \\ &= \mathbf{x}_i^T\,\mathrm{Bias}(\hat{\boldsymbol{\beta}}) - x_{u,i}\beta_u,\end{aligned}$$

and

$$\mathrm{Bias}(\hat{\boldsymbol{\eta}}) = \mathbf{X}\,\mathrm{Bias}(\hat{\boldsymbol{\beta}}) - \mathbf{x}_u\beta_u.$$

For variance, we can get

$$\mathrm{Var}(\hat{\boldsymbol{\eta}}) = \mathbf{X}\,\mathrm{Var}(\hat{\boldsymbol{\beta}})\mathbf{X}^T.$$

For $\hat{\boldsymbol{\beta}}$, since

$$\begin{aligned}\mu_{T,i} = h(\eta_{T,i}) &\approx h(\eta_i) + (\eta_{T,i} - \eta_i)\frac{\partial h(\eta_i)}{\partial \eta_i} \\ &= \mu_i + x_{u,i}\beta_u \exp(\mathbf{x}_i^T\boldsymbol{\beta}_0).\end{aligned}$$

By 4.4.3, we have

$$\mathrm{Bias}(\hat{\boldsymbol{\beta}}) \approx \mathbb{H}_n^{-1}\tilde{\mathbf{b}}$$

$$
\begin{aligned}
&= (\frac{1}{n\phi}\mathbf{X}^T\Delta_{\boldsymbol{y}}\mathbf{X})^{-1}(\frac{1}{n\phi}\mathbf{X}^T\Delta(\boldsymbol{\mu}_T - \boldsymbol{\mu})) \\
&= (\mathbf{X}^T\Delta_{\boldsymbol{y}}\mathbf{X})^{-1}\mathbf{X}^T\Delta(\boldsymbol{\mu}_T - \boldsymbol{\mu}) \\
&\approx (\mathbf{X}^T\Delta_{\boldsymbol{y}}\mathbf{X})^{-1}\mathbf{X}^T\mathbf{x}_u\beta_u,
\end{aligned}
$$

and

$$
\begin{aligned}
\mathrm{Var}(\hat{\boldsymbol{\beta}}) &\approx \mathbb{H}_n^{-1}\widetilde{\mathbb{H}}_n\mathbb{H}_n^{-1} \\
&= (\frac{1}{n\phi}\mathbf{X}^T\Delta_{\boldsymbol{y}}\mathbf{X})^{-1}\frac{1}{n^2}\mathbf{X}^T\Delta\mathbf{W}_T\Delta\mathbf{X}(\frac{1}{n\phi}\mathbf{X}^T\Delta_{\boldsymbol{y}}\mathbf{X})^{-1} \\
&= \phi^2(\mathbf{X}^T\Delta_{\boldsymbol{y}}\mathbf{X})^{-1}\mathbf{X}^T\Delta\mathbf{W}_T\Delta\mathbf{X}(\mathbf{X}^T\Delta_{\boldsymbol{y}}\mathbf{X})^{-1}.
\end{aligned}
$$

So we have

$$
\begin{aligned}
&\mathrm{MSE}(\hat{\boldsymbol{\mu}}) = \mathrm{Var}(\hat{\boldsymbol{\mu}}) + \mathrm{Bias}(\hat{\boldsymbol{\mu}})\,\mathrm{Bias}^T(\hat{\boldsymbol{\mu}}) \\
\approx&\mathbf{D}(\boldsymbol{\eta}_T)\,\mathrm{Var}(\boldsymbol{\eta})\mathbf{D}(\boldsymbol{\eta}_T) + \mathbf{D}(\boldsymbol{\eta}_T)\,\mathrm{Bias}(\hat{\boldsymbol{\eta}})\,\mathrm{Bias}^T(\hat{\boldsymbol{\eta}})\mathbf{D}(\boldsymbol{\eta}_T) \\
=&\mathbf{D}(\boldsymbol{\eta}_T)\mathbf{X}\,\mathrm{Var}(\hat{\boldsymbol{\beta}})\mathbf{X}^T\mathbf{D}(\boldsymbol{\eta}_T) \\
&+ \mathbf{D}(\boldsymbol{\eta}_T)(\mathbf{X}\,\mathrm{Bias}(\hat{\boldsymbol{\beta}}) - \mathbf{x}_u\beta_u)(\mathbf{X}\,\mathrm{Bias}(\hat{\boldsymbol{\beta}}) - \mathbf{x}_u\beta_u)^T\mathbf{D}(\boldsymbol{\eta}_T) \\
\approx&\mathbf{D}(\boldsymbol{\eta}_T)\phi^2\mathbf{X}(\mathbf{X}^T\Delta_{\boldsymbol{y}}\mathbf{X})^{-1}\mathbf{X}^T\Delta\mathbf{W}_T\Delta\mathbf{X}(\mathbf{X}^T\Delta_{\boldsymbol{y}}\mathbf{X})^{-1}\mathbf{X}^T\mathbf{D}(\boldsymbol{\eta}_T) \\
&+ \mathbf{D}(\boldsymbol{\eta}_T)(\mathbf{X}(\mathbf{X}^T\Delta_{\boldsymbol{y}}\mathbf{X})^{-1}\mathbf{X}^T\mathbf{x}_u\beta_u - \mathbf{x}_u\beta_u) \\
&\cdot (\mathbf{X}(\mathbf{X}^T\Delta_{\boldsymbol{y}}\mathbf{X})^{-1}\mathbf{X}^T\mathbf{x}_u\beta_u - \mathbf{x}_u\beta_u)^T\mathbf{D}(\boldsymbol{\eta}_T) \\
=&\mathbf{D}(\boldsymbol{\eta}_T)\phi^2\mathbf{X}(\mathbf{X}^T\Delta_{\boldsymbol{y}}\mathbf{X})^{-1}\mathbf{X}^T\Delta\mathbf{W}_T\Delta\mathbf{X}(\mathbf{X}^T\Delta_{\boldsymbol{y}}\mathbf{X})^{-1}\mathbf{X}^T\mathbf{D}(\boldsymbol{\eta}_T) \\
&+ \mathbf{D}(\boldsymbol{\eta}_T)(\mathbf{X}(\mathbf{X}^T\Delta_{\boldsymbol{y}}\mathbf{X})^{-1}\mathbf{X}^T - \mathbf{I})\mathbf{x}_u\beta_u[(\mathbf{X}(\mathbf{X}(\mathbf{X}^T\Delta_{\boldsymbol{y}}\mathbf{X})^{-1}\mathbf{X}^T - \mathbf{I})\mathbf{x}_u\beta_u]^T\mathbf{D}(\boldsymbol{\eta}_T)
\end{aligned}
$$

$$
\begin{aligned}
=&\mathbf{D}(\boldsymbol{\eta}_T)\phi^2\mathbf{X}(\mathbf{X}^T\Delta_{\boldsymbol{y}}\mathbf{X})^{-1}\mathbf{X}^T\Delta\mathbf{W}_T\Delta\mathbf{X}(\mathbf{X}^T\Delta_{\boldsymbol{y}}\mathbf{X})^{-1}\mathbf{X}^T\mathbf{D}(\boldsymbol{\eta}_T)\\
&+\mathbf{D}(\boldsymbol{\eta}_T)((\mathbf{X}(\mathbf{X}^T\Delta_{\boldsymbol{y}}\mathbf{X})^{-1}\mathbf{X}^T-\mathbf{I}))\mathbf{x}_u\beta_u\beta_u\mathbf{x}_u^T((\mathbf{X}(\mathbf{X}^T\Delta_{\boldsymbol{y}}\mathbf{X})^{-1}\mathbf{X}^T-\mathbf{I}))\mathbf{D}(\boldsymbol{\eta}_T).
\end{aligned}
$$

For MSE($\hat{\boldsymbol{\mu}}_T$), it is unbiased and we have

$$
\begin{aligned}
&\mathrm{MSE}(\hat{\boldsymbol{\mu}}_T)=\mathrm{Var}(\hat{\boldsymbol{\mu}}_T)\\
\approx&\mathbf{D}(\boldsymbol{\eta}_T)\,\mathrm{Var}(\hat{\boldsymbol{\eta}}_T)\mathbf{D}(\boldsymbol{\eta}_T)\\
=&\mathbf{D}(\boldsymbol{\eta}_T)\widetilde{\mathbf{X}}\,\mathrm{Var}(\hat{\boldsymbol{\beta}}_T)\widetilde{\mathbf{X}}^T\mathbf{D}(\boldsymbol{\eta}_T)\\
=&\mathbf{D}(\boldsymbol{\eta}_T)(\mathbf{X},\mathbf{x}_u)(\widetilde{\mathbf{X}}^T\widetilde{\mathbf{X}})^{-1}\phi\begin{pmatrix}\mathbf{X}^T\\ \mathbf{x}_u^T\end{pmatrix}\mathbf{D}(\boldsymbol{\eta}_T)\\
=&\phi\mathbf{D}(\boldsymbol{\eta}_T)(\mathbf{X},\mathbf{x}_u)(\begin{pmatrix}\mathbf{X}^T\\ \mathbf{x}_u^T\end{pmatrix}(\mathbf{X},\mathbf{x}_u))^{-1}\begin{pmatrix}\mathbf{X}^T\\ \mathbf{x}_u^T\end{pmatrix}\mathbf{D}(\boldsymbol{\eta}_T)\\
=&\phi\mathbf{D}(\boldsymbol{\eta}_T)(\mathbf{X},\mathbf{x}_u)\begin{pmatrix}\mathbf{X}^T\mathbf{X} & \mathbf{X}^T\mathbf{x}_u\\ \mathbf{x}_u^T\mathbf{X} & \mathbf{x}_u^T\mathbf{x}_u\end{pmatrix}^{-1}\begin{pmatrix}\mathbf{X}^T\\ \mathbf{x}_u^T\end{pmatrix}\mathbf{D}(\boldsymbol{\eta}_T)\\
=&\phi\mathbf{D}(\boldsymbol{\eta}_T)\{\mathbf{X}[(\mathbf{X}^T\mathbf{X})^{-1}+(\mathbf{X}^T\mathbf{X})^{-1}\mathbf{X}^T\mathbf{x}_u\\
&\cdot(\mathbf{x}_u^T\mathbf{x}_u-\mathbf{x}_u^T\mathbf{X}(\mathbf{X}^T\mathbf{X})^{-1}\mathbf{X}^T\mathbf{x}_u)^{-1}\mathbf{x}_u^T\mathbf{X}(\mathbf{X}^T\mathbf{X})^{-1}]\mathbf{X}^T\\
&+\mathbf{x}_u[-(\mathbf{x}_u^T\mathbf{x}_u-\mathbf{x}_u^T\mathbf{X}(\mathbf{X}^T\mathbf{X})^{-1}\mathbf{X}^T\mathbf{x}_u)^{-1}\mathbf{x}_u^T\mathbf{X}(\mathbf{X}^T\mathbf{X})^{-1}]\mathbf{X}^T\\
&+\mathbf{X}[-(\mathbf{X}^T\mathbf{X})^{-1}\mathbf{X}^T\mathbf{x}_u(\mathbf{x}_u^T\mathbf{x}_u-\mathbf{x}_u^T\mathbf{X}(\mathbf{X}^T\mathbf{X})^{-1}\mathbf{X}^T\mathbf{x}_u)^{-1}]\mathbf{x}_u^T\\
&+\mathbf{x}_u(\mathbf{x}_u^T\mathbf{x}_u-\mathbf{x}_u^T\mathbf{X}(\mathbf{X}^T\mathbf{X})^{-1}\mathbf{X}^T\mathbf{x}_u)^{-1}\mathbf{x}_u^T\}\mathbf{D}(\boldsymbol{\eta}_T)\\
=&\phi\mathbf{D}(\boldsymbol{\eta}_T)\mathbf{X}(\mathbf{X}^T\mathbf{X})^{-1}\mathbf{X}^T\mathbf{D}(\boldsymbol{\eta}_T)\\
&+\phi\mathbf{D}(\boldsymbol{\eta}_T)(\mathbf{X}(\mathbf{X}^T\mathbf{X})^{-1}\mathbf{X}^T-\mathbf{I})\mathbf{x}_u
\end{aligned}
$$

$$\cdot (\mathbf{x}_u^T\mathbf{x}_u - \mathbf{x}_u^T\mathbf{X}(\mathbf{X}^T\mathbf{X})^{-1}\mathbf{X}^T\mathbf{x}_u)^{-1}\mathbf{x}_u^T(\mathbf{X}(\mathbf{X}^T\mathbf{X})^{-1}\mathbf{X}^T - \mathbf{I})\mathbf{D}(\boldsymbol{\eta}_T).$$

By condition $S0$, compare MSE($\hat{\boldsymbol{\mu}}$) and MSE($\hat{\boldsymbol{\mu}}_T$), we complete the proof. □

4.4.2 Simulations

In this section, we firstly run the simulation for Gamma GLM with canonical link, based on mosquito abundance data and weather data from Peel Region. Then we run the simulation for Gamma GLM with log link.

For Gamma GLM with canonical link, based on mosquito abundance surveillance data and weather data from Peel Region in year 2008, recall model (4.9) as following,

$$\begin{aligned}
E(\rho_{k,t}) =& \mu_{k,t},\\
g(\mu_{k,t}) =& log(\mu_{k,t}) = \eta_{k,t},\\
\eta_{k,t} =& \beta_0 + \beta_1\ (ddm_{k,t}^{[12]})^2 + \beta_2\ ddm_{k,t}^{[12]} + \beta_3\ (ppm_{k,t}^{[42]})^2\\
&+ \beta_4\ ppm_{k,t}^{[42]} + \beta_5\ ddm_{k,t}^{[12]}\ ppm_{k,t}^{[42]},
\end{aligned}$$

and recall model (4.10) as following,

$$\begin{aligned}
E(\rho_{k,t}) =& \mu_{k,t},\\
g(\mu_{k,t}) =& log(\mu_{k,t}) = \widehat{\eta}_{k,t},\\
\widehat{\eta}_{k,t} =& \beta_0 + \beta_1\ (ddm_{k,t}^{[12]})^2 + \beta_2\ ddm_{k,t}^{[12]} + \beta_3\ (ppm_{k,t}^{[12]})^2
\end{aligned}$$

$$+ \beta_4 \; ppm_{k,t}^{[42]} + \beta_5 \; ddm_{k,t}^{[12]} \; ppm_{k,t}^{[42]} + z_k.$$

In our simulation, we use model 4.9 as the fitting model, use model 4.10 with $\alpha * \widehat{z}_k$ as the truth model. $\widehat{z}_k$ is the missing information found in Section 4.2, $\rho = \beta_u^{-2} * (\mathbf{x}_u^T W_T \mathbf{x}_u - \mathbf{x}_u^T W_T \mathbf{X} (\mathbf{X}^T W_T \mathbf{X})^{-1} \mathbf{X}^T W_T \mathbf{x}_u)^{-1}$. In Table 4.4 and Table 4.5, it is shown that if $\rho > 1$, $M_1 < M_2$ by Theory 4.4.2 and Theory 4.4.4.

Table 4.4 shows simulation results for Gamma GLM with the conical link. It verified that when the condition is satisfied, the MSE of the fitting model is smaller than the truth model. Also, the hidden dimension model can reach a smaller MSE than the fitting model, but larger than the truth model.

ρ	MSE of the fitting model (M_1)	MSE of the hidden dimension model	MSE of the truth model (M_2)
0.0195	6.5541	4.4452	0.8846
0.1288	0.3842	1.0909	0.1780
1.0003	0.1119	0.6933	0.1112
2.4667	0.0947	0.6401	0.1052
10.0829	0.0801	0.5956	0.0957

Table 4.4: Gamma-GLM with canonical link.

Simulation results for Gamma GLM with log link. Table 4.5 shows more details

ρ	MSE of the fitting model (M_1)	MSE of the hidden dimension model	MSE of the truth model(M_2)
0.0079	18.9654	6.3986	5.7508
0.1025	0.5157	1.2212	0.2748
1.0219	0.1443	0.8557	0.1459
2.1829	0.1244	0.7983	0.1369
8.3005	0.1165	0.7804	0.1346

Table 4.5: Gamma-GLM with log link.

4.5 Conclusion and discussion

In this chapter, we extend the dimension expansion method by Bornn et al. (2012) to generalized linear modeling for spatio-temporal processes with unobserved information. This method allows us to model certain environmental driven processes with limited data available. The method works by collecting all the unobservable information through a carefully designed objective function. The proposed method is a valuable tool to extend the application of GLMs to data with missing information.

As an application, we model mosquito abundance using surveillance data in Peel Region, Ontario, Canada, assuming certain information can not be observed. Numerical simulations show that the method can significantly improve the accuracy of the GLM results of Wang et al. (2011). We also compare the performance of our method and the GLMM when applied to real data and simulation data. The results

show that our method can reduce more errors of the GLM than the GLMM. Our method could be a valuable modeling tool to understand the processes when collected samples do not contain all important relevant information.

We also give the conditions when GLM with missing information has smaller MSE than that of GLM without missing information and verified it through simulations.

5 Forecasting mosquito abundance and WNV risk in Peel Region

5.1 Forecasting *Culex* mosquito trap counts in Peel Region

We use our model in the weekly forecasting of average *Culex* mosquito trap counts in Peel Region LAMPS, York University. For each year, starting from mid-June, we receive mosquito trap counts data from local health unit (Peel Region), then we use the latest mosquito data and weather data to update the estimated coefficients of our model (2.3). After we get updated model, we use the forecasted weather as weather input of our model to predict the average trapped mosquito abundance in Peel Region. We extended the mosquito abundance forecasting work to Halton, City of Toronto and Peel in 2014. In 2016, we do the forecasting for all five regions of GTA.

The forecast results are posted on the website of LAMPS. The following figures

show the screenshots of the forecasting work,

Figure 5.1: Screenshot of average *Culex* mosquito trap counts forecasting in 2013 from LAMPS website. Available at `http://www.lamps.yorku.ca/weeklyforecast2013`.

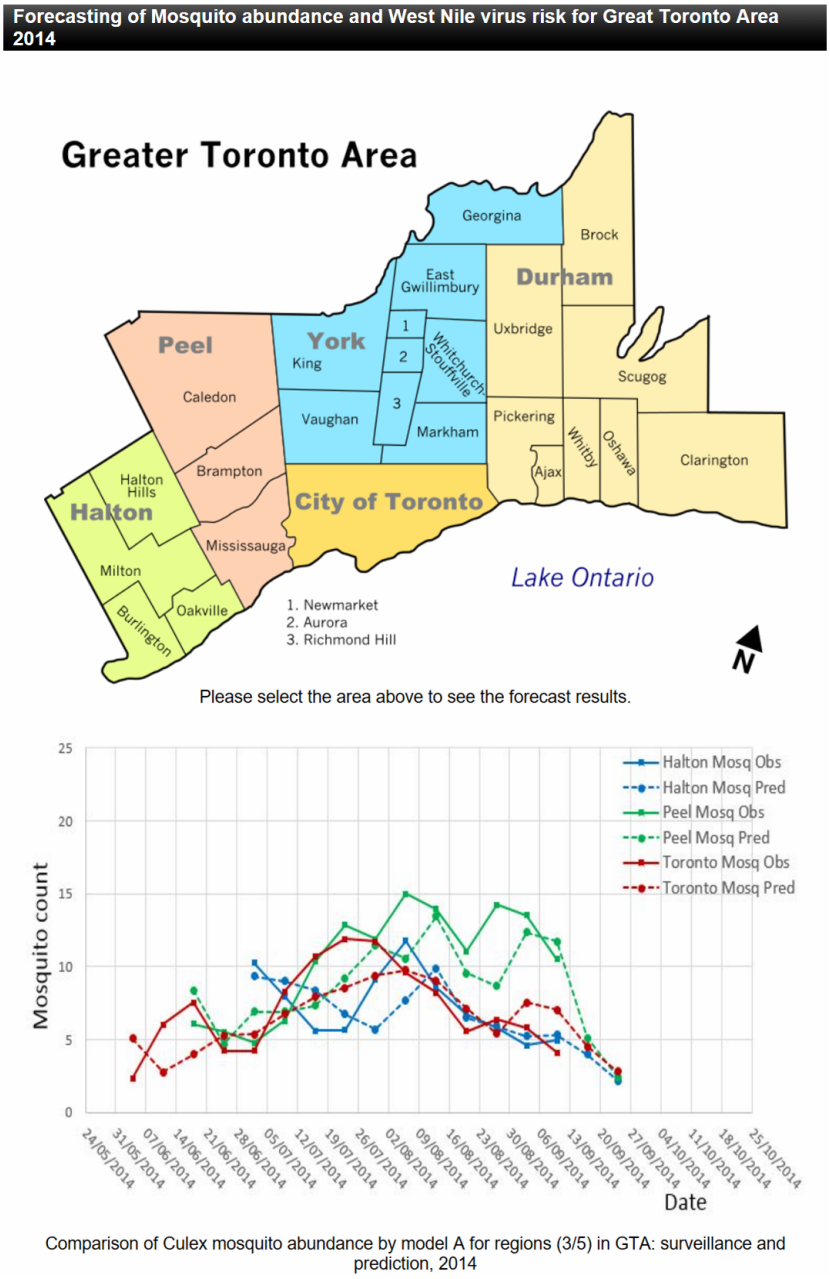

Figure 5.2: Screenshot of average *Culex* mosquito trap counts forecasting in 2014 from LAMPS website. Available at `http://www.lamps.yorku.ca/node/226`.

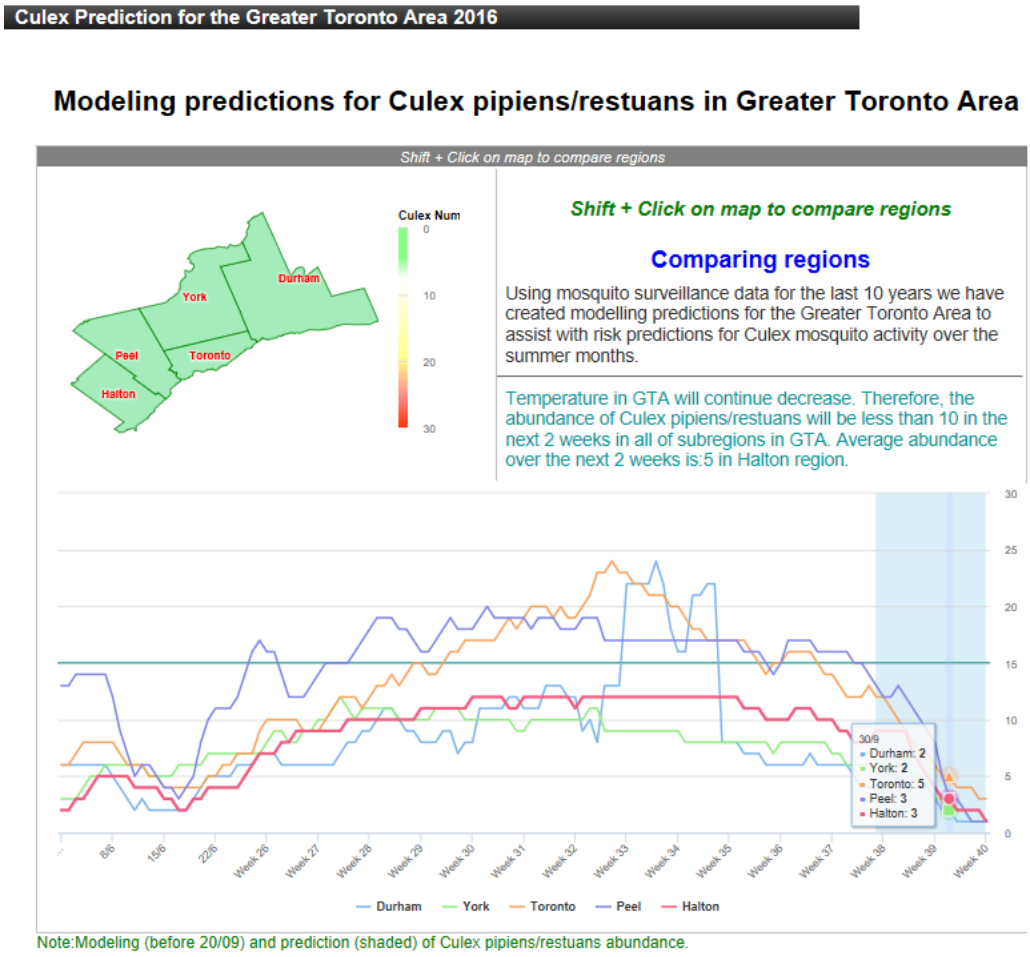

Figure 5.3: Screenshot of average *Culex* mosquito trap counts forecasting in 2016 from LAMPS website. Available at `http://www.lamps.yorku.ca/node/331`.

5.2 Forecasting WNV risk in Peel Region

R_0 is usually used as the indicator to decide if there will be an epidemic or not in compartmental WNV transmission models. However, local health unit (like Peel

Region) usually uses minimum infection rate (**MIR**) as the risk index for WNV human infection (Nasci et al. 2001, PEE 2002). It is defined as

$$\mathbf{MIR} = \frac{\text{total number of positive pools}}{\text{total number of tested mosquitoes}} * 1000. \tag{5.1}$$

MIR assume that there is one positive mosquito for each positive pool, however this assumption may not be correct since it is possible that there is two or more positive mosquitoes for a positive pool. We employ the vector infection rate (**VIR**) as our risk indicator, it is defined as

$$\mathbf{VIR}(t) = \frac{M_i(t)}{N_m(t)}. \tag{5.2}$$

The **VIR**(t) measures the portion of mosquitoes vectors that carry the virus at time t. If **VIR** is large (small), the probability that one mosquito bite is from the infected mosquito is high (low), and therefore the WNV human risk is high (low).

As an example, Figure 5.4 shows the simulated and predicted WNV human infection cases and rescaled **VIR** in Peel Region on August 22, 2017. It shows that WNV risk will keep stable in the following two weeks from August 22, 2017.

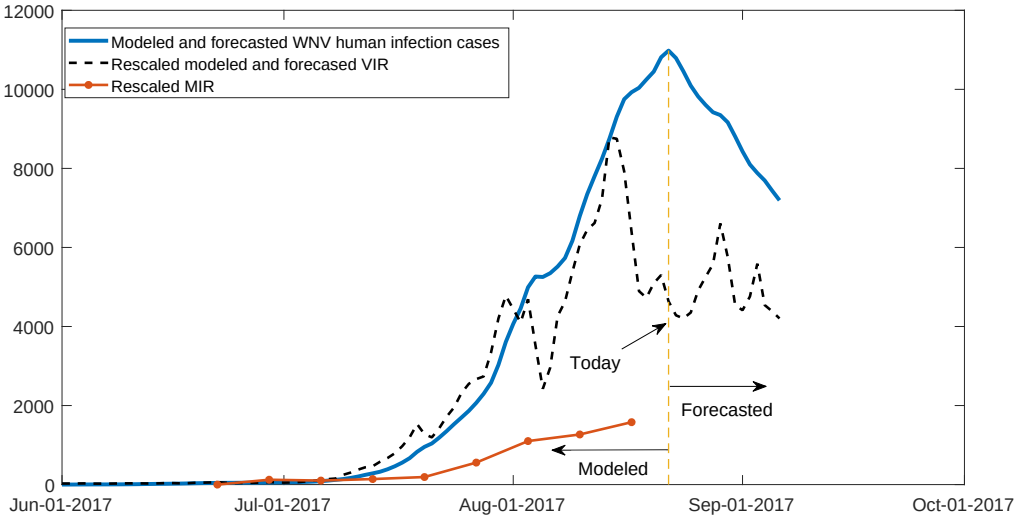

Figure 5.4: Simulated and predicted WNV human infection cases and rescaled **VIR** in next two weeks, and recorded rescaled **MIR**.

5.3 Discussion

We have forecasted the average *Culex* mosquito trap counts in Peel Region during summer time. It has been tested during the practice that our model can capture the trend of observed mosquito count.

In addition, we have shown an example of forecasting weekly WNV risk for Peel Region. We can also forecast other 4 regions of GTA with little adjustment of our model. This would be of great value for WNV control and prevention in GTA.

6 Conclusions and future work

As an emerging mosquito-borne disease, WNV is a serious public health issue. *Culex* mosquitoes play the key role in the transmission process of the diseases as the primary vector. In addition, weather conditions have the huge impact on mosquito behaviors, mosquito populations, and WNV transmission process. Although there are many studies about weather impact on mosquito abundance and WNV transmission dynamics, forecasting *Culex* mosquito abundance and WNV risk with real weather conditions are still challenging topics. We use mathematical methods and statistical methods to study the impact of weather conditions on *Culex* mosquito population and the transmission WNV. And we provide a novel approach to forecast *Culex* mosquito abundance and WNV risk with real weather conditions.

In Chapter 1, we present the background of WNV, mosquito abundance models, and WNV transmission models. In Chapter 2, we first introduce a GLM for *Culex* mosquito abundance, then we integrate the GLM with a compartmental model for WNV transmission. We incorporate the effect of temperature and precipitation on

the mosquito behaviors in the hybrid model. What's more, we consider the mosquito biting preference in our model. For some unknown parameters, we use grid search algorithm to find the parameter values. We also compare the effect of different weather patterns on WNV transmission process. Simulation results show that the hybrid model fits the trend of the number of reported WNV human infection cases very well in Peel Region. The results also indicate that the impact of temperature is more significant than that of precipitation. This hybrid model is a novel tool to forecast WNV risk with real weather data.

The mosquito overwintering diapause plays the key role in the survival of mosquitoes and WNV in Peel Region of Ontario, Canada. In Chapter 3, we first divide the year into two periods depending on temperature and photoperiod, then we build a matrix mosquito population model for each period. We employ heat accumulation as a measurement for the effect of temperature on mosquito development in our matrix model. We analyze the theoretical properties of our model when we assume temperature is constant. Again, we estimate some of the unknown parameter values. Our simulation results indicate that our model fits very well to the trend of mosquito surveillance data in Peel Region.

In Chapter 4, we study the spatio-temporal distribution of mosquito population. We estimate the collective impact of all the unobservable information for each trap

through a hidden dimension method. We apply the method to mosquito surveillance data in Peel Region, Ontario, Canada. The results indicate significantly improves of modeling accuracy compared with the model without missing information. Our model reaches a good match with the observed mosquito abundance data. We also derive the conditions when the MSE of GLM with missing information is smaller than that without missing information.

In Chapter 5, we show the application of using our model to forecast weekly average trapped mosquito abundance in Peel Region during summer in LAMPS of York University. We also show an example of forecasting WNV in Peel Region. In Chapter 6, we conclude this thesis and provide the future works.

There still are many questions to be discussed in future. Firstly, we develop the matrix mosquito population model which can capture the trend of *Culex* mosquito abundance. An extension should be to incorporate the WNV transmission process with the matrix mosquito population model in Chapter 3.

Secondly, although our models in Chapter 2 and Chapter3 can capture the trend of *Culex* mosquito trap count and reported human cases very well, we do not incorporate the effect of mosquito control on mosquito abundance and the effect of public education on WNV infection. We will incorporate these effects in future studies.

Thirdly, all our works are based on the *Culex* mosquitoes in Peel Region, Ontario,

Canada. The models can be adopted to study other species of mosquitoes or other areas.

Lastly, we focus on WNV in this dissertation, the model in Chapter 2 can be adopted to study other mosquito-borne diseases such as Zika, Dengue fever, and malaria.

Bibliography

[1] Abdelrazec, A., Lenhart, S., and Zhu, H. (2013). Transmission dynamics of west nile virus in mosquitoes and corvids and non-corvids. *Journal of Mathematical Biology*, 68(6):1553–1582.

[2] Adewale, A. J. and Xu, X. (2010). Robust designs for generalized linear models with possible overdispersion and misspecified link functions. *Computational Statistics & Data Analysis*, 54(4):875–890.

[3] Ahumada, J. A., Laoointe, D., and Samuel, M. D. (2004). Modeling the population dynamics of culex quinquefasciatus (diptera: Culicidae), along an elevational gradient in hawaii. *Journal of Medical Entomology*, 41(6):1157–1170.

[4] Alto, B. W. and Juliano, S. A. (2001). Precipitation and temperature effects on populations ofAedes albopictus(diptera: Culicidae): Implications for range expansion. *Journal of Medical Entomology*, 38(5):646–656.

[5] Anderson, J. F. and Main, A. J. (2006). Importance of vertical and horizontal

transmission of west nile virus byCulex pipiensin the northeastern united states. *The Journal of Infectious Diseases*, 194(11):1577–1579.

[6] Arino, J., Wang, L., and Wolkowicz, G. S. (2006). An alternative formulation for a delayed logistic equation. *Journal of Theoretical Biology*, 241(1):109 – 119.

[7] Bacar, N. (2011). *A Short History of Mathematical Population Dynamics*. Springer London.

[8] Becker, N., Petric, D., Zgomba, M., Boase, C., Madon, M., Dahl, C., and Kaiser, A. (2010). *Mosquitoes and Their Control*. Springer Berlin Heidelberg.

[9] Bernardelli, H. (1941). Population waves. *Journal of the Burma Research Society*, 31:3–18.

[10] Blythe, S., Nisbet, R., and Gurney, W. (1982). Instability and complex dynamic behaviour in population models with long time delays. *Theoretical Population Biology*, 22(2):147 – 176.

[11] Bornn, L., Shaddick, G., and Zidek, J. V. (2012). Modeling nonstationary processes through dimension expansion. *Journal of the American Statistical Association*, 107(497):281–289.

[12] Bowman, C., Gumel, A. B., den Driessche, P. V., Wu, J., and Zhu, H. (2005). A

mathematical model for assessing control strategies against west nile virus. *Bulletin of Mathematical Biology*, 67(5):1107–1133.

[13] Bradshaw, W. E. and Holzapfel, C. M. (1977). Interaction between photoperiod, temperature, and chilling in dormant larvae of the tree-hole mosquito, toxorhynchites rutilus coq. *The Biological Bulletin*, 152(2):147–158.

[14] Brady, O. J., Johansson, M. A., Guerra, C. A., Bhatt, S., Golding, N., Pigott, D. M., Delatte, H., Grech, M. G., Leisnham, P. T., de Freitas, R. M., Styer, L. M., Smith, D. L., Scott, T. W., Gething, P. W., and Hay, S. I. (2013). Modelling adult aedes aegypti and aedes albopictus survival at different temperatures in laboratory and field settings. *Parasites & Vectors*, 6(1):351.

[15] C. Bowman, A. B. Gumel, P. V. d. D. J. W. and Zhu, H. (2005). A mathematical model for assessing control strategies against west nile virus. *Bulletin of Mathematical Biology*, 67(5):1107–1133.

[16] Cailly, P., Tran, A., Balenghien, T., L'Ambert, G., Toty, C., and Ezanno, P. (2012). A climate-driven abundance model to assess mosquito control strategies. *Ecological Modelling*, 227:7–17.

[17] Canada, S. (2012). Peel, ontario (code 3521) and ontario (code 35) (table). census profile. 2011 census. Technical report, Statistics Canada.

[18] CDC (2012a). Tables: West nile virus disease cases by state, 2012. *Centers for Disease Control and Prevention*. Accessed August 3, 2017. Available at `http://www.cdc.gov/westnile/statsMaps/finalMapsData/data/2012WNVHumanInfectionsbyState.pdf`.

[19] CDC (2012b). West nile virus symptoms, diagnosis, and treatment. *Centers for Disease Control and Prevention*. Accessed August 24, 2017. Available at `https://www.cdc.gov/westnile/symptoms/index.html`.

[20] Chesson, J. (1978). Measuring preference in selective predation. *Ecology*, 59(2):211–215.

[21] Ciota, A. T., Drummond, C. L., Ruby, M. A., Drobnack, J., Ebel, G. D., and Kramer, L. D. (2012). Dispersal of culex mosquitoes (diptera: Culicidae) from a wastewater treatment facility. *Journal of Medical Entomology*, 49(1):35–42.

[22] Cooke, K., van den Driessche, P., and Zou, X. (1999). Interaction of maturation delay and nonlinear birth in population and epidemic models. *Journal of Mathematical Biology*, 39(4):332–352.

[23] Cressie, N. and Cassie, N. A. (1993). *Statistics for Spatial Data*. JOHN WILEY & SONS INC.

[24] Cruz-Pacheco, G., Esteva, L., Montaõ-Hirose, J. A., and Vargas, C. (2005). Modelling the dynamics of west nile virus. *Bulletin of Mathematical Biology*, 67(6):1157–1172.

[25] Cushing, J. M. and Zhou, Y. (1994). The net reproductive value and stability in matrix population models. *Natural Resource Modelling*, 8(4):297–333.

[26] Dee, D. and National Center for Atmospheric Research Staff (Eds) (2017). The climate data guide: Era-interim. Accessed August 3, 2017. Available at `https://climatedataguide.ucar.edu/climate-data/era-interim`.

[27] Dee, D. P., Uppala, S. M., Simmons, A. J., Berrisford, P., Poli, P., Kobayashi, S., Andrae, U., Balmaseda, M. A., Balsamo, G., Bauer, P., Bechtold, P., Beljaars, A. C. M., van de Berg, L., Bidlot, J., Bormann, N., Delsol, C., Dragani, R., Fuentes, M., Geer, A. J., Haimberger, L., Healy, S. B., Hersbach, H., Hólm, E. V., Isaksen, L., Kållberg, P., Khler, M., Matricardi, M., McNally, A. P., Monge-Sanz, B. M., Morcrette, J.-J., Park, B.-K., Peubey, C., de Rosnay, P., Tavolato, C., Thépaut, J.-N., and Vitart, F. (2011). The ERA-interim reanalysis: configuration and performance of the data assimilation system. *Quarterly Journal of the Royal Meteorological Society*, 137(656):553–597.

[28] DeGaetano, A. T. (2004). Meteorological effects on adult mosquito (culex) popula-

tions in metropolitan new jersey. *International Journal of Biometeorology*, 49(5):345–353.

[29] Denlinger, D. L. and Armbruster, P. A. (2014). Mosquito diapause. *Annual Review of Entomology*, 59(1):73–93.

[30] Dickerson, A. K., Shankles, P. G., Madhavan, N. M., and Hu, D. L. (2012). Mosquitoes survive raindrop collisions by virtue of their low mass. *Proceedings of the National Academy of Sciences*, 109(25):9822–9827.

[31] Diekmann, O., Heesterbeek, J., and Metz, J. (1990). On the definition and the computation of the basic reproduction ratio r 0 in models for infectious diseases in heterogeneous populations. *Journal of Mathematical Biology*, 28(4):356–382.

[32] Dohm, D. J., O'Guinn, M. L., and Turell, M. J. (2002). Effect of environmental temperature on the ability of culex pipiens(diptera: Culicidae) to transmit west nile virus. *Journal of Medical Entomology*, 39(1):221–225.

[33] Duchon, J. (1976). Interpolation des fonctions de deux variables suivant le principe de la flexion des plaques minces. *ESAIM: Mathematical Modelling and Numerical Analysis*, 10(R3):5–12.

[34] Duchon, J. (1977). Splines minimizing rotation-invariant semi-norms in sobolev

spaces. In *Constructive Theory of Functions of Several Variables*, pages 85–100. Springer Berlin Heidelberg.

[35] Fahrmexr, L. (1990). Maximum likelihood estimation in misspecified generalized linear models. *Statistics*, 21(4):487–502.

[36] Fan, G., Liu, J., van den Driessche, P., Wu, J., and Zhu, H. (2010). The impact of maturation delay of mosquitoes on the transmission of west nile virus. *Mathematical Biosciences*, 228(2):119–126.

[37] Focks, D. A., Haile, D. G., Daniels, E., and Mount, G. A. (1993). Dynamic life table model for aedes aegypti (diptera: Culicidae): Analysis of the literature and model development. *Journal of Medical Entomology*, 30(6):1003–1017.

[38] Gardner, A. M., Hamer, G. L., Hines, A. M., Newman, C. M., Walker, E. D., and Ruiz, M. O. (2012). Weather variability affects abundance of larval *culex* (diptera: Culicidae) in storm water catch basins in suburban chicago. *Journal of Medical Entomology*, 49(2):270–276.

[39] Gong, H., DeGaetano, A. T., and Harrington, L. C. (2010). Climate-based models for west nile culex mosquito vectors in the northeastern US. *International Journal of Biometeorology*, 55(3):435–446.

[40] Hamer, G. L., Kitron, U. D., Goldberg, T. L., Brawn, J. D., Loss, S. R., Ruiz, M. O., Hayes, D. B., and Walker, E. D. (2009). Host selection by culex pipiens mosquitoes and west nile virus amplification. *The American journal of tropical medicine and hygiene*, 80(2):268–278.

[41] Hayes, E. B., Sejvar, J. J., Zaki, S. R., Lanciotti, R. S., Bode, A. V., and Campbell, G. L. (2005). Virology, pathology, and clinical manifestations of west nile virus disease. *Emerging Infectious Diseases*, 11(8):1174–1179.

[42] Hutchinson, G. E. (1948). Circular causal systems in ecology. *Annals of the New York Academy of Sciences*, 50(4):221–246.

[43] Hutchinson, M. F. (1995). Interpolating mean rainfall using thin plate smoothing splines. *International journal of geographical information systems*, 9(4):385–403.

[44] Impoinvil, D. E., Cardenas, G. A., Gihture, J. I., Mbogo, C. M., and Beier, J. C. (2007). Constant temperature and time period effects on anopheles gambiae egg hatching. *Journal of the American Mosquito Control Association*, 23(2):124–130.

[45] Jarvis, C. H. and Stuart, N. (2001). A comparison among strategies for interpolating maximum and minimum daily air temperatures. part ii: The interaction between number of guiding variables and the type of interpolation method. *Journal of Applied Meteorology*, 40(6):1075–1084.

[46] Jones, C. E., Lounibos, L. P., Marra, P. P., and Kilpatrick, A. M. (2012a). Rainfall influences survival ofCulex pipiens(diptera: Culicidae) in a residential neighborhood in the mid-atlantic united states. *Journal of Medical Entomology*, 49(3):467–473.

[47] Jones, C. E., Lounibos, L. P., Marra, P. P., and Kilpatrick, A. M. (2012b). Rainfall influences survival ofCulex pipiens(diptera: Culicidae) in a residential neighborhood in the mid-atlantic united states. *Journal of Medical Entomology*, 49(3):467–473.

[48] Kenkre, V. M., Parmenter, R. R., Peixoto, I. D., and Sadasiv, L. (2005). A theoretical framework for the analysis of the west nile virus epidemic. *Mathematical and Computer Modelling*, 42(3-4):313–324.

[49] Kennedy, J., Dilworth-Christie, P., and Erskine, A. (1999). *The Canadian breeding bird (mapping) census database*. Canadian Wildlife Service.

[50] Kilpatrick, A. M., Kramer, L. D., Jones, M. J., Marra, P. P., and Daszak, P. (2006). West nile virus epidemics in north america are driven by shifts in mosquito feeding behavior. *PLoS Biology*, 4(4):606–610.

[51] Koenraadt, C., Paaijmans, K. P., Githeko, A. K., Knols, B. G., and Takken, W. (2003). Egg hatching, larval movement and larval survival of the malaria vector anopheles gambiae in desiccating habitats. *Malaria Journal*, 2(1):20.

[52] Komar, N., Langevin, S., Hinten, S., Nemeth, N., Edwards, E., Hettler, D., Davis, B., Bowen, R., and Bunning, M. (2003). Experimental infection of north american birds with the new york 1999 strain of west nile virus. *Emerging Infectious Diseases*, 9(3):311–322.

[53] Kredler, C. (1986). Behaviour of third order terms in quadratic approximations of LR-statistics in multivariate generalized linear models. *The Annals of Statistics*, 14(1):326–335.

[54] Lefkovitch, L. P. (1965). The study of population growth in organisms grouped by stages. *Biometrics*, 21(1):1–18.

[55] Leslie, P. H. (1945). On the use of matrices in certain population mathematics. *Biometrika*, 33(3):183–212.

[56] Leslie, P. H. (1948). Some further notes on the use of matrices in population mathematics. *Biometrika*, 35(3/4):213.

[57] Lewis, E. G. (1942). On the generation and growth of a population. *Sankhy: The Indian Journal of Statistics (1933-1960)*, 6(1):93–96.

[58] Lewis, M., Rencławowicz, J., and van den Driessche, P. (2006). Traveling waves and spread rates for a west nile virus model. *Bulletin of Mathematical Biology*, 68(1):3–23.

[59] Lončarić, Ž. and Hackenberger, B. K. (2013). Stage and age structured aedes vexans and culex pipiens (diptera: Culicidae) climate-dependent matrix population model. *Theoretical Population Biology*, 83:82–94.

[60] Lura, T., Cummings, R., Velten, R., Collibus, K. D., Morgan, T., Nguyen, K., and Gerry, A. (2012). Host (avian) biting preference of southern CaliforniaCulex-Mosquitoes (diptera: Culicidae). *Journal of Medical Entomology*, 49(3):687–696.

[61] Macdonald, G. (1957). *The Epidemiology and Control of Malaria*. Oxford University Press.

[62] Manly, B. F. J. (1974). A model for certain types of selection experiments. *Biometrics*, 30(2):281–294.

[63] Moon, T. E. (1976). A statistical model of the dynamics of a mosquito vector (culex tarsalis) population. *Biometrics*, 32(2):355.

[64] Murdoch, W. W. (1969). Switching in general predators: Experiments on predator specificity and stability of prey populations. *Ecological Monographs*, 39(4):335–354.

[65] Nasci, R. S., White, D. J., Stirling, H., Oliver, J., Daniels, T. J., Falco, R. C., Campbell, S., Crans, W. J., Savage, H. M., Lanciotti, R. S., Moore, C. G., Godsey, M. S., Gottfried, K. L., and Mitchell, C. J. (2001). West nile virus isolates from

mosquitoes in new york and new jersey, 1999. *Emerging Infectious Diseases*, 7(4):626–630.

[66] Nelder, J. A. and Baker, R. (1972). Generalized linear models. *Encyclopedia of Statistical Sciences*.

[67] Pearl, R. and Reed, L. J. (1920). On the rate of growth of the population of the united states since 1790 and its mathematical representation. *Proceedings of the National Academy of Sciences of the United States of America*, 6(6):275–288.

[68] Pearson, K. (1896). Mathematical contributions to the theory of evolution. III. regression, heredity, and panmixia. *Philosophical Transactions of the Royal Society A: Mathematical, Physical and Engineering Sciences*, 187(0):253–318.

[69] Pecoraro, H. L., Day, H. L., Reineke, R., Stevens, N., Withey, J. C., Marzluff, J. M., and Meschke, J. S. (2007). Climatic and landscape correlates for potential west nile virus mosquito vectors in the seattle region. *Journal of Vector Ecology*, 32(1):22–28.

[70] PEE (2002). West nile virus in region of peel 2002. *Region of Peel*. Accessed August 3, 2017. Available online at `https://www.peelregion.ca/health/vbd/files/technical-report-2002/wnv-techreport-june302002-as.pdf`.

[71] Perrin, O. and Meiring, W. (2003). Nonstationarity in r¡sup¿n¡/sup¿ is second-order stationarity in r¡sup¿2n¡/sup¿. *Journal of Applied Probability*, 40(3):815–820.

[72] PHAC (2012). West nile virus monitor, 2012. *Public Health Agency of Canada*. Accessed August 3, 2017. Available at `http://www.phac-aspc.gc.ca/wnv-vwn/mon-hmnsurv-2012-eng.php`.

[73] Reisen, W. K. (1995). Effect of temperature on culex tarsalis (diptera: Culicidae) from the coachella and san joaquin valleys of california. *Journal of Medical Entomology*, 32(5):636–645.

[74] Reisen, W. K., Milby, M. M., and Meyer, R. P. (1992a). Population dynamics of adult culex mosquitoes (diptera: Culicidae) along the kern river, kern county, california, in 1990. *Journal of Medical Entomology*, 29(3):531–543.

[75] Reisen, W. K., Milby, M. M., Meyer, R. P., Pfuntner, A. R., Spoehel, J., Hazelrigg, J. E., and Webb, J. P. (1991). Mark–release–recapture studies with culex mosquitoes (diptera: Culicidae) in southern california. *Journal of Medical Entomology*, 28(3):357–371.

[76] Reisen, W. K., Milby, M. M., Presser, S. B., and Hardy, J. L. (1992b). Ecology of mosquitoes and st. louis encephalitis virus in the los angeles basin of california, 1987-1990. *Journal of Medical Entomology*, 29(4):582–598.

[77] Richardson, C. W. and Wright, D. A. (1984). *WGEN: A model for generating daily*

weather variables. US Department of Agriculture, Agricultural Research Service Washington, DC.

[78] Rizzoli, A., Bolzoni, L., Chadwick, E. A., Capelli, G., Montarsi, F., Grisenti, M., de la Puente, J. M., Muñoz, J., Figuerola, J., Soriguer, R., Anfora, G., Luca, M. D., and Rosà, R. (2015). Understanding west nile virus ecology in europe: Culex pipiens host feeding preference in a hotspot of virus emergence. *Parasites & Vectors*, 8(1):213–225.

[79] Robich, R. M. and Denlinger, D. L. (2005). Diapause in the mosquito culex pipiens evokes a metabolic switch from blood feeding to sugar gluttony. *Proceedings of the National Academy of Sciences*, 102(44):15912–15917.

[80] Ross, R. (1911). The prevention of malaria murray. *London, UK*.

[81] Rubel, F., Brugger, K., Hantel, M., Chvala-Mannsberger, S., Bakonyi, T., Weissenbck, H., and Nowotny, N. (2008). Explaining usutu virus dynamics in austria: Model development and calibration. *Preventive Veterinary Medicine*, 85(3-4):166–186.

[82] Sanburg, L. L. and Larsen, J. R. (1973). Effect of photoperiod and temperature on ovarian development in culex pipiens pipiens. *Journal of Insect Physiology*, 19(6):1173–1190.

[83] Schaeffer, B., Mondet, B., and Touzeau, S. (2008). Using a climate-dependent model to predict mosquito abundance: Application to aedes (stegomyia) africanus and aedes (diceromyia) furcifer (diptera: Culicidae). *Infection, Genetics and Evolution*, 8(4):422–432.

[84] Seiberg, N. and Witten, E. (1999). String theory and noncommutative geometry. *Journal of High Energy Physics*, 1999(09):032–032.

[85] Sota, T. and Mogi, M. (1989). Effectiveness of zooprophylaxis in malaria control: a theoretical inquiry, with a model for mosquito populations with two bloodmeal hosts. *Medical and Veterinary Entomology*, 3(4):337–345.

[86] Tait, A., Henderson, R., Turner, R., and Zheng, X. (2006). Thin plate smoothing spline interpolation of daily rainfall for new zealand using a climatological rainfall surface. *International Journal of Climatology*, 26(14):2097–2115.

[87] Thomas, D. and Urena, B. (2001). A model describing the evolution of west nile-like encephalitis in new york city. *Mathematical and Computer Modelling*, 34(7-8):771–781.

[88] Trawinski, P. and MacKay, D. (2008). Meteorologically conditioned time-series predictions of west nile virus vector mosquitoes. *Vector-Borne and Zoonotic Diseases*, 8(4):505–522.

[89] Tsuda, Y., Komagata, O., Kasai, S., Hayashi, T., Nihei, N., Saito, K., Mizutani, M., Kunida, M., Yoshida, M., and Kobayashi, M. (2008). A mark–release–recapture study on dispersal and flight distance of culex pipiens pallens in an urban area of japan. *Journal of the American Mosquito Control Association*, 24(3):339–343.

[90] van den Driessche, P. and Watmough, J. (2002). Reproduction numbers and subthreshold endemic equilibria for compartmental models of disease transmission. *Mathematical Biosciences*, 180(1-2):29–48.

[91] Wahba, G. and Wendelberger, J. (1980). Some new mathematical methods for variational objective analysis using splines and cross validation. *Monthly Weather Review*, 108(8):1122–1143.

[92] Walsh, A. S., Glass, G. E., Lesser, C. R., and Curriero, F. C. (2007). Predicting seasonal abundance of mosquitoes based on off-season meteorological conditions. *Environmental and Ecological Statistics*, 15(3):279–291.

[93] Wan, H. and Zhu, H. (2010). The backward bifurcation in compartmental models for west nile virus. *Mathematical Biosciences*, 227(1):20–28.

[94] Wan, H. and Zhu, H. (2012). The impact of resource and temperature on malaria transmission. *Journal of Biological Systems*, 20(03):285–302.

[95] Wan, H. and Zhu, H. (2014). A new model with delay for mosquito population dynamics. *Mathematical Biosciences and Engineering*, 11(6):1395–1410.

[96] Wang, J., Ogden, N. H., and Zhu, H. (2011). The impact of weather conditions on culex pipiens and culex restuans (diptera: Culicidae) abundance: A case study in peel region. *Journal of Medical Entomology*, 48(2):468–475.

[97] Witten, E. (1995). String theory dynamics in various dimensions. *Nuclear Physics B*, 443(1-2):85–126.

[98] Wonham, M. J., de Camino-Beck, T., and Lewis, M. A. (2004). An epidemiological model for west nile virus: invasion analysis and control applications. *Proceedings of the Royal Society B: Biological Sciences*, 271(1538):501–507.

[99] Wonham, M. J., Lewis, M. A., Renclawowicz, J., and van den Driessche, P. (2006). Transmission assumptions generate conflicting predictions in host-vector disease models: a case study in west nile virus. *Ecology Letters*, 9(6):706–725.

[100] Yang, H. M., Macoris, M. L. G., Galvani, K. C., Andrighetti, M. T. M., and Wanderley, D. M. V. (2009). Assessing the effects of temperature on the population of aedes aegypti, the vector of dengue. *Epidemiology and Infection*, 137(08):1188.